Bicycle Wheel Test Machine

Specialized Bicycle Components

Dylan Harper
dyharper@calpoly.edu

Kevin Hom
kphom@calpoly.edu

Ross Williams
rwilli02@calpoly.edu

Statement of Confidentiality

The complete senior project report was submitted to the project advisor and sponsor. The results of this project are of a confidential nature and will not be published at this time.

Statement of Disclaimer

Since this project is a result of a class assignment, it has been graded and accepted as fulfillment of the course requirements. Acceptance does not imply technical accuracy or reliability. Any use of information in this report is done at the risk of the user. These risks may include catastrophic failure of the device or infringement of patent or copyright laws as the machine described is a prototype design not fully-compliant with all necessary safety codes. California Polytechnic State University at San Luis Obispo and its staff cannot be held liable for any use or misuse of the project.

Table of Contents

Statement of Confidentiality 2
Statement of Disclaimer 3
Introduction 7
Objectives 7
Background 8
Components 8
Bicycle Loading Considerations 9
Rider Weight 9
Chain Load 10
Dropout Stiffness 11
Wheel Speed 12
Quick Release Clamping Force 13
Loss Comparison 14
Existing Products 15
Bearing Research 16
Rolling Element Bearings 16
Air Bearings 16
Magnetic Bearings 17
Force Actuators and Speed Controllers 17
Onboard Dynamometers 18
Measurement Devices 19
Control Systems 19
Safety 19
Design Development 20
Initial Designs and Brainstorming 20
Conceptual Designs 21
Two-Test Fixture Concept 22
Additional Preliminary Concepts 24
Single Test Fixture with Rotating Dropouts 24
Spinning the Axle Concept 27
Initial Cost Analysis and Considerations 30

Final Design 31
Design Layout 31
Procedure 32
Final Design Componentry 33
Rotating-Dropout Positioning Mechanism 33
Load-actuating Systems 33
Table –top Design 34
Bearing Selection 35
Dropout Chip Development 36
Motor Control and DAQ Subsystem 38
Cost Analysis 44
Safety and Maintenance Considerations 44
Machine Fabrication and Final Performance 45
Frame and Indexing 45
Sub-assemblies 45
Motor Control System Enclosure 46
VI Development 47
Final Machine Performance 48
Design Verification Plan 48
Rear Dropout Stiffness Determination and Verification 48
Support Bearing Power Loss 49
Servo System Tuning 50
Appendices 51
Appendix A: Works Cited 51
Background Research 51
Bearing Research 53
Control and Data Acquisition Systems 54
Dynamometer Research 54
Coupling Considerations 55
Load-Actuating Systems 56
Appendix B: Management Plan 57
Team Members 57

Collective Assignments 58
Project Phases and Milestones 58
Appendix C 61
QFD House of Quality 61
Engineering Requirement Pair wise Comparison 62
Appendix D: Conceptual Design Schematics 63
Preliminary Concept # 2: Regression Method 63
Preliminary Concept # 3: Two-Test Method with One Fixture 65
Appendix E: Detail Design Drawing Packet 66
Appendix F: Contact Information 68
Specialized Correspondent 68
Team Advisor 68
Vendors and Suppliers 68
Appendix G: Vendor Technical Data Sheets 70
Appendix H: Supporting Analysis 71
Appendix I: Team Gantt Chart 72

Introduction

In recent years, the cycling industry has witnessed huge advancements in bicycle components and materials. The age old goals of speed and low weight are still present today, but the pursuit of these goals may be reducing the structural stability of various components integral to wheel performance, including the wheel hub bearings. These bearings are invaluable to bicycles but little is known about how the forces and loads applied to a bicycle affect the performance of these bearings. Broken axles and hubs are indicators of significant stresses within the hub, but little is known about how the resulting deformation affects the performance of the bearings. Specialized Bicycle Components asked the team to produce a custom test machine to help them study this problem.

The team's goal was to design a machine able to simulate rider and chain loading conditions and measure the corresponding power loss within the hub bearings. Through the implementation of this machine, Specialized hopes to gain vital information about the efficiencies of various hub, axle, and bearing combinations

The team consists of three mechanical engineering seniors, Kevin Hom, Dylan Harper, and Ross Williams. Dr. Joseph Mello will be advising the team, and all contact to Specialized will be through the project sponsor Sam Pickman.

Objectives

The goal of this project is to design and build a test machine capable of measuring the hub power loss of a bicycle wheel under various loading conditions. To maximize performance, hub and axle assemblies have been minimized in size and weight. It is unclear, however, how deflection of these smaller components affects the overall power loss. Specialized hopes to use the machine to directly compare the efficiencies of different hub/axle/bearing assemblies under load. The machine must be able to simulate rider load, chain load, and quick release clamping force, as well as offer a range of dropout stiffness. These dropout stiffnesses must accurately represent the actual boundary conditions at the dropouts while not over-constraining the axle. It must also be able to locate the chain load at each individual cog on the cassette. Ideally the machine will consist of a single test fixture to eliminate variance between tests and enhance repeatability. Beyond these concrete objectives, the team wants to design the machine to be as simple as possible, while retaining a high level of precision. Below is a table of the specifications the team has defined for the project. Many of the values and ranges were given to by the sponsor directly. The other specifications were developed using the QFD method. The house of quality can be found in Appendix C.

Table 1. Project Engineering Specifications

Spec #		Range	Tolerance	Verfication
1	Power Loss	NA	±1 W	Test
2	Chain Load	0-5000 N	±5 N	Test
3	Rider Load	0-1000 N	±2 N	Test
4	Wheel Speed	1-60 km/h	±2 mm/h	Test
5	Front/Rear Hubs	Y/N	NA	Inspection
6	QR Clamp Force	0-2500 N	±2 N	Test
7	Dropout Stiffness	9-13 mm	NA	Inspection, Similarity
8	Loads ON/OFF	Y/N	NA	Inspection, Test
9	Cost	< $10,000	NA	Inspection
10	%Employees Easy Use	85 %	NA	Test
11	Volume	< 105 m^3	NA	Inspection
12	Maintenance	<5 h/mo	NA	Test

Background

Components

In designing a machine that will hold multiple types of front and rear bicycle wheels, the determining factor is the spacing of the hub. In today's bicycle market, the most common hub spacing for front and rear wheels ranges from 100-110mm and 130-135mm respectively. The wheel team at specialized, however, has specified that they intend to test hubs up to 190mm. Therefore the machine must be capable of handling 100-190mm hub widths.

A variety of axle styles and sizes exist within the industry. These range from 10-25mm and are available as through or quick-release axles. Our machine will be primarily designed to handle 10mm quick-release axles but will be capable of being modified to handle up to 20mm diameters and through axles.

There are two types of bearings found in bicycle hubs. The first type of hub bearings are loose ball bearings that are contained in a channel formed by the hub body and a cup fastened onto the axle. These bearings are referred to as cup and cone bearings and are the most common solution found on many cheaper hubs. Newer hubs contain sealed ball bearings that are manufactured as standalone cartridge bearings and then pressed into the hub. High-end cartridge bearings, while usually more efficient, vary drastically in price but also have much more data available in industry due to large manufacturers like SKF providing calculations on power loss in their bearings given different loads. This calculation tool can be found on the SKF website

Bicycle dropouts are typically integrated into the frame of the bicycle, but some new cycle designs have utilized adjustable dropouts that can be changed in order to adjust geometry of the bike. The team has been unable to find information on local dropout stiffness as most studies and tests currently conducted in industry do not measure this directly, but instead measure overall frame stiffness. Rather than try to quantify this stiffness exactly for the machine, the team will instead produce dropouts of varying stiffnesses to account for variation between frames.

Bicycle Loading Considerations

The sponsor had already indicated which loads the machine had to replicate, so the purpose of the team's research was not to analyze which loads to include. Instead, the team wanted to better understand how each load could possibly affect the hub/axle assembly to ensure that the machine would accurately model real conditions. The provided information suggests that dropout stiffness will greatly affect the hub loads, but will be difficult to model. Thus, the team will need to design the dropout component of the test carefully to ensure useful results. The team also must design the loads so that they can be applied independently, or in unison.

One of the most difficult aspects of this project will be to match the precision and repeatability requirements defined by Specialized. Reaching these goals will require high-precision instrumentation and careful experiment design. Both the machine and test method must be designed to eliminate and isolate sources of loss. Wheel speed measurement will be particularly important, and will drive the accuracy of the power measurement.

Rider Weight

Perhaps the most obvious load placed on the bicycle system is the static weight of the rider. The rider applies this load at three main points: the saddle, the pedals, and the handle bars. How the force is distributed though the frame is a function of the location of

the rider's center of gravity, frame geometry, and the terrain conditions on which the wheels are rotating. The variance of weight distribution on different frames or varying the rider's position (i.e. standing vs. sitting) is outside the scope of this project as Specialized has asked the team to simply apply a variable static load up to 1000 N (~225 lb). This load causes bending stresses to occur within the axle which in turn lead to bearing misalignment and power lost. The bending profile of the hub due to rider weight is shown in the free body diagram below.

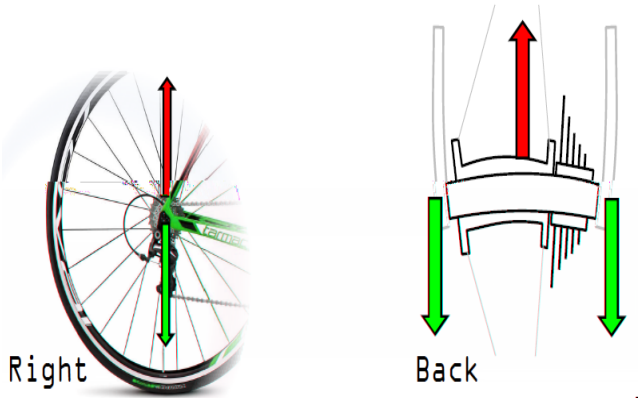

Figure 1. Free body diagram (FBD) and bending profile from a static vertical load

Chain Load

The drive load through the chain is the largest force placed onto the hub. This load is transmitted from the rider to the pedals then through the chain which effectively pulls the hub forward creating the bending profile shown below. The magnitude of this force can range upward of 5000 N (1125 lb) and is directly related to the rider's level of fitness as well as the tractive resistance seen by the tires. Because of the large variance in magnitude due to these two factors, Specialized has required this force be replicated with the ability to vary the load up to 5000 N.

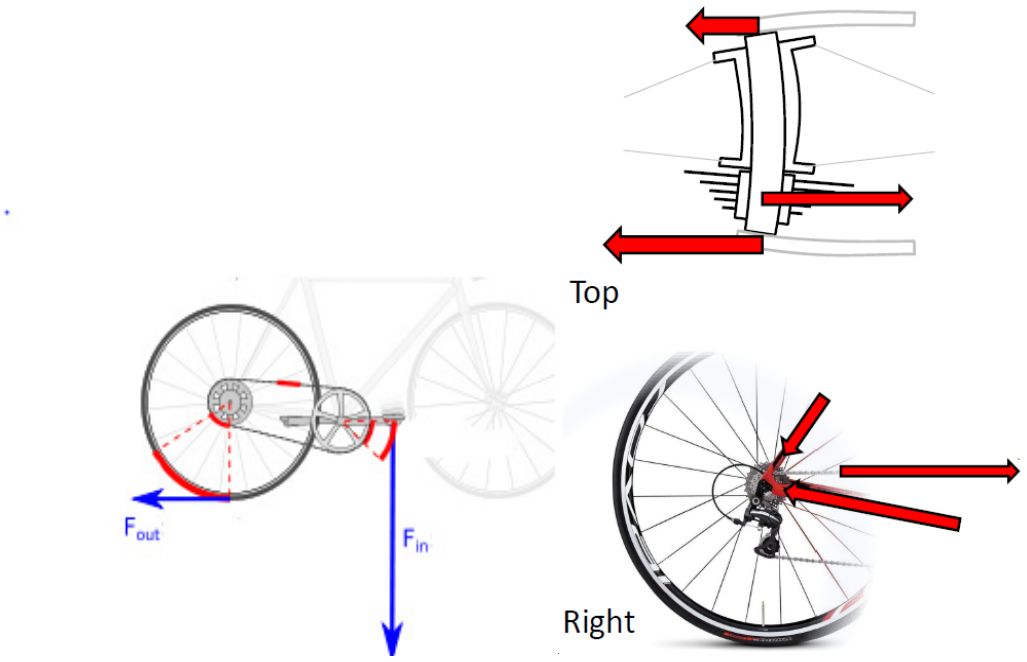

Figure 2. Force transference and bending profile in the axle due to drive load

Dropout Stiffness

The amount of relative misalignment within the hub is greatly affected by the material and mechanical properties of the dropouts. This boundary condition created by the axle being locked into the frame is a function of the stay and dropouts' stiffness, geometry, and cross-sectional area. The team must be careful to replicate the actual stiffness at the dropouts to match real conditions as closely as possible.

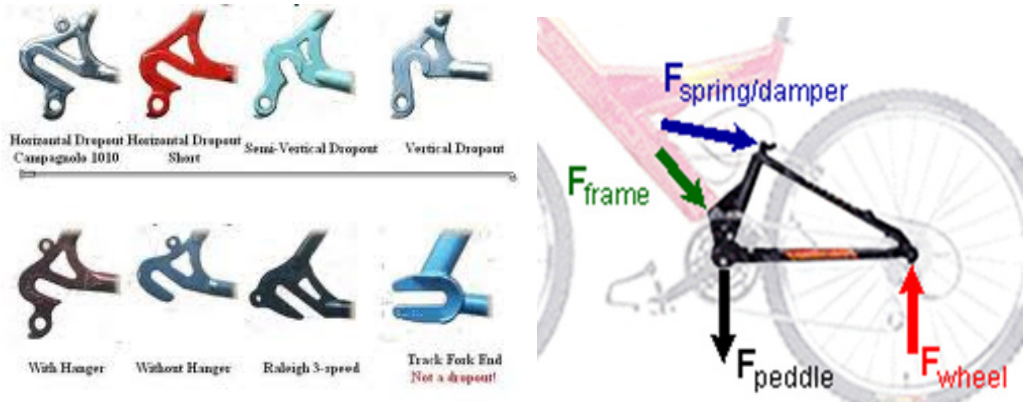

Figure 3. Examples of varying dropout designs and stay FBD

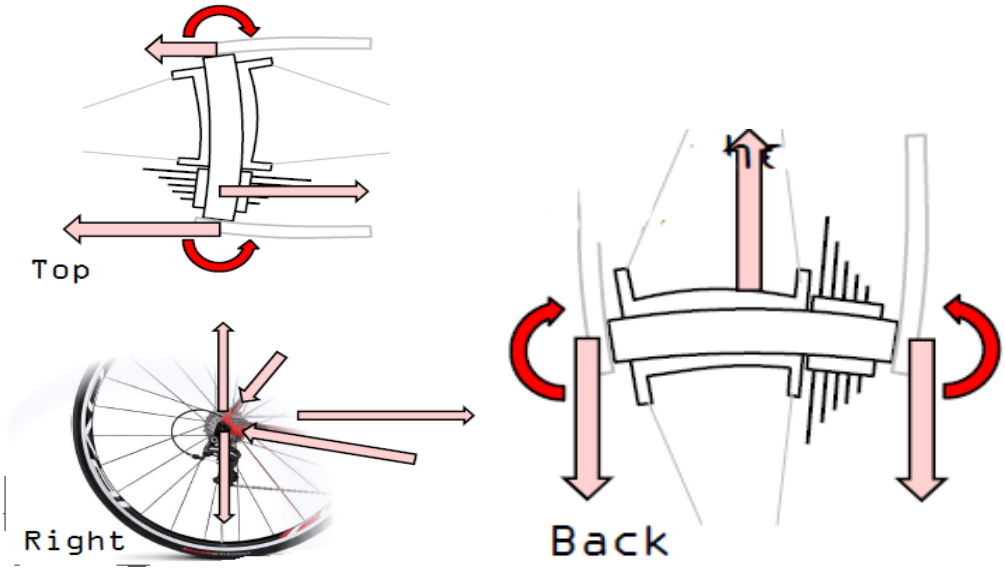

Figure 4. FBD depicting the boundary conditions placed on the axle by the dropouts

Wheel Speed

As said above, the speed at which the wheel is driven will be a large determinant of power lost within the hub bearings. This fact makes the method in which wheel speed is controlled a critical factor in the final design. Making matters more complicated is the overpowering presence of aerodynamic losses at wheel speeds greater than 20 kph (see Figure 5 below). Because the power necessary to overcome air resistance is much larger than that required to compensate for friction in the bearings, the team must devise a test method that definitively quantifies bearing loss without the concern of aerodynamic losses preventing any relative difference between wheel configurations. The team must also account for the resistance formed by the wheel's contact point with the ground. This additional power loss is directly proportional to the vertical load being applied on the system and thus will increase as the simulated rider weight increases. The team must account for this fact in the final design in the same manner as it must with air resistance.

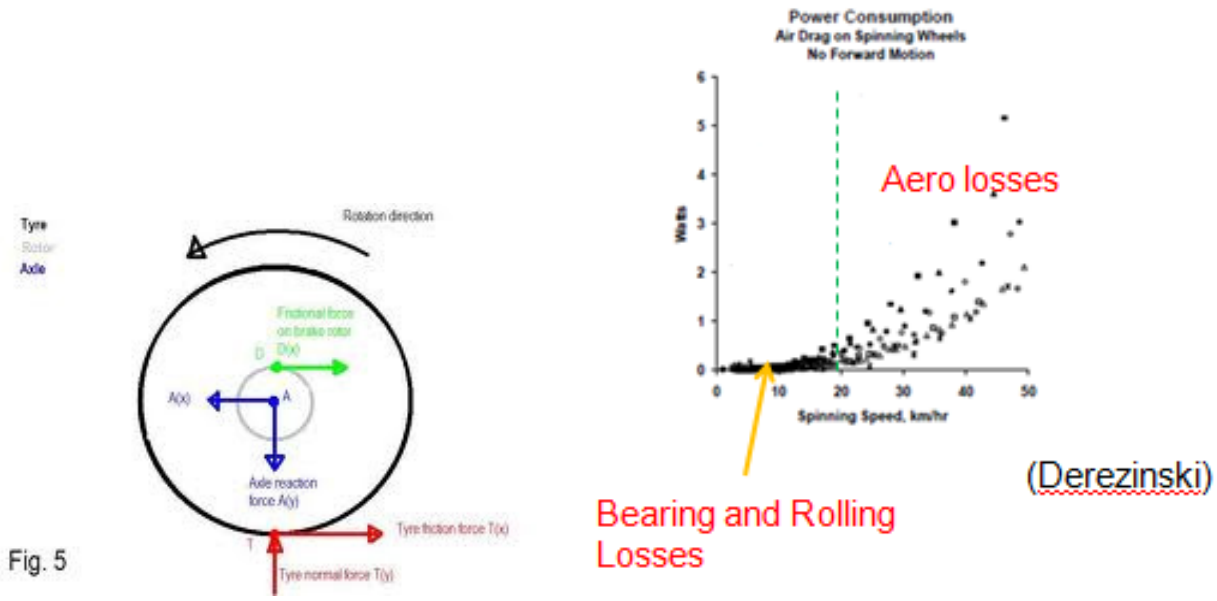

Figure 5. Wheel FBD and graph of power required to run a wheel at varying speeds

Quick Release Clamping Force

Most bikes today use the quick release mechanism to lock the wheel to the frame. A quick release uses a threaded cam-lever mechanism that is tightened then clamped down to ensure the axle stays in place. It does this by placing a compressive force on the axle while tensioning the skewer running through axle. These forces can reach magnitudes of 3200 N of compressive force on the axle when the quick release is fully tightened. The figure below shows a diagram of the components within a typical quick release and a basic pictorial of how it is used.

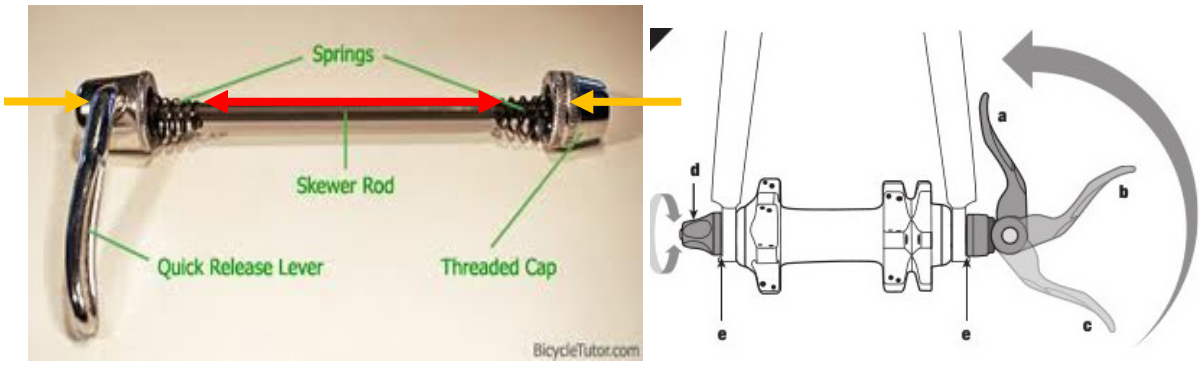

Figure 6. Quick Release FBD with system components and application

Loss Comparison

As said above in the discussion on wheel speed, aerodynamic and rolling resistance losses present during the system's normal operation have the ability to prevent the team from finding any meaningful data used to determine the performance characteristics of a specific wheel configuration. In response to this, the team estimated the magnitudes it could expect from each of the three modes of loss through research of previous studies, prior course training, and publically-available calculation methods. The magnitudes shown below were taken from a 1998 article in the Journal of Applied Biomechanics and show the extent at which power required to overcome bearing friction is masked by aerodynamic and rolling losses. As said above, the relative magnitudes of these losses demonstrate the importance of choosing the proper test method to ensure the team can confidently quantify bearing loss.

- P_{aero}=159 W
- P_{road}=24 W
- $P_{bearing}$=1.4 W

  - Data calculated for 177 lb rider at 20 mph on flat ground with 7 mph headwind

An additional calculation method used to estimate loss specifically within the bearings was provided via the SKF Group, a worldwide bearing manufacturer. This calculation takes into account the frictional moment within the bearing due to rolling, sliding, seal, and hydrodynamic drag and was especially useful during the conceptual design phase when quantifying the power lost in any added support bearings was needed to determine the concept's feasibility. The calculation can be found at SKF's website and is shown below.

- $N_R = 1.05 \times 10^{-4}$ *M*n (SKF)
  - N_R= power lost due to bearing
  - M=total frictional moment
    - » Includes rolling, sliding, and seal resistance as well as hydrodynamic drag
  - n= wheel speed

*Calculation later used for conceptual validation

Existing Products

Preliminary online research found multiple manufacturing companies devoting entire departments to the design and production of commercially-available test machines. In fact, the keywords “bicycle test machine” will yield over 2,200 results on Alibaba alone. The machines sold on websites such as Alibaba or McMaster-Carr come from corporations producing testing devices investigating frame durability, seat tube fatigue, disk brake forces, etc. Many of these machines use hydraulic, pneumatic, or mechanical position-control systems to apply loads to specific points on a bicycle frame. These loads simulate performance-determining loads such as rider weight, chain load, and impact forces. The designs and force actuation processes of these machines provide a platform from which ideas can be generated so that the loading conditions on the machine can be as accurate and realistic as possible.

When looking specifically at bearing test machines, it was found that much of the research and machinery had been done and built by large manufacturers such as SKF, Koyo, Timken, etc. This research included studies investigating bearing parameters such as optimal lubrication viscosities or power lost under a given load. Machines of a potentially-applicable scope to the project are discussed below. SKF was a particularly useful source as they provide design specifications for all their products as well as the performance (i.e. power lost due to friction) of said products under specified operating conditions. SKF also produces and sells measurement/testing devices that could potentially be used or adapted for the project. One of these devices is their Sensor-Bearing Unit, an apparatus mounted similar to other ball bearings that is capable of measuring speed and position of the shaft it supports. Such a precision device could be useful in maintaining wheel speed accuracy as wheel speed is the critical determining factor on the amount of power lost due to bearing friction and aerodynamic effects.

Other companies such as Magtrol, SKF, and General Bearing have developed machines designed to test a bearing’s load carrying capabilities. These machines are able to apply loads in both the axial and radial directions and can provide a means for determining how such technology can be adapted specifically to the wheel hub of a bicycle. Studying these machines can also aid research of how a bicycle’s operating loads are transferred through the front and rear wheel hubs to the bearings and could potentially yield a simpler, more cost-efficient means of force application. Having said this, the team must take into account that these machines produce forces applied directly to the bearing itself whereas the proposed machine would ideally simulate hub bearing loads as accurately as possible. This goal requires the team to apply loads at points not directly in contact with the hub.

Bearing Research

Applying multiple different loads into a system with rotating components necessitates the incorporation of bearings into any proposed conceptual design. Adding bearings to any design, however, requires a comprehensive understanding of how different types of bearings support loads and potentially add losses to the system. Performing preliminary research of bearing performance characteristics enables the team to choose the correct set of bearings and thus avoids having extra losses introduced into the system overshadowing the losses trying to be measure. If the team were to use the wrong type of bearings to support the applied loads, the test would be unable to show any relative difference between wheel set-ups and thus would have inconclusive results. The types of bearings researched as candidates for the machine include rolling contact bearings and several types of noncontact bearings.

Rolling Element Bearings

Rolling element bearings ("contact bearings") are the most popular bearing for industrial and recreational applications due to their high performance to cost characteristics. The most common type of contact bearing is the radial ball bearing. Radial ball bearings are named as such because they are very useful in supporting loads normal to their races' axis of rotation. While radial ball bearings can support some axial load, other types of contact bearings such as the tapered roller or the spherical bearing are specifically designed to handle axial forces of much higher magnitudes.

Besides different variations of how the rolling elements of contact bearings support a load, the material of which the bearing is made of also has a significant impact on the bearing's performance characteristics. The bearing material selection process is nothing new to the bicycle industry as ceramic ball bearings have become increasingly popular over the past several years. Commonly made of Silicon Nitride or Zirconia, ceramic bearings are able to reduce rolling friction by roughly 20 times that of steel while being up to 60% lighter and capable of handling a higher load.

Air Bearings

Air bearings use pressurized air flowing out of porous pads placed at varying radial locations which form a thin layer of fluid allowing rotation without any contact whatsoever. Because of this, the only resistance to rotation is the near-negligible friction encountered in the pressurized air. Air bearings are also often considered the smoothest running of all bearings due to fact that they "average out local irregularities" found within component inaccuracies (Xie, 2003). One would think with these superior performance characteristics that air bearings would be the ideal solution for the

machine. However, when examining the total cost of implementing air bearings into the system the final amount came to be roughly $ 7000 with only the bare minimum componentry included. These additional features included the bearings' housings, filters, airlines, etc. Combining this factor with the fact that air bearings can support only one-fifth the load of typical hydrodynamic bearings quickly yielded the conclusion that air bearings are most likely not a feasible solution for the system.

Magnetic Bearings

Like air bearings, magnetic bearings draw their performance benefits from their non-contact relationship with the shaft they support. Magnetic bearings are also incredibly strong with near-infinite stiffness at steady-state giving it a decided strength advantage over air bearings. Another advantage of using magnetic bearings is that its performance characteristics are largely dictated by the electrical and/or control system components involved in its operation and are seemingly independent of mechanical properties such as stiffness or yield strength. Like air bearings, though, magnetic bearings require many additional components to mitigate heat loss and provide system control and are thus very expensive. These parts plus the inherently large size of magnetic bearings (~2-10 times greater than ball bearings) add a large amount of unnecessary space to the system's apparatus.

The type of bearing arrangement implemented into the machine will be the combination resulting in the least additional power required to run the system provided such bearings can be obtained at a reasonable cost. As stated above, air and magnetic bearings have nearly negligible power lost due to friction but come at an exorbitant cost severely limiting the team's spending capabilities on material and other necessary project components (i.e. sensors, motors, etc.). More than likely, rolling element bearings will be used which necessitates quantifying approximately how much power loss is being introduced into the system. The calculation from SKF makes the comparison between rolling element bearings very efficient and allows the team to confidently select the appropriate bearing size and type for the test.

Force Actuators and Speed Controllers

In choosing a means of force application, the team must take into account the required forces' magnitudes, direction, and placement on the frame. Given the varying loads the team must apply to the machine, it soon becomes obvious that no one machine can be specifically applied to the team's design and budget constraints. Almost certainly, the resulting machine will comprise several subsystems able to be operated and controlled independently of one another. These systems could range in complexity from an

automated press operating under PLC control to a reverse carjack cranked to a certain height.

Electromechanical devices could also provide a means of producing forces with varying magnitudes. These devices are particularly useful as they come with built-in control systems capable of holding a sustained output which could in turn be used to produce a static load. Another very practical aspect of these devices is that their remote interface allows the user to apply and control the load a safe distance away from the point of application. When dealing with rotating machinery and forces upwards of 5000 N, safety concerns can never be neglected. An example of one of these electromechanical devices that immediately comes to mind is the stepper motor. The stepper motor is a rotary machine whose shaft rotates in predetermined "steps" in either angular direction. A common step magnitude is 1.8 degrees which gives the user 200 positions in which the output shaft can be placed. The stepper motor, in conjunction with lever arms, could be used to produce the magnitudes of loads at specific points on the frame. Linear motors could also be utilized as they have a similar actuation process and also provide very high resolutions.

Perhaps the most important feature of the design is controlling the speed of the wheel. As mentioned above, a bearing's rotational speed is the critical factor in determining its performance characteristics (i.e. life, power lost due to friction toque, etc.). An obvious and very common means of producing the accuracy required in such a key component comes via a dynamometer or "dyno." A dyno is an electromechanical device whose output shaft rotates at a user-input speed or torque while measuring both. From these known quantities, the power required to run the dyno at said torque or speed can be calculated.

Onboard Dynamometers

One of the ways riders are able to gauge their ability to produce work is via an onboard computer reading the power supplied to one of several key areas on the bike. These commercially-available devices are attached to the rear hub, the wheelset, or the crankset and measure the angular speed of the hub, crank, or wheel and multiply the reading with the torque applied, thus giving power. These power meters, made by PowerTap, Quarq, Power2Max, and SRM can be accurate to within ±1.5%, and provide the team a way of directly measuring the power at the hub via strain gauges placed in the hub or bottom bracket.

Onboard measurement tools can also be used to isolate the loads which the rider's power output must overcome to reach a certain speed. Through measuring loads at the ends of the front and rear wheel axles as well as the chain load via "instrumented force

pedals," the reaction loads at the ground-tire contact point could be calculated. These forces can be used to calculate total power output required by the rider.

Measurement Devices

The devices used to measure the applied loads and the additional power lost due to each added load are just as if not more important than the method by which these forces are actuated. They could include strain gauges to measure deflection and forces in the axle, a rotary torque transducer for computing the power required to run the dynamometer, load cells to quantify rider load, as well as other similar instruments used for determining chain load and quick release clamping force. Properly specifying each sensor, transducer, and gauge is crucial to ensuring the stringent accuracy requirements dictated by the sponsor are met.

Control Systems

After defining how the forces will be applied, a way of controlling these force's magnitudes needs to be found. This problem can be neglected should the team find devices with preprogrammed controllers already providing the machine's required accuracy. If not, however, it becomes necessary to find a control system applicable to the final design. In order to ensure the precise resolution required and to account for outside disturbances that may occur in operation, a feedback control system will most likely be needed.

Two popular forms of controllers are the PID (proportional-integral-derivative) and PLC (programmable logic controller). A PID controller takes the system's error (difference between system output and desired output) and reduces it by reading the error's magnitude and rate of change. This type of controller is the most popular form in industry and represents the type the team is most familiar with as a group. PLC controllers are useful in that they are widely used in motion control, can support multiple inputs and outputs, and are often built to support operation in extreme weather conditions. Given that this machine will be used in a machine shop and lack of group knowledge in PLC control, a PID controller will most likely be used when or if needed.

Safety

This machine will have multiple rotating parts as well as very high loads, both in tension and compression, applied to the wheel being tested. Aside from adequate factors of safety applied to each manufactured component, there is a need for shielding from the user and others who may be near the machine at any given time. There are many companies that produce pre-fabricated, impact resistant, polycarbonate shields that can

be oriented in many different positions as needed. The shields described are also clear therefore allowing safe visibility of the entire system.

All constraints of this test machine must meet OSHA safety requirements to be used in an open space on the shop floor. The safety equipment included will follow the guide lines laid out by the OSHA requirements for machine safeguarding and the occupational noise exposure guide. With respect to these standards and ease of operation it would be ideal to not need eye or ear protection when operating the machine

Design Development

Initial Designs and Brainstorming

Before the initial meeting with the team sponsor to determine the specific requirements for the test machine, the team brainstormed ideas allowing questions to be formulated regarding the parameters of the sponsor-defined requirements. The first question that arose was what range of bikes should be able to be tested by the machine. From team research and knowledge of bicycle wheels it was known that a variety of different standards existed between mountain and road bicycles with a wide range of hub widths and axle diameters. It was also unclear from the initial proposal what parts of the bike were to be included in the test. Was this machine going to be used on hubs before they are laced to wheels? Wheels taken off of bicycles? Or entire Bicycles loaded into the machine? Another concern was if all of the desired loads needed to be present in one test simultaneously or if multiple tests could be conducted. Another problem the team ran into was the potential losses through a conventional chain drive train and how the loads would be applied to the rear hub without an actual force on a pedal. Going into the meeting with the sponsor the team also had a desire to know how the data collected from this machine was going to be used, and what comparisons would be made between different wheels for a better understanding of the scope of the project.

After the first meeting with team advisor, Dr. Joseph Mello, it was determined that a table of losses should be built to establish the range and magnitudes of the losses that the team should expect to see from each loading component involved. The prominent values can be found in the loss comparison section.

In the team's first meeting with Specialized Test Lab Manager, Sam Pickman, the team was able to identify all of the relevant requirements necessary to move forward with the initial design of the project. It was stated that the machine should be able to handle a fully assembled wheel as well as a variety of hub widths and axle diameters. The team also learned that the data gathered from this machine was to be used in comparison

with other wheel assemblies in order to determine the effect on bearing friction each setup has at different values of rider and chain load at different speeds. The problem of chain loading was also clarified as Sam stated that a static chain load is acceptable in order to get even and consistent modeling parameters.

From prior individual experience, the group had a combined knowledge base that allowed the team to start creating concepts for the machine. Considering the fact that power loss was to be measured, it was decided that one method of attempting to solve the problem would definitely involve a dynamometer. Another method conceived of during the initial sponsor meeting was a regression test that would yield a velocity curve vs. time from which power curves could be analytically separated in order to determine losses. All of these initial thoughts and brainstorming sessions led the team to discover that before designing a machine, the team needed to develop a test that would accurately measure these losses, not predict them through calculations. Herein lies the challenge of the project as the team anticipated defining this test method to be a more difficult task then fabricating the resulting machine.

When attempting to initially design this test the team concluded that the only way to measure the hub bearing losses while eliminating all other losses was to run two tests. The first test would spin the entire wheel locking the hub and axle so that the hub bearings were not spinning. In the next test the axle will be locked, allowing the wheel to spin on the hub bearings. The data from the first test can then be subtracted from the data of the second test in order to yield the isolated hub bearing losses. The team attempted to find solutions to this test setup in many different ways. One idea was to load the wheel onto the shaft of a dynamometer, locking the hub to the shaft so that the power loss is then recorded for all losses induced by the wheels except that of the hub bearings. This would be the first step in the test. The second step would be a regression test, locking the axle so that the wheel spins on the hub bearings in order to gain power losses including the bearings. The losses calculated from step one could then be subtracted from the losses in step two to yield the isolated power loss of the hub bearings.

Conceptual Designs

Three initial concepts were originally developed and presented to Sam, the sketches for which can be found in Appendix D. The first and initially most-developed concept is shown below.

Two-Test Fixture Concept

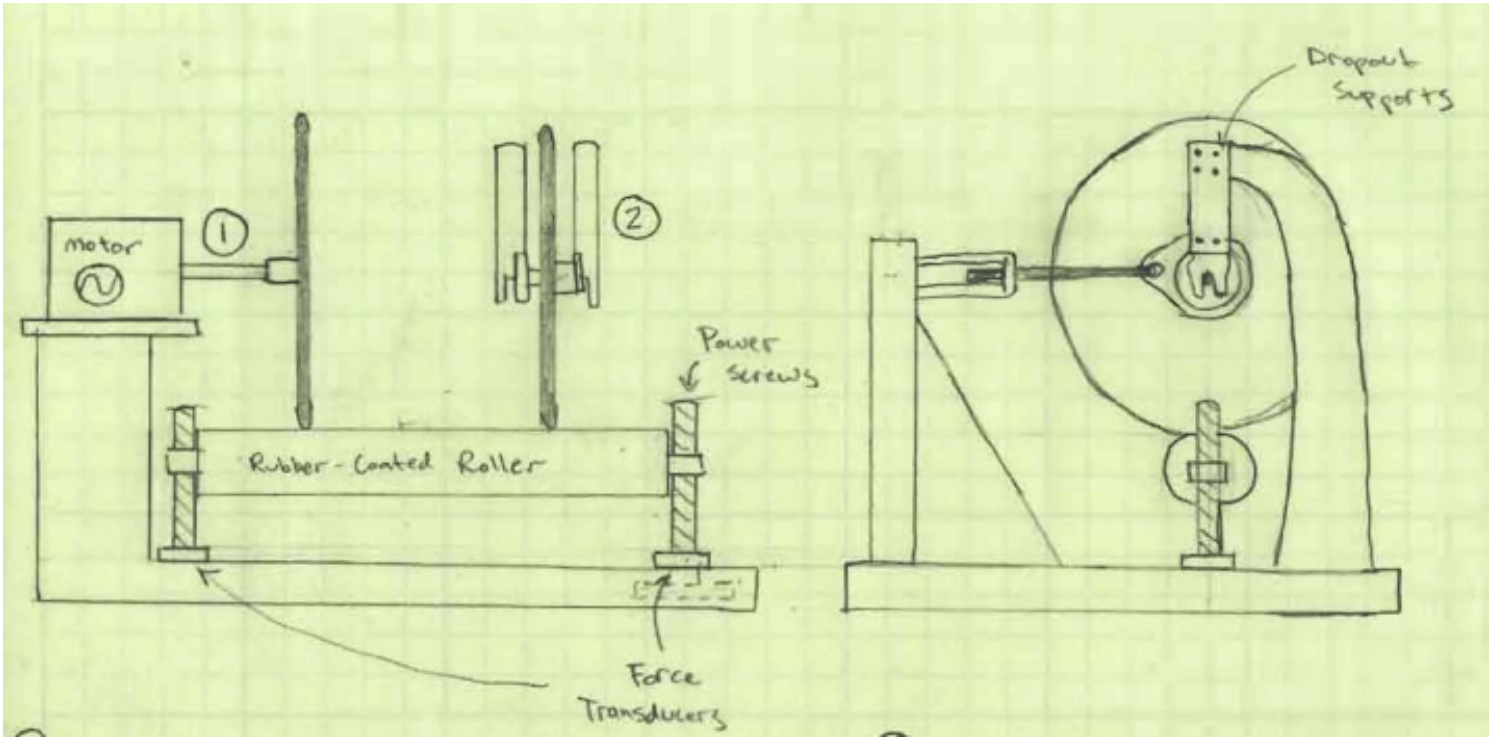

Figure 7. Initial Design Approach

Concept #1 was designed to be run in two separate tests in order to isolate hub bearing losses. The first test fixture would secure the hub and axle together, and power the wheel from the center. This way the wheel could be ran under various loading conditions and the team could then quantify the system losses from the machine. The second test was planned to be a regression (or step-down) test run on the actual hub bearings. The idea was to measure the speed of the wheel as it naturally decelerated, and calculate out the energy losses by derivation of the overall kinetic energy. The only difference in measured power loss between the two tests should have been the loss due solely to the bearings in the hub.

The team's main concern with this design, however, was that the first test was designed so that the motor shaft would be loaded similar to a cantilever beam. This loading condition could potentially create a large moment at the motor and consequently create losses within the motor's bearings. The problem was the team could not support the rotating shaft without adding at least one bearing. Any bearing that was added to the first fixture would not be accounted for in the second test, and thus would skew power loss data. Despite this issue, the team strongly favored concept #1 at this point. After reviewing the sketches with the team, Sam agreed that it looked to be the most

promising design, but expressed similar concerns about the unsupported motor shaft. He told the team he would review the design with other engineers at Specialized, while the meantime the group set about supporting the motor shaft with a coupled shaft system, shown below.

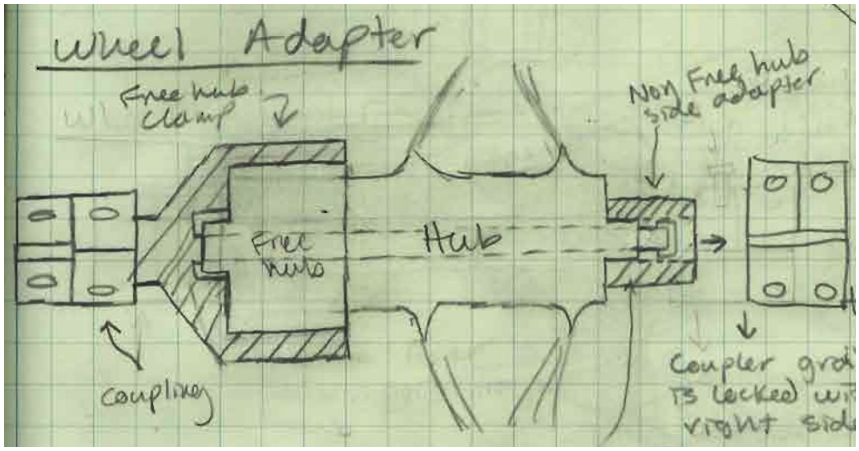

Figure 8. Coupled Shaft Design Detail

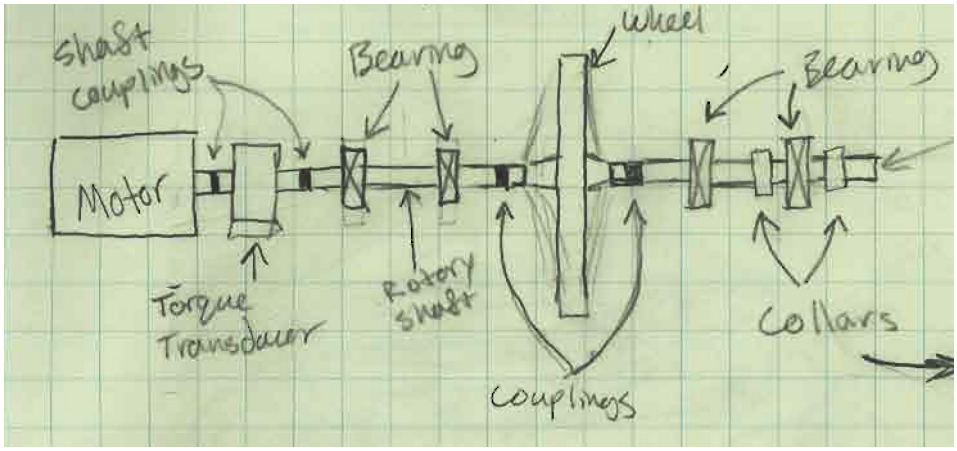

Figure 9. Coupled Shaft General Design

To solve the problem, the team designed a coupled shaft system to fit around the hub. The entire purpose of this mechanism was to add a bearing for support on the driving shaft and eliminate large moments at the motor. The team knew that adding this bearing would generate some unaccounted loss, but was willing to sacrifice a bit of accuracy in order to reach a plausible design. Sam, however, had immediate concerns when this design was presented to him. With so many couplers and intermediate pieces of shaft, he was worried that the design would be inconsistent and unreliable. To eliminate the loss created by the support bearing he suggested the team research air bearings. With almost frictionless bearings, the shaft could be supported and thus allow for precision

measurements. Sam also had feedback from other Specialized engineers about the first concept.

One main concern they had was that the first test was designed to hold the wheel on the free hub, and would not work for front wheels. Also, the chain load device was designed to fit over the entire free hub, and could not be moved side to side as a chain does on a rear cassette. Thus, the team received an extra requirement that the chain load device must be able to vary in location as well as apply a load to replicate more realistic bending of the axle. Additionally, some engineers were concerned that by running two separate tests in different fixtures, unaccounted for losses could be created. They suggested the team try to simplify the machine down to one single fixture.

Additional Preliminary Concepts

Two other initial concepts were developed simultaneously with the two-test fixture design utilizing the aforementioned regression and two-test methods described above. These concepts were also presented to the team sponsor where it was decided they had too many concerns to plausibly represent a solution for the final design. For the regression test method, there were was worry the concept would be unable to consistently separate orders of losses without excess variance between wheel set ups. Concept # 3, like the two-test fixture concept above, utilizes a two-step test enabling additional losses (i.e. rolling resistance, air drag, etc.) to be quantified and separated when calculating bearing loss. This test differs from the two-test concept in that in uses only one fixture. The test was designed this way to eliminate any additional variance that could occur when re-constraining the wheel for the second test. Though neither of these two preliminary concepts were chosen as a solution for the final design, they help represent the team's conceptual design methodology and were very useful in that features of both concepts were incorporated into the final design. The schematics for the two described tests represent this merging of features and can be seen in Appendix D.

Single Test Fixture with Rotating Dropouts

With all this in mind the team set about generating the next concept. At this point the team still planned on running two tests, but wanted to consolidate both to one fixture. The challenge was that in the first test the hub and axle were to be locked together and spun as a unit. The second test, however, was to be run on a fixed axle. The fixture would need to both spin and not spin. At first this sounded impossible, but through Sam's suggestion of air bearings the team was able to generate a working solution. The developed idea to support the axle on a pair of rotating dropout chips supported in air bearings is shown below.

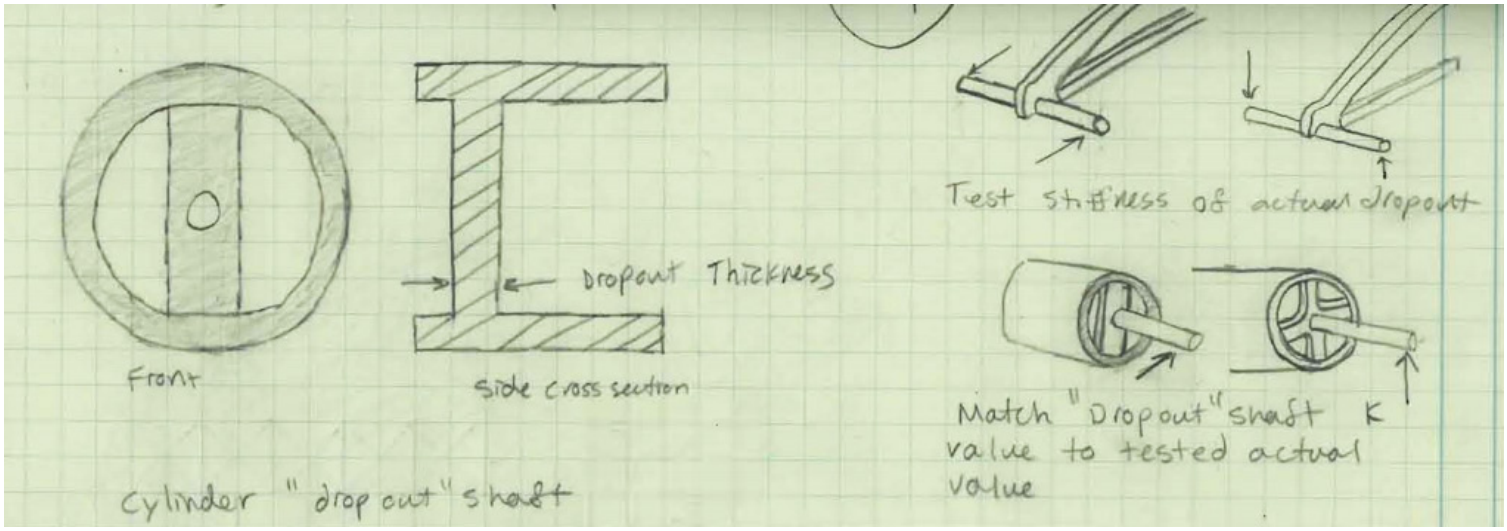

Figure 10. Rotating Dropout Chip Detail

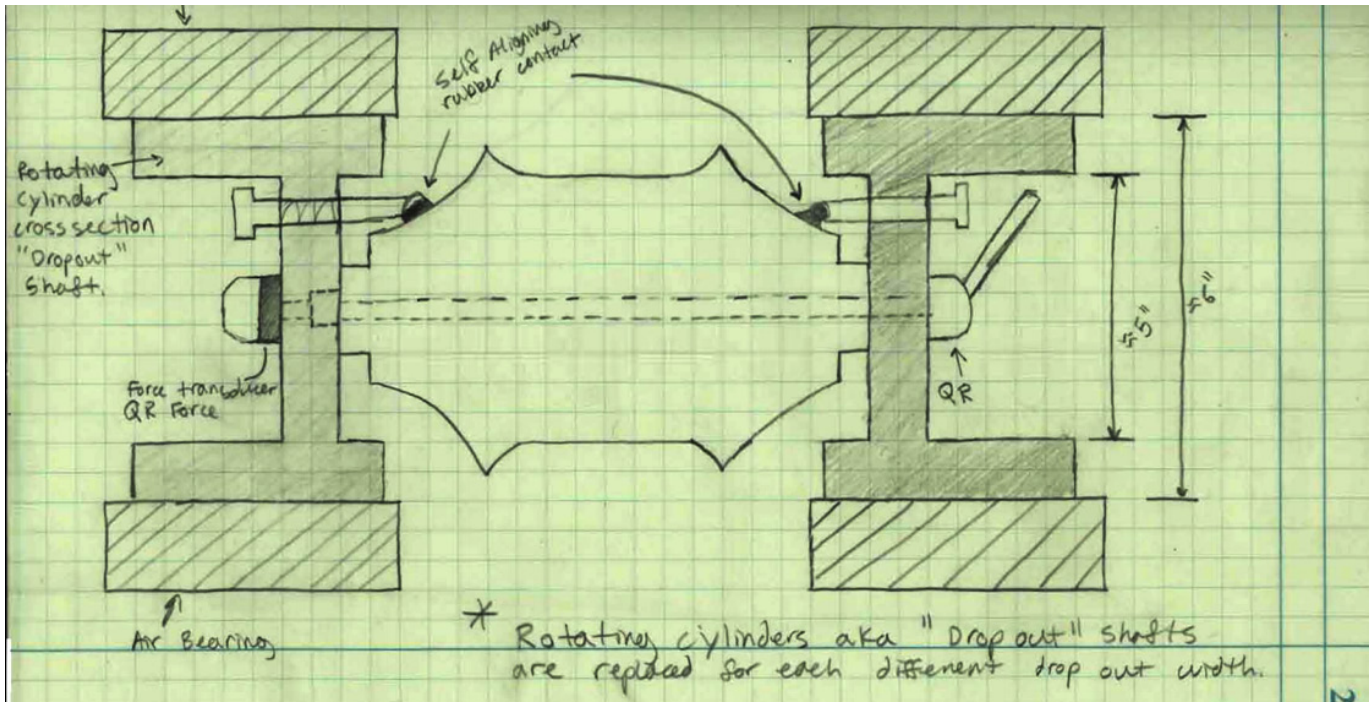

Figure 11. Dropout Chips within Air Bearing Detail

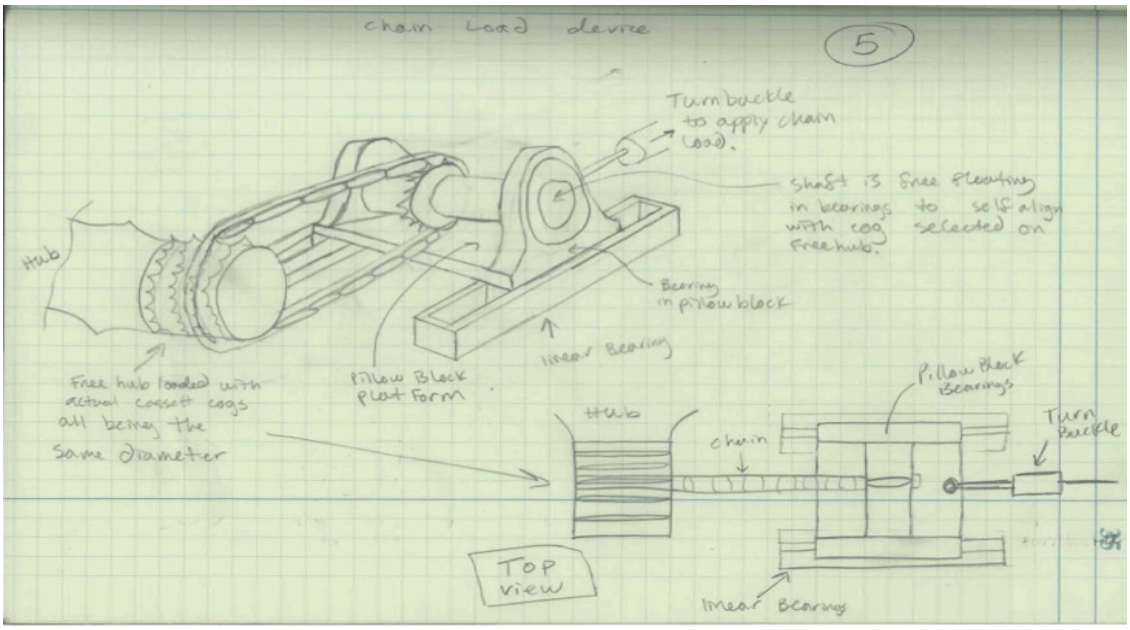

Figure 12. Chain loading device

The chain-loading device will use a standard bicycle chain connecting a custom cassette with all cogs being the same size to a single cog located on a shaft housed between two bearings in pillow blocks. This cassette allows variable placement of the load due to accurately placed industry standard cogs. A turnbuckle will apply a pulling force to the platform, which both pillow blocks are fastened to providing tension on the free hub.

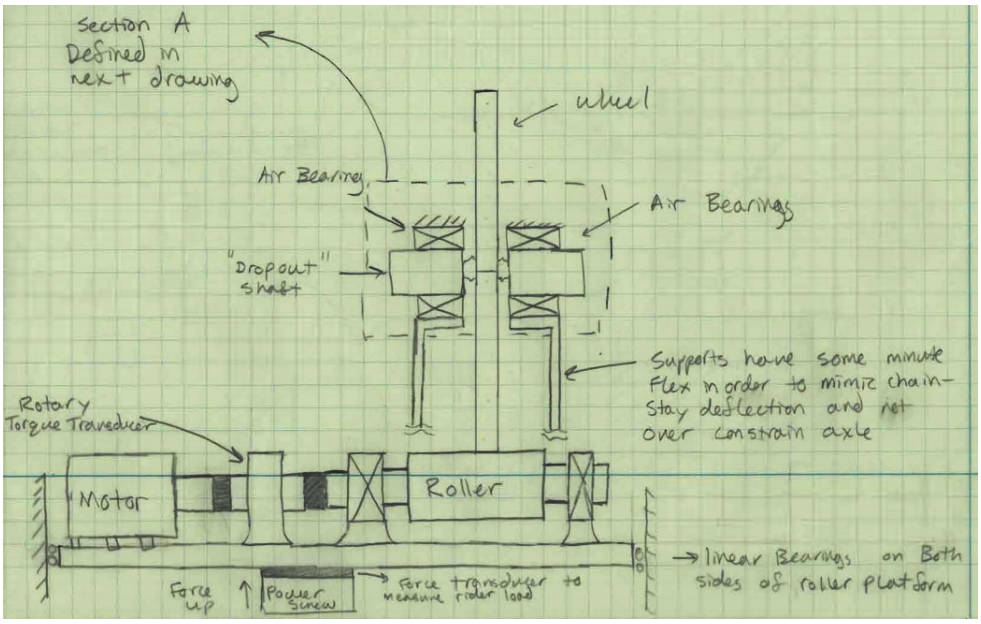

Figure 13. Air Bearing Design General

In one test, the hub and axle would be locked together and the whole unit would rotate within the bearings. Then, the hub and axle could simply be de-coupled and the dropout chips could be locked. With these chips locked in place the second test would be run on a stationary axle. The difference in power loss between the two tests would be due only to the hub bearings. Additional benefits of this design were that front and rear wheels could be tested with very little adjustment, and the loading conditions between tests would be identical since they would be run in the same fixture.

Spinning the Axle Concept

When discussing the most current design with Professor Mello, the variability of the loss measurements compared to the magnitude of the hub bearing losses was again brought up. In the team's discussion with Dr. Mello, the idea of rotating the axle instead of the wheel was revisited, the goal being to eliminate all discrepancies due to air drag and contact losses. This solution, the team decided, is ideal as the only losses measured by the dynamometer would be the bearings inside of the hub and the method of holding the axle steady (i.e. oversized support bearings).

This design can be adapted from the previous concept, which used rotational dropouts to mimic the stiffness of the dropouts while being secured to the axle in the same way the wheel is secured to a frame. Even though the losses of the other bearings aside from the hub are present, they will be constant from test to test and over-designing these bearings should allow for minimal power losses. This test setup will allow for significantly reduced variance in dynamometer power readings during the experiment as the largest loss during the wheel's usual operation, aerodynamic drag, is not present. This method also makes the fabrication process much simpler due to having an assembly of less moving parts and not having to deal with the alignment of a wheel on a roller since the rim can be set into a stationary holder and locked down. The same method for providing rider load with a power screw can be applied, with the load forcing the stationary holder upwards towards the hub assembly.

The only concern with this test setup is the ability of the rotational dropouts to mimic the actual dropout stiffness of a bicycle frame. The difference between this setup and the previous iteration is that the rotational dropout is always spinning therefore forcing the stiffness to be uniform instead of varying in the vertical and horizontal directions. This uniform stiffness can still be varied with additional dropouts to accommodate the small, medium, and large stiffness's desired for the machine.

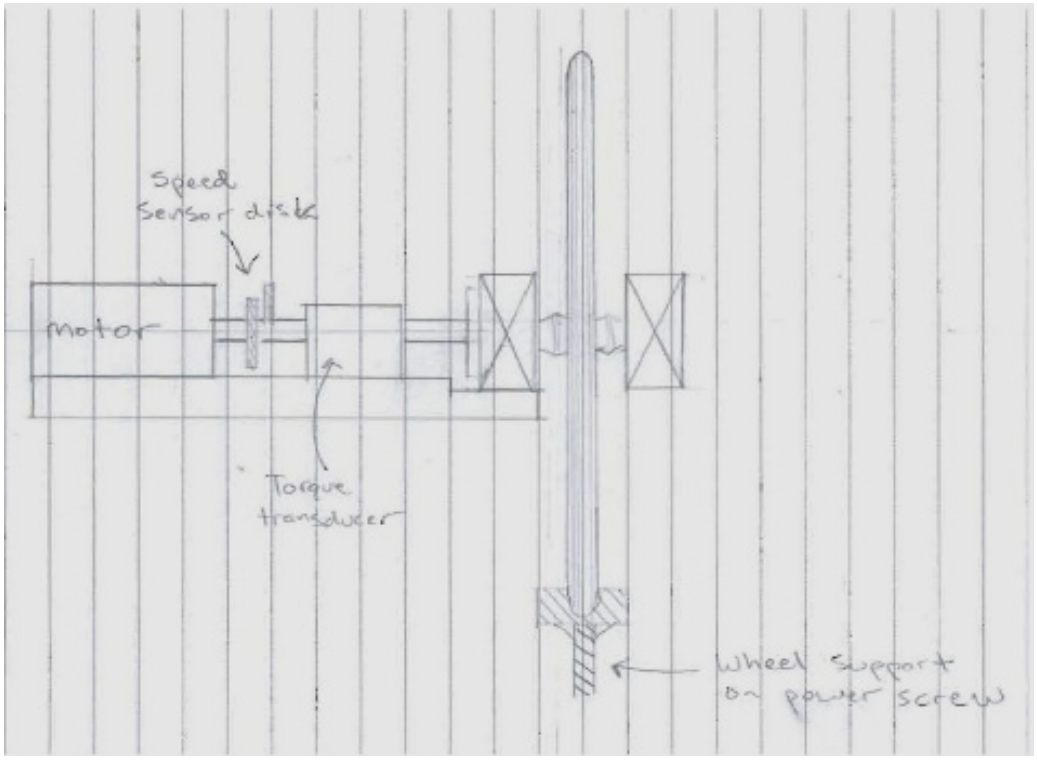

Figure 14. Spinning Axle Design

The spinning axle design uses the same method of attaching the hub to the rotating dropouts as seen in Figure 11. The difference in this setup is that the test is only run once, with the axle spinning with the rotating dropouts.

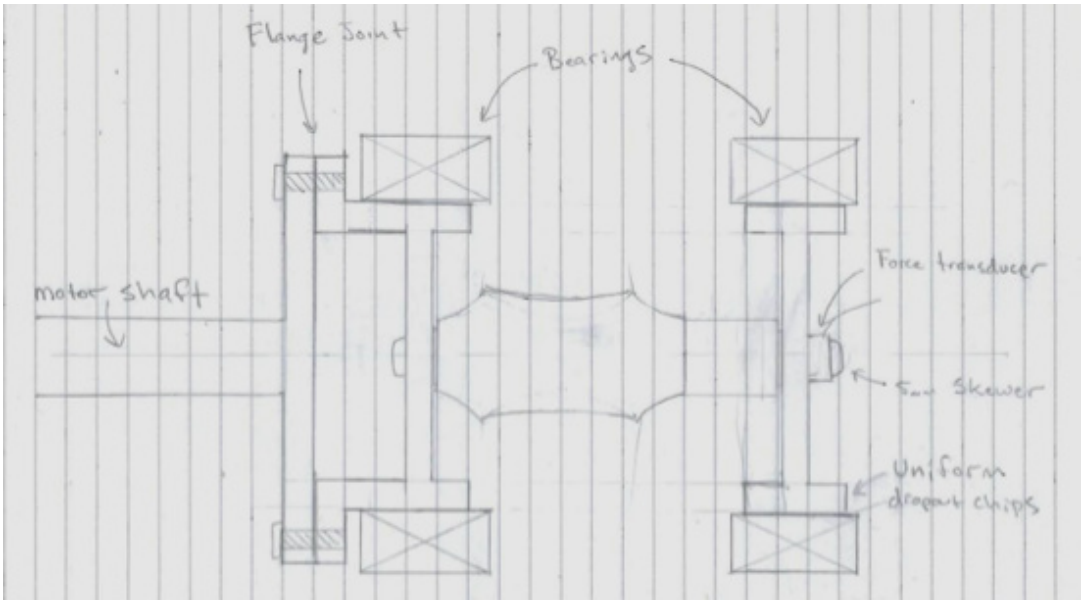

Figure 15. Motor shaft flange adapter connected to rotating dropouts.

Since the hub is locked, the flange adapter on the motor shaft turns the rotating dropouts and axle as one unit, allowing the rider load and chain loading devices to apply forces to the hub bearings.

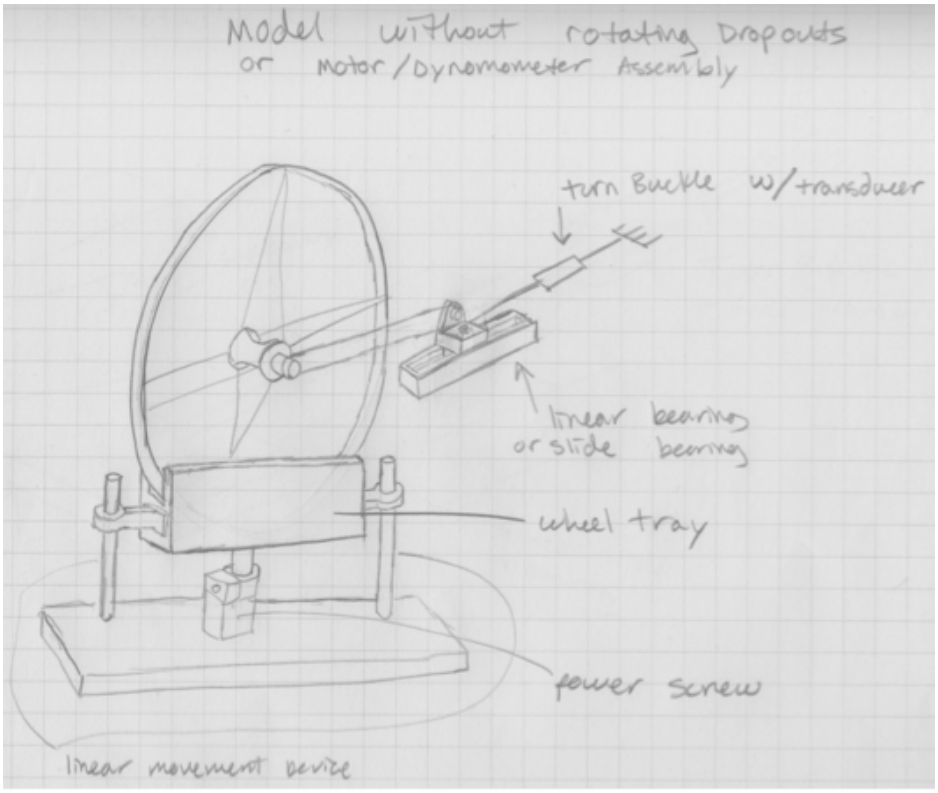

Figure 16. General rider load and chain loading devices

The rider load will be applied using a wheel tray to apply pressure to the rim, which is actuated by a power screw. The wheel tray will move vertically along a linear slide or bearing.

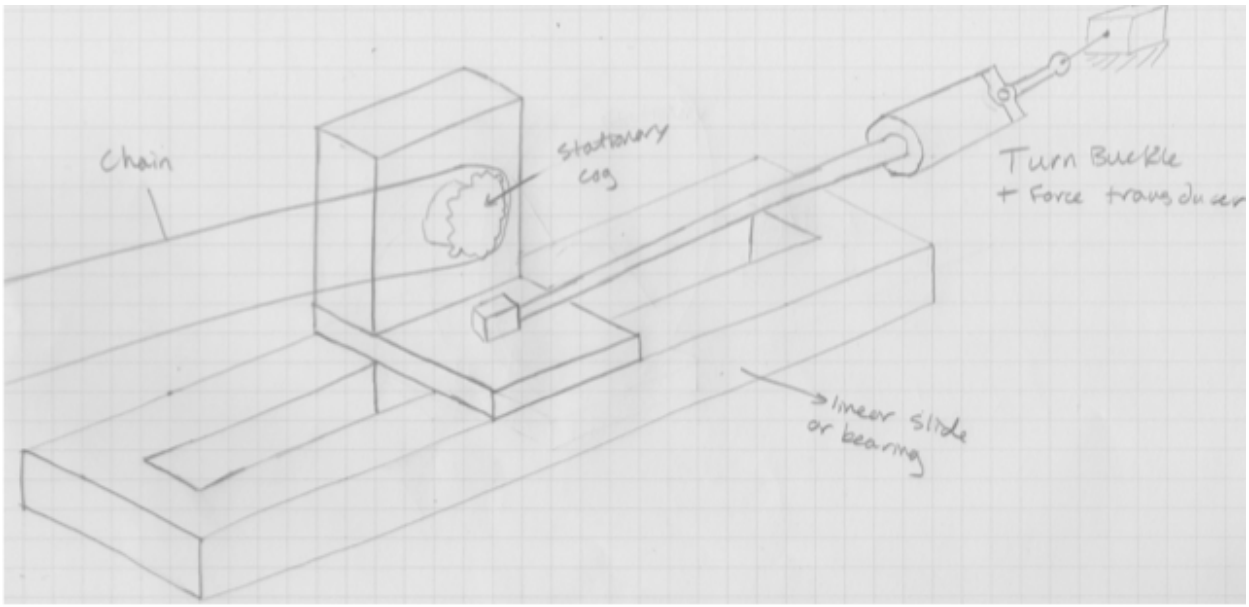

Figure 17. Detail view of idea for chain loading device

The chain-loading device will be actuated by a turnbuckle applying a tensional force to the custom cassette shown in Figure 12. This idea can be completed with or without the use of a linear bearing. Without a linear bearing the cog would be suspended in free air until pulled tight by the turnbuckle.

With respect to the minimal amount of moving parts and the decreased number of losses to account for, it was concluded the spinning axle design is by far the most feasible and accurate conceptual design.

Initial Cost Analysis and Considerations

With a decision made on a conceptual design, the team can now research the price of all individual components to obtain an estimate of the project's total cost. Table 2 below represents this research and shows a large variability in final costs dependent on the choice of support bearings to house the rotating dropouts. As mentioned in the conceptual design section, this choice of using low friction air or magnetic bearings over more-common roller bearings will depend on the other costs associated with fabricating the machine. Not accounted for in Table 2 is the total time required by the three group members to create and develop the test machine. In industry, the cost associated with the amount of hours worked on a year-long project would be quite substantial and would most likely dwarf the cost estimates below.

Table 2. Cost estimates of machine componentry

Motor	$ 200
Speed Sensor	$ 150
Torque Transducer	$ 500
Shaft	$ 60
Bearings	$300-4000
Structure	$300
Load Cells (x3)	$2000
Misc. (dropout chip material, wheel support)	$200
Power Screw	$50

Total Estimated Cost= $3750-7500

Final Design

Design Layout

The overall layout of the final design can be seen below in Figure 18. The machine consists of a square flat table with a slot cut for the wheel to fit into. On either side of the slot sits two bearings housed in machined blocks. Both bearings have concentric locking collars built into the inner race in order to fix the dropout chips into each bearing. The locking collars allow the operator to easily remove and replace the individual dropout chips to vary dropout stiffnesses between tests. The pillow block opposite the motor is attached to an adjustable slide thus allowing for a variety of hub widths. The motor-side bearing is placed on a block to account for the height added by the linear slide. The motor shaft runs in line with the bearing centers, and attaches to the motor-side dropout chip by means of a flange. A helical spring coupler exists between the motor and flange adapter to accommodate for any possible shaft misalignment. The motor itself is housed between two bearings in pillow blocks to allow for free rotation about the drive shaft's axis. These pillow blocks are similarly mounted on a block to accommodate for additional height from the linear slide. A torque arm extends from the face of the motor and rests on an ultra-precision compressional load cell for power measurement. Two power screw jacks actuate the rider and chain loads. The chain load jack is placed in line with the pulley, and will be used in tension. The rider load jack sits on a platform under the table and will be loaded in compression. The chain load mechanism contains and s-type load cell, and the rider load uses a pancake-style cell for load measurement. All three load cells feed into a digital acquisition system and sent to a computer via USB for display. The motor speed is controlled by an analog voltage signal from the computer, and can be configured in Labview.

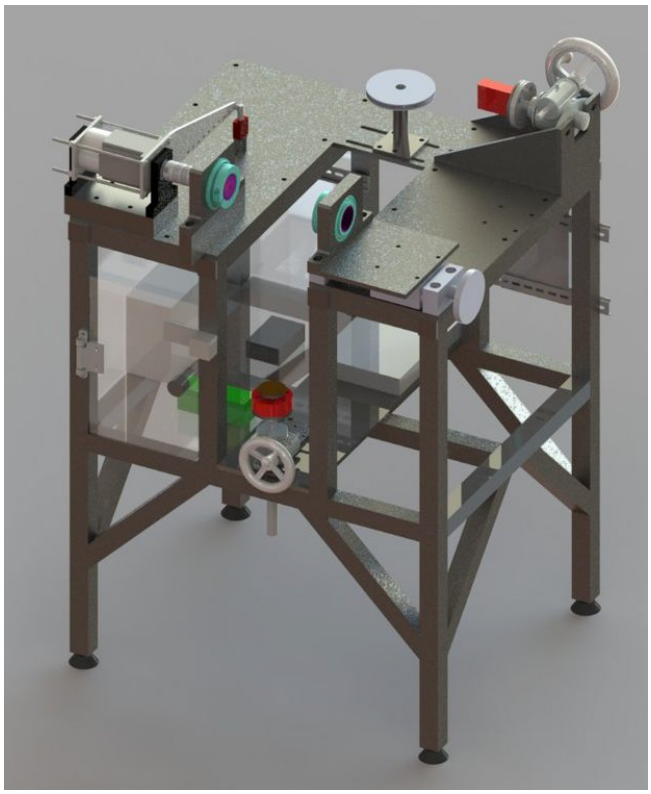

Figure 18. Test Machine Assembly

Procedure

In order to test a wheel, the operator must first install the desired dropout chips into the bearings. On the motor side, the chip will be secured to the motor shaft flange and locked within the collar of the bearing. The wheel will then be placed into the wheel tray on the lower screw jack, and raised to be concentric with the dropout chips. The operator will then adjust the linear slide so the dropouts sit flush with either side of the hub. A skewer will be run through the whole assembly, and pick up the nut housed behind the motor-side dropout chip. Once the skewer has been secured to the desired load, the chain and rider loads can be actuated by adjusting each power screw jack until the desired forces are read by the load cells. With the wheel fully locked and loaded, the test can begin. The motor speed profile for the test will be fed into the motor from the computer, and the shaft will spin the dropout chip and axle assembly as a unit. The reaction from the friction within the hub will cause the motor to spin, and place a force on the torque arm load cell. The computer will take the reading from the load cell, along with the torque arm distance and speed measurement, and calculate power required to spin the axle.

Final Design Componentry

Rotating-Dropout Positioning Mechanism

A manual-positioning slide provides the best option for consistent and simple movement of the rotating dropout to allow for different hub sizes. This industrial product features high load capacity and solid construction, which is suitable to the application required within the test machine. Forgoing electronic and hydraulic powered alternatives keeps the slide within the given budget while still providing a precise method of moving the dropout. The simplest solution to this problem would have been to outfit the test plate with slots. This would allow bolts to be loosened and the pillow block moved in line with the slots. This solution caused concern due to the accuracy of machining slots given equipment available and the possibility of misalignment disrupting the machine's required accuracy. The Generic Slides MS400 was chosen because of its robust shaft construction when compared to similarly priced options. This style of slide is more desirable than a dovetail type slide because of its ability to withstand forces from all directions, whereas a dovetail slide can only withstand proficient loading from the top down. This is a vital requirement due to the fact that the load applied to the slide is from the bottom up as simulated by the rider load. The MS400 is priced affordably when considering the budget and can be easily mounted to the test table and pillow block bearings with manufacturer machined mounting holes. The MS400 features an aluminum slider, which creates concerns over fatigue and wear when compared to the test stand's stronger steel components. The concern over Aluminum degradation over time is negligible in this application due to the use of a steel adapter plate which allows the Aluminum plate to be left assembled over long periods of time. The steel slider option also doubles the cost of the MS400, which is undesirable given the project budget.

Load-actuating Systems

To apply both the rider and chain load forces, a device was required that would provide an accurate and easily adjustable static force load on the bicycle wheel. Considering the simplest solution, a turnbuckle, would provide a static force but may be hard to accurately adjust as well as not having the ability to be automated. To best meet predefined requirements it was decided to use machine screw jacks to actuate forces to the wheel. Screw jacks are very customizable, allowing the selection of the desired load capacity and required travel for each application. Joyce Dayton was selected for the manufacturer of the needed screw jacks due to the availability of solid modeling information and the modular upgradeability of each jack. The initial units can be purchased with varying sized hand wheels to manually apply the load with 20:1 worm gear ratios providing accurate load distribution. These jacks are fully functional in the vertical and horizontal position, as well as rated for loads in tension and compression. By nature, the screw jacks are self-locking and thus negate possible concerns over

backlash. To apply the chain load force the Joyce Dayton WJ201 was selected with a one-ton load capability, 2” of travel, and a 20:1 worm gear ratio. For the rider load, the W250 was selected with a ¼ ton load capability and a 5:1 worm gear ratio. Both of these screw jacks meet the required loading conditions specified in the engineering requirements and can be upgraded with a motor/encoder assembly to automate the loading process. Initially the screw jacks will be actuated manually via hand wheels. Two angle plates will be used to mount the WJ201 horizontally, with a 4 hole-mounting pattern to fasten the plates to the table-top.

Table –top Design

The surface for the test machine was designed to keep relative flatness as accurate as possible. Therefore, one steel plate will serve as the table-top with a slot machined down the middle to allow for placement of the wheel. This design eliminates the need to exactly align separately-machined sides. Steel was chosen as the table-top’s material to preserve test facility cleanliness conditions as well as its low cost and high durability over an extended period of time. Low carbon A36 Steel will be used due to its combination of relatively-low cost, sound structural properties (i.e. high tensile strength), and ability to be applied in nearly all material fabrication processes. The use of mounting blocks to fasten the pillow block assemblies to the plate allows for the use of shimming materials to provide level bearing alignment. This eliminates the need to precision grind the surface of the plate. The wheel slot will be reinforced on each side with square tubing bolted to the table-top surface to provide structural support in the direction of the chain load.

The remaining material used for the completion of the test stand will be composed of the same A36 steel, with multiple areas using ¼ in thick plating and the structure composed of 1.5” x 1.5” x 3/16” square tubing. The welded frame assembly will be a separate unit from the table-top and bolted to the table top to complete the test stand assembly.

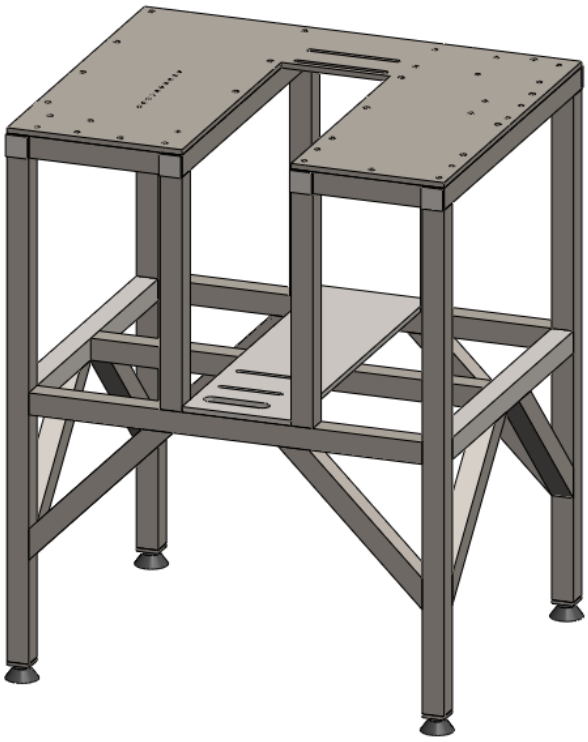

Figure 19. Machine Table Design

Bearing Selection

The two driving factors in bearing selection were the ability to lock the dropout chips within the inner race, and the lowest possible power loss. The first bearing types considered for the machine were non-contact bearings, including air, magnetic and hydrodynamic bearings. These bearing types boast the lowest frictional losses, but were quickly abandoned due to excessive cost and complexity. Hydrodynamic bearings were also found to have an unacceptably high uncertainty in power loss based on factors such as temperature, which would vary between tests (Appendix H). The next type considered were ceramic ball bearings, which perform a bit better than steel bearings for the specified requirements. The main benefits to ceramic bearings include lower friction than steel and relatively long life in dry conditions. Unfortunately there are no available distributors that offer ceramic bearings with concentric locking collar s within the price range of the project. This led to the decision to use relatively large-bore steel ball bearings mounted in pillow blocks.

There are a variety of companies that offer concentric locking collar steel ball bearings within the desired size range. These include AMI, FYH, Timken, Dodge and many others. AMI Bearings Inc. was found to have the most readily available distribution,

price information, and solid models. The SUE210 Model was selected for use in the machine due to appropriate bore size and locking mechanism, and a price within the pre-described limits. These bearings come housed in cast-iron pillow blocks, and will be run either entirely dry or with a thin oil to minimize frictional losses. As stated previously, preliminary calculations through SKF predict that losses from these bearings will not overshadow hub frictional losses, and will allow for viable comparison between hub/axle assemblies. A picture of the selected bearing can be found below.

Figure 20. AMI SUE210 Concentric Locking Collar Bearing

Dropout Chip Development

Under normal conditions a bike wheel is secured between stationary dropouts. This setup holds the axle stationary to these dropouts and allows the hub to rotate freely around this axis. This configuration, however, would require the wheel to spin and generate a large amount of power loss due to aerodynamic drag. It would also require a support roller to spin along with the wheel which would provide associated power losses as well. For the design to match the required precision outlined by the sponsor, it made sense to eliminate these losses and focus the test more finely on the hub bearings themselves. To accomplish this, the decision was made to eliminate wheel rotation and instead spin the axle within a stationary hub. This design, however, required the development of a method to secure the axle between dropouts capable of spinning along with the axle. This led to the creation of rotating dropout chips.
The dropout chip design was fueled by two requirements; the ability to be locked into the inner race of a bearing, and accurate replication of stiffness at the dropouts. To fulfill the first requirement, the dropout chips will be milled to a consistent outside diameter matching the bore of the two bearings. The chips will be slid into the inner race of the bearings, and secured through a setscrew on the locking collar. In order to replicate

boundary condition stiffness for the axle, the dropout chips will be milled to a certain face width. By testing the dropout stiffness of a variety of frames we will be able to define ranges of stiffness to be modeled by the dropout chips. The face width of these chips will then be determined through FEA analysis to match the stiffness ranges defined by the tests. A section view of the dropout design can be found below.

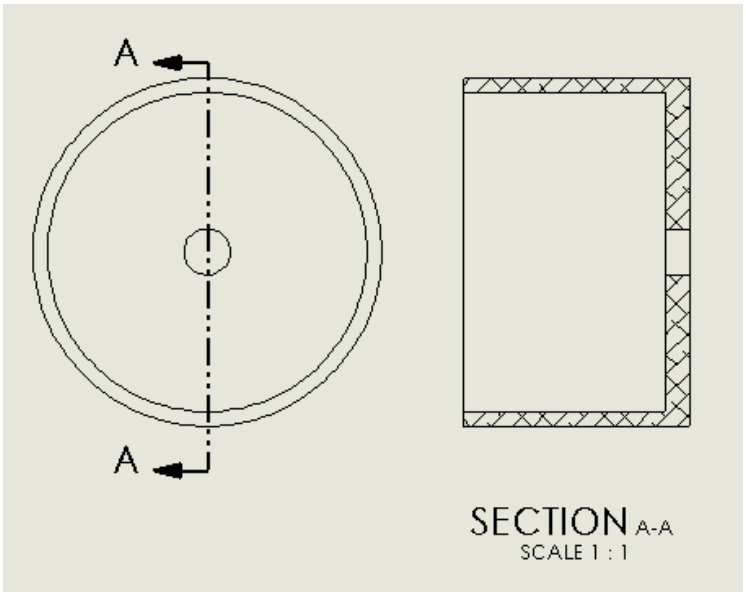

Figure 21. Dropout Chip Sectional View

An additional requirement for the drive-side dropout chip is the need to secure to the motor shaft. This connection will allow the motor to drive the dropout chip, and consequently the axle within the hub. A section view of the drive-side dropout can be found below.

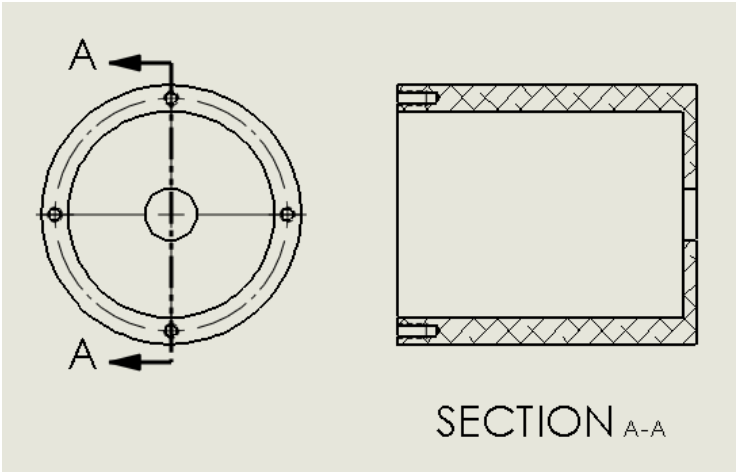

Figure 22. Drive-Side Dropout Section View

Motor Control and DAQ Subsystem

As previously stated, wheel speed is the driving factor in determining power loss in a bicycle system. Even when isolating and removing major losses occurring at the wheels (i.e. air resistance, road contact), the remaining power lost due to bearing friction is significant enough to determine the difference between winning and losing a race. As this loss is linearly proportional to speed, it becomes increasingly important in determining power loss to control wheel speed as accurately as possible. As such, selecting proper speed control and data acquisition (DAQ) instruments is vital to the accuracy of the chosen test concept.

Motor Selection

Three main parameters are used in selecting an electric motor: required accuracy, angular speed, and torque. Based on the sponsor given speed accuracy requirement (2 mm at 5 km/hr), it was found that servo motors, motors with built-in high-precision position, velocity, and torque control, would represent the simplest, most cost-efficient solution. DC motors and other basic electric motor types (i.e. AC motors), though cheaper as a single component, require the purchasing and constructing of a “custom solution” where each system component (motor drive, cables, controller, etc.) must be specified individually. Furthermore, these alternative solutions offer much wider accuracy tolerances compared to servo control systems, which are rated to within 0.1 %. Servo systems, however, are offered in complete packages that can be quickly implemented with PC configuration software and DAQ/graphical user interface (GUI) programs (i.e. Labview, Simulink). With this in mind, the search for servo packages meeting the accuracy requirement began and included companies such as Omega, Anaheim Automation, Parker, Automation Direct, and Allen-Bradley. Due to group familiarity and prior success with Automation Direct (ADC) as well as their extensive catalog offering better prices than their competitors (see Cost Analysis), ADC’s Sureservo represented the best combination of parameters for the machine.

After selecting a vendor, it then becomes necessary to find the motor offering the system’s required speed and torque within its rated values. To do so requires the use of statics and material properties to define said torque. This was done through use of several conservative assumptions made for calculating system component mass moments of inertia (i.e. density, material) in conjunction with published vendor data. Combining these values with the system’s needed angular acceleration (0-300 rpm in 5 sec) allowed the system’s running torque to be determined as ~1.25 N-m. This value is

largely driven by torque needed to overcome friction occurring in the bearings housing the rotating dropouts and was calculated using SKF's frictional moment calculator with the bearings running at top speed (270 rpm) under full load (5200 N radial load, 3200 N axial load). In order to ensure a motor with sufficient power would be selected and to add factors of safety into the machine, SKF's calculated value for starting torque was used rather than the calculated value for running torque. As starting torque is much greater than the bearing's running frictional torque, using the value for starting torque ensures the motor can drive the system at full load without danger of the motor overheating or stalling.

Through use of Sureservo's published torque-speed curves, the motor needed to meet the running torque requirement was found to be the SV-207. This motor's rated power output (750 W) is far more than the necessary power needed for the system (~40 W); however, this motor is needed to meet the system's torque requirement. A smaller motor could've been used through the implementation of a servo reducer, which is a very precise variable gear reduction made specifically for servo applications. The reducer would've allowed the motor to run at rated values for speed (3000 rpm) and torque (2.2 N-m). Though this would have resulted in a cheaper, more energy efficient solution, there are several obstacles preventing the use of a reducer. These obstacles include adding power losses to the system as well as increased complexity and inaccuracy to the torque measurement used to calculate bearing power loss.

Motor Control System Enclosure

In order for the system to fully comply with all relevant electrical codes (i.e. NEMA, UL), the lower level of the support frame was used to mount all system electrical components and the wire/cabling connecting them within a lockable enclosure made of 1/8" acrylic paneling. Designing this enclosure involved determining the best arrangement of components given constraints imposed on the system by factors such as required spacing/ventilation as well as given wire length. The components housed within the enclosure include the motor drive and ZipLINK communication board, the load cell power supply and data acquisition system, as well as two disconnect switches mounted on 35-mm DIN Rail on the frame exterior allowing for system power to be immediately shut off in an emergency. Construction of this stage began upon the frame assembly's completion and required thorough research into all system component specifications (i.e. voltage, amperage, etc.) so that the machine posed minimal hazard in a laboratory setting. This involved researching the required cable, wire, and fuse sizes as well as how to properly route and connect them between the machine's mounted components (see Appendix G). Upon completion of this fabrication stage, the system can finally be ran and optimized to meet all required specifications and engineering targets. Refer to

the Design Verification Plan Section below for further detail into the testing/tuning of system electrical components.

Torque-Arm Assembly

As seen in the top-level system schematic, the motor is interfaced with a torque arm with a cylindrical extrusion mounted in between two pillow block bearings. This mounting procedure ensures the motor is able to freely rotate about the shaft's axis of rotation without introducing extra losses into the system, a key requirement to accurately determine torque and thus, power. When in operation, the long side of torque arm contacts a load cell which reads the reaction force needed to hold the arm horizontal; at zero speed, the balance weight on the short side keeps the arm horizontal. The reasoning for these design parameters is specified below in the Power Measurement Method section. The cylindrical sections extruded from arm base and the back plate have their outer surfaces pressed against the inner races of the pillow block bearings while the inner surface of the arm extrusion is dimensioned to allow clearance for the motor shaft to rotate.

MiSUMi-USA's T-Shaped Retained Bearing Base Mount was selected for the pillow blocks due to the vendor's good standing with Cal Poly, their extremely-competitive pricing and shipping times, and most importantly, their ability to handle custom orders with no additional cost. MiSUMi's website provides an instant computer-aided design (CAD) configurator which allows the precise implementation of a product's dimensions into a system design. For the test stand design, the only parameter needed to be configured was the precise location of the pillow block bearing's axis as concentricity is critical to producing an accurate power measurement. This requirement made defining a custom height for the bearing's axis necessary as the outer surface of the base plate and torque arm's cylindrical extrusions were designed to fit common bearing bore sizes. The exact values for these dimensions can be seen in the detail drawings section of the Appendices.

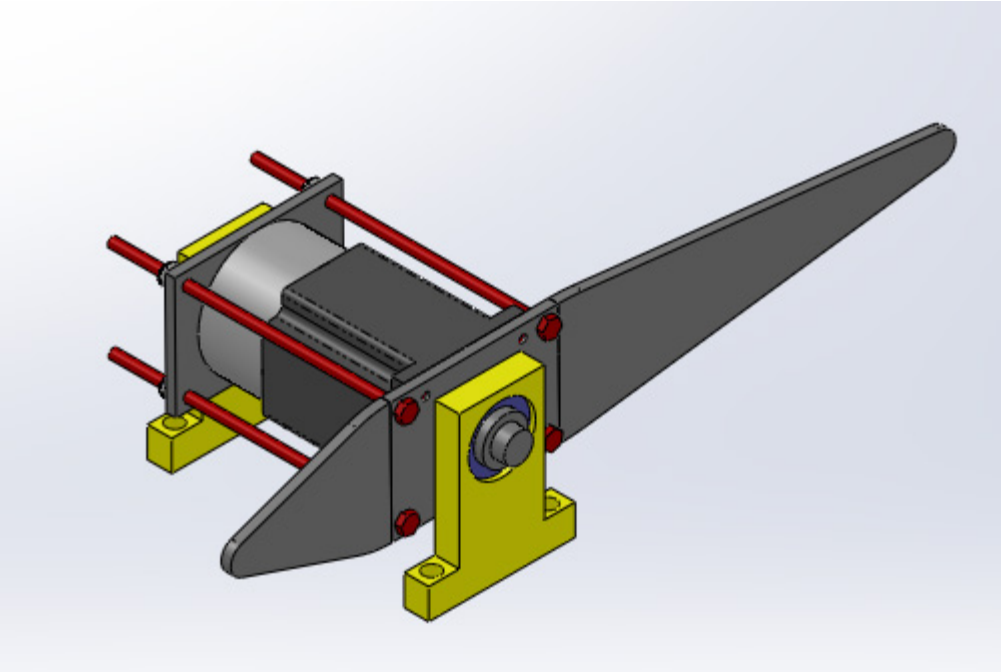

Figure 23. Torque Arm Assembly

Coupler Selection

In order for the shaft to accurately transmit power and speed to the driven axle and to account for possible misalignment between shafts under load, a flexible coupling is needed. Three coupling models were found fulfilling these requirements, the Bellows/helical coupler, the Oldham coupler, and the U-Joint or Cardan coupler. Due to the Oldham and Cardan's considerable mass/inertia, reliance on properly-lubricated joints, higher backlash, and smaller allowance for misalignment, it was decided that a Bellows type coupler would represent the best solution. A Bellows coupler is essentially a three-piece helical coupling with additional material removed between shaft interfaces. This three-piece construction allows larger parallel misalignment while maintaining comparable torsional rigidity. This coupling will be used to connect the motor shaft to the shaft driving the axle and was selected by defining the shafts' outer diameter as well as the transmitted torque and speed. With torque, speed, and motor shaft size already determined via the motor selection process, the only parameter left undefined was the driven shaft size. Using DE-Goodman Criteria for fatigue life and conservatively modeling the shaft as loaded in pure torsion, the required shaft size was found to 21.2 mm. With this size defined, Helical Products Company Inc. was approached due to their past friendliness toward Cal Poly ME senior project groups. Giving them the aforementioned parameters allowed for them to specify and provide their WAC50-19mm-19mm model at minimal cost. (Richard G. Budynas, 2011)

Load Cell and Data Acquisition Instrument Selection

Four main parameters play a factor in selecting the proper load cell: cell type, load range, linearity over said range, and cost. As all parameters are inter-related, each must be weighed in analyzing a cell's rated values and method of measurement. Load cells can measure both compressive and tensile forces with most being strain gauge based instruments using a Wheatstone bridge circuit to measure changes of resistance within the gauges. Other, less common cell types use hydraulic, pneumatic, and/or piezo-resistive methods to convert their measured force into a voltage signal. In more exotic cases, fiber optics can also be used as a transduction method. Given their high accuracy-to-cost ratio and due to sponsor guidance toward using an "S-type" transducer, Transducer Technique's SBO Series was selected as the chosen model for the chain load measurement. The SBO series is the ideal solution given the cost restraints as it provides an accurate, calibratable signal in both compression and tension while being easily interfaced with other system components. The ability to measure tension was especially important in the case of cells used in conjunction the chain loading device as this is the only type of force a chain can experience in operation. The two other load cells selected are also produced by transducer techniques. The rider load will be measured by an LPU series pancake-style load cell. An S-type cell was considered for this measurement, but the LPU series was chosen for its low profile geometry and through-hole bolt mounting system. The SBO series cell was simply too tall and required a complex loading mechanism. For torque arm force measurement an MDB series precision load cell was selected. The torque loads from the hub bearings are expected to be relatively small, and will require a low-capacity load cell. The MDB series provided the proper balance between precision and load capacity for our requirements.

With the load cells properly selected, a means of sending signals to and from a PC needs to be defined. Two options for this method of collecting data from the specified measurement instruments were defined by the inclusion or exclusion of a signal conditioner. This instrument represents a single assembly used to both amplify the cell's transduced signal into a larger voltage and convert said signal into a filtered, digital output. Prior to sponsor input, Vishay's D4 DAQ Conditioner was specified as the most cost-effective way to acquire data from multiple sources. However, using the D4 would necessitate the purchase of an additional controller should the loading mechanisms need to be automated. Because of this, National Instrument's X Series Data Acquisition line of multifunction devices was suggested as a non-signal conditioning solution that could also send and control signals to both the motor and load actuators. An additional benefit of the X Series is that its USB interface allows for efficient computer and GUI-program set-up. One caveat of not using a signal conditioner, however, is the purchase of an additional 10 V power supply as well as the increased importance for proper

grounding. A detailed system signal flow diagram showing how data is acquired can be found in Appendix E.

Power Measurement Method

By interfacing the motor with a torque arm and allowing the assembly to freely rotate about the shaft's axis, the motor can effectively be converted into a driven dynamometer. This type of dyno-torque arm assembly used with a rotation-constraining load cell is analogous to a brake dynamometer's balancing torque arm as the methods for calculating power are essentially the same. However, as opposed to applying a variable brake pressure on the shaft to balance the moment of the torque arm's suspended weight (see Figure 24), the designed driven dyno will use a load cell to hold the torque arm in a horizontal position. The use of the torque arm assemblys' balancing weights are also analogous, with the brake dyno using the weight to keep the arm horizontal in operation and the driven dyno using the weight to hold the torque arm horizontal at zero speed. It is necessary for the driven dyno to function in this manner as it prevents the arm's weight to be factored into the load cell's force reading. With the known weight hung from the brake dyno torque arm and the measured reaction force at the driven dyno's load cell, the torque for each can be calculated knowing the horizontal distance to the weight or load cell. From here, power is easily computed through accurate control of the shaft's angular speed. The schematics below show this process of balancing the torques on the shaft in order to calculate power.

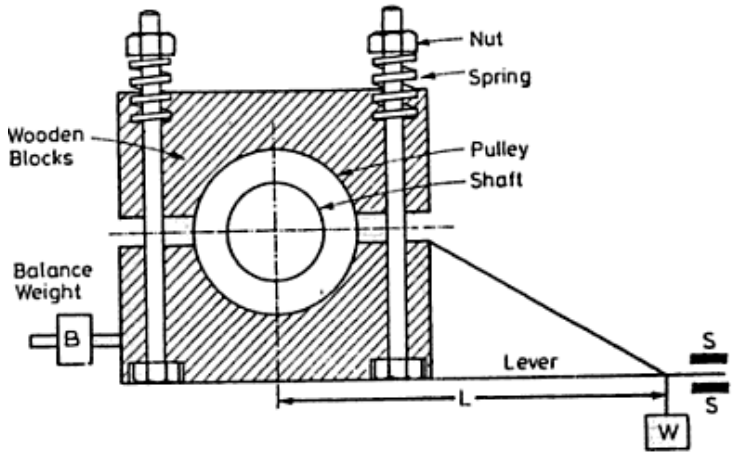

Figure 24. Proney Brake Absorption Dynamometer for measuring power (J. S. Brar, 2004).

Cost Analysis

As stated before, product and material costs are a driving factor in selecting a particular catalog item. The ultimate decision on a particular component, however, represented the best balance of cost, assembly efficiency, previous experience with a particular vendor, etc. The following table summarizes estimated costs for each component. These figures are based on listed prices and quotes from the vendors, and have been inflated to account for extra costs from tax and shipping.

Table 3. Cost Analysis

Motor and Control System	$1,500
Load Cells	$1,200
DAQ	$1,500
Power Screw Jacks	$1,000
Building Materials/ Labor	$1,850
Linear Slide	$600
Bearings (concentric locking collar)	$250
Bearings (motor)	$100
Total	$8000

Safety and Maintenance Considerations

When dealing with rotating machinery there must always be safety precautions taken to prevent user injury. Exposed rotational equipment on this machine is limited to the helical spring coupler between the motor and flanged dropout. All other rotational components are housed either in bearings or within the hub itself. Currently this exposure is considered within safe limits, but in the future the team will consider adding a plastic guard around the coupler for additional safety.

There are few maintenance concerns for the machine, barring unpredicted failures that may occur. The dropout bearings will need to be monitored closely since they will be run either dry or lightly oiled. To ensure maximum life and efficient performance these will

need to be checked regularly and cleaned or oiled when necessary. Additionally, the load cells may need occasional calibration for accurate force measurement.

Machine Fabrication and Final Performance

Frame and Indexing

The first step of fabrication was to get the top plate, bottom plate, and all other small parts cut and indexed. This was accomplished using water jet machining, which provided for accurate hole alignment as well as minimal distortion of the material during the cutting process. The frame for the test machine is constructed out of ASTM A36 steel. Fifty eight inches of 3/16" wall thickness, 1.5"x 1.5" square tubing was used to complete the structural support for the bottom and top plates which support each component. The square tubing and bottom plate were joined using gas metal arc welding (MIG) to ensure a secure and non-flexing support. The top plate is fastened to the frame by through bolts to allow for shimming and to avoid the distortion that would occur with welding the top plate to the frame. Each leg of the frame is equipped with a load leveling vibration isolator to allow for a level table surface as well as dampening any errant vibrations. The top plate and all other adapter plates were drilled and tapped to provide the threads for fastening components directly to the table.

Sub-assemblies

The rider load assembly is composed of three adapter plates; two which space and fasten the screw jack to the bottom plate, and one that connects the LPU 250 load cell to the screw jack. The load is applied to the cell by a custom machined loading plate which was fabricated from aluminum round stock using a lathe to machine the profile and a die to cut the threads which interface with the load cell.

The chain load assembly is mounted to the table through the screw jack mount. The mount is assembled from four 3/8" thick plates which were cut during the water jet process. These plates were welded together using gas tungsten arc welding (TIG). An adapter plate fastens the S type load cell to the screw jack which in turn tensions the chain loading mechanism.

The non-drive dropout side uses an adapter plate to join the pillow block to the linear slide allowing for adjustable hub width. The pillow blocks were CNC machined out of ASTM A36 steel to in order to eliminate any self-aligning attributes. The bearings were press fit into these pillow blocks to force all misalignment to occur in the dropout faces. The drive side pillow block is mounted to the table plate by an aluminum mounting block

which was machined to set the pillow blocks in the same horizontal plane.

The motor pillow blocks are also mounted on an aluminum block to concentrically align the motor spindle with the bearing bores. The torque arm was constructed from one 1/4" thick plate and a CNC machined motor adapter which allows the motor to rest freely inside of the pillow block bearings. The motor adapter and the plate were TIG welded together. The torque arm is tapped in order to be fastened to the link arm which applies pressure to the MDB 5 load cell. The MDB load cell is also mounted on a round aluminum mounting block in order to keep the cell level with the torque arm. A matching CNC machined motor back plate is fastened to the opposing plate using 6.5" long bolts effectively sandwiching the motor between the two plates.

The aluminum dropouts as well as the flange adapter were machined out of round aluminum on a lathe to ensure concentricity and the tight tolerances needed for alignment as well as the slip fight for the locking mechanism of the bearings. The skewer nut was machined out of ASTM A36 steel because of the fact that quick release skewers will be frequently threaded in and out of the nut. The skewer for the test machine was constructed out of an existing 135mm rear skewer and a 7/16 steel bolt. The bolt was chucked up in a lathe and a hole the diameter of the skewer was dilled down the center of the bolt. The threads of the bolt were then cut of using and abrasive saw and the skewer was slipped through the hole. The top side of the bolt was then TIG welded to the skewer resulting in a QR skewer that can be tightened by a socket wrench.

The disconnect boxes as well as multiple power components are mounted via din rails to the exterior and interior of the frame. The protective acrylic walls are riveted to the frame.

Motor Control System Enclosure

Upon finishing constructing the frame assembly, system electrical components were mounted on the frame's lower level within an acrylic enclosure to provide a barrier between the user and any design feature posing a shock hazard. Cal Poly Technical Support representative Jim Gerhardt oversaw this stage of the fabrication process and was extremely helpful in providing instruction and ensuring all aspects of the enclosure design were properly considered before fabrication. Construction of the enclosure began with cutting and mounting the acrylic onto the frame. Special considerations taken into account while dimensioning the acrylic panels included allowing for the appropriate clearance from the frame's tubing as well as ensuring the servo drive had proper spacing and ventilation. A door equipped with a lockable hasp was also made from acrylic paneling allowing an additional safeguard between system operators and electrical components.

Once the panels were mounted into place with rivets, 3/32” holes of were drilled into the frame so that the three lengths DIN Rail could be placed on the frame exterior and one length on the interior. The outside rails were used to mount the two disconnect switches controlling the supply of 220V and 110 V power while the inside rail was used to mount the ZipLINK communication board and the fuses regulating control power to the drive. Also mounted on the interior rail is a receptacle allowing for two plugs to be connected to the 110 V power supplied by the compact disconnect. These two plugs are used to provide the load cell’s excitation signals as well as the DAQ’s power supply. Also drilled into the frame were M5 holes allowing the door hinge and hasp to be mounted on the frame’s front face.

The next step in enclosure construction involved mounting the components and routing their respective wires. The servo drive was mounted vertically into the base plate such that heat built up in the drive during operation could be efficiently expelled into the surrounding air without posing a fire hazard to the other components. The DAQ and the load cell power supply were then fastened into place on the lower level plate at a safe distance from the rider load cell assembly. Wires were routed such that the 220 V and 110 V signals were separated as much as possible so that excess noise possibly skewing data measurements could be minimized. Any excess length of wire was tied off using zip ties. This allowed for space saved within the enclosure as well as giving our sponsor’s options should they choose to mount components differently. For enclosure detail drawings and complete wiring diagram, see Appendix E.

VI Development

The team developed a LabView VI in order to control the motor and simplify test runs. The front panel of the VI displays three user inputs, Wheel speed, rollout distance, and torque arm distance. Rollout distance will need to be measured and input for each wheel, and torque arm distance will need to be adjusted only when the load cell is moved. Initially the wheel speed will be set to zero to allow for loading. Once the wheel has been installed between the dropouts, the operator will run the VI and load the wheels. Once the front panel reads that the desired loads have been reached the wheel is ready to test. At this point the operator is free to vary the desired road speed to any value. The block diagram calculates the necessary motor speed using the rollout distance and sends a proportional analog voltage to the motor. The block diagram also calculates and displays the overall system power loss.

Final Machine Performance

Overall the machine performs rather well, but will need some additional work to meet specifications. The major issue currently is that our large diameter dropout bearings were pressed too tightly, which adds a huge amount of loss to the system. With this additional loss we believe it will be difficult to identify bearing power loss. Specialized plans to un-press the bearings and bore the holes out larger. When the bearings are re-pressed they should rotate more freely. Additionally, the load cell and power loss readings are outside of the specified tolerances. Although these readings are currently not within acceptable ranges, the team believes that with some effort the signals can be cleaned up to operate within tolerance. The load cell signals are mostly clean, but contain sharp spikes at a frequency of about 4 Hz. With some filtering or conditioning these spikes may be mitigated.

Despite these concerns, the machine operates fairly well for how little it has been tinkered with. At low speeds, around 20-30 km/h, the machine demonstrated that it was capable of measuring around 3-5 W of power loss with an acceptable uncertainty of about 0.75-1 W. Although this uncertainty increased with wheel speed, the team believes that this can be solved through the methods discussed above. After some discussion with the team sponsor and advisor it was decided that the machine will be delivered in the current mostly finished state. Specialized will then take control of the project and finalize the machine.

Design Verification Plan

The chosen test design relies on several factors and/or assumptions that must be confirmed before and during the various stages of fabrication. As such, several experiments must be performed In order to assess test method validity. These experiments are vital for proving the chosen concept meets all engineering targets and that the correct measurements/ data are being taken. After analyzing where the selected test method may be fundamentally weak and areas where uncertainty may be introduced into the test procedure, three such experiments were designed and are described below.

Rear Dropout Stiffness Determination and Verification

The fundamental idea leading to the conceptualization of the chosen test method was that aero and road losses could be eliminated by holding the wheel stationary and instead spinning the axle. The logic for this choice lies in that the relative velocity of the

axle to the hub bearings would be the same as in real world operation, however backwards it may initially seem. The critical hypothesis leading to the decision of spinning the axle instead of the rim was that the dropout stiffness, a key boundary requirement for determining axial misalignment in the hub, could be accurately modeled by designing rotating enclosures with uniform stiffnesses for the axle ends to fit into. As such, it becomes necessary to define said stiffness through empirically taken data. To do so, a threaded rod with a stiffness value much greater than that of the dropouts will be placed into the dropouts' slots. This rod will be loaded with weights of a known magnitude at a predefined distance from the longitudinal axis of the bike or center of the wheel. By measuring the angular deflection of the rod in the direction of the chain load (the largest load the dropouts must support), the critical stiffness of the dropouts can be found. Another key parameter in conducting this experiment is that the frame must be properly constrained to ensure only local deformation at the dropouts is being measured. This requires proper constraining of the rear triangle as well as the bottom bracket to ensure "global" deflections of the system's major axes don't skew measured data. In order to ensure the range of stiffnesses for the rear dropouts were properly determined, a follow-up experiment will be conducted on the fully-constructed machine where the axle deflection under load will be compared to the deflection seen in real world operation. Modeled accuracy of ±10 % has been tentatively selected as the verification acceptance criteria.

Support Bearing Power Loss

Another major assumption made in the design of the chosen concept is that power used to run the bearings supporting the rotating dropouts would not overshadow the power required to run the hub bearings. If such a case were to occur, the designed test method would show no meaningful data as there would be no difference between wheel-axle-bearing configurations. This reason, as discussed before, is why substantial time and resources were put into researching non-contact and zero-friction bearings (i.e. hydrodynamic, air, electromagnetic). Given the cost and spatial constraints of these types of bearings, rolling contact (i.e. steel or ceramic deep-groove ball bearings) bearings were selected as the most feasible solution for the test. However, due to the inherent friction associated with rolling contact bearings, the power required to run said bearings under load must be quantified. This is true even with the bearings' grease replaced with low viscosity oil. In order to quantify this additional power loss, we plan on running the support bearings at various speeds under load without the axle assembled. The success of the support bearing loss hypothesis will be determined by whether or not their required power is less than 20 % of the power required with to run the fully-assembled system. With these measurements, we can also determine the optimum oil

viscosity that will provide the best balance between maximum friction reduction and minimal required maintenance.

Servo System Tuning

The Sureservo SVA-2100 drive controlling the motor can be configured in a myriad of different combinations depending if the user wants to control the motor's position, velocity, or torque. The Sureservo User Manual was thoroughly studied and used to set the drive's parameters to the configuration most applicable to our test. With this test machine speed control is of primary importance as it is a key determinant in calculating the power required to spin the rotating dropout-axle assembly under load. To control motor speed the drive was set to Velocity Mode as LabVIEW is used as an external controller feeding the drive a voltage proportional to the motor's desired speed. Internal Velocity Mode was also used while the group familiarized itself with how the servo system operated. This mode involves setting specific drive parameters to allow the motor to cycle between three different speeds set internally on the drive. Though this mode was not ultimately used to control motor speed, learning how it operates was a vital step in determining how to manually cycle through or change drive parameters. Through use of the Sureservo Pro Software enabling the drive to be connected to an onsite PC, these manually-changed parameters can be quickly uploaded allowing the user to see what each parameter's value is. This software also allows for PC-to-drive communication where the user can instantly change drive parameters without using the panel located on the front of the drive. Though this capability is convenient and very efficient, its use is not recommended as many drive parameters require cycling supply power in order for their new values to take effect.

The SVA-2100 uses PID control to optimize the motor's response characteristics such as time to respond (steady state), peak overshoot, damped frequency, steady-state error, etc. Applying control theory to each of these characteristics allows easy adjustment by properly setting the system control gains. For the full list of drive parameters and how they apply to our application, see the Sureservo User Manual located in Appendix G.

Appendices

Appendix A: Works Cited

Background Research

Bicycle Manufacturing Equipment. (n.d.). Retrieved September 30, 2012, from Taiwan Trade: http://www.taiwantrade.com.tw/shuztung/products-category-list/en_US/144917/Bicycle_manufacturing_equipment

BIBLIOGRAPHY Drouet, J.-M., & Champoux, Y. (2010). A novel dynamometric hubset design to measure wheel loads in. *Procedia Engineering*, June.

This source was used in giving an accurate free body diagram of the hub in operation and allowed the team to confidently estimate the bearing power losses within the hub under different loading conditions.

James B. Spicer, C. J. (2001). Effects of Frictional Loss on Bicycle Chain Drive Efficiency. *Transactions of the ASME*, 8.

James C. Martin, D. L. (1998). Validation of a Mathematical Model for Road Cycling Power. *Journal of Applied Biomechanics*, 16.

Kusumba, S. (2004). *Dynamometer Proportional Load Control.* Cleveland State University.

Liteville. (n.d.). *Why and How We Test*. Retrieved October 2, 2012, from Liteville: http://www.liteville.de/t/25_37.html-weights

Schraner, G. (1999). *The Art of Wheel Building: a bench reference for neophytes, pros, and wheelaholics* . Buonpane Publishers.

SKF. (n.d.). *Frictional Moment-Power Loss*. Retrieved September 30, 2012, from SKF: http://www.skf.com/skf/productcatalogue/calculationsFilter?lang=en&newlink=&prodid=&action=Calc5

Universal Transmissions. (n.d.). *Gates Frame Stiffness Test Instruction Manual.* Retrieved October 2, 2012, from Carbon Drive Systems: http://www.g-boxx.com/pdf/pdf-23-03-10_2/GATES-Frame-stiffness-EN.pdf

Wilson, D. G. (2004). *Bicycling Science.* Cambridge, Massachusetts: MIT Press.

These sources were used in the initial research/introductory phase of the project when it was necessary to define all the power losses during a bicycle's operation and their corresponding magnitudes. Analyzing the findings of these reports allows the team to narrow the scope of feasible conceptual designs by defining which bicycle system components represent power losses that must be isolated from the final design. These articles were particularly helpful in aiding the conceptualization of how to eliminate losses in the drive train (chain, sprockets, etc.) and due to aerodynamics. Also supporting the team's background research was the fact that several of these sources defined the friction power losses in the wheel bearings in equation form and thus allowed the team to see which factors contributed most to this loss.

Bicycle Manufacturing Equipment. (n.d.). Retrieved September 30, 2012, from Taiwan Trade: http://www.taiwantrade.com.tw/shuztung/products-category-list/en_US/144917/Bicycle_manufacturing_equipment

Kusumba, S. (2004). *Dynamometer Proportional Load Control.* Cleveland State University.

Liteville. (n.d.). *Why and How We Test*. Retrieved October 2, 2012, from Liteville: http://www.liteville.de/t/25_37.html-weights

Universal Transmissions. (n.d.). *Gates Frame Stiffness Test Instruction Manual.* Retrieved October 2, 2012, from Carbon Drive Systems: http://www.g-boxx.com/pdf/pdf-23-03-10_2/GATES-Frame-stiffness-EN.pdf

The above four sweces were found at the onset of the brainstorming phase. During this time, the team was trying to develop as many ideas of how to apply and control the loads that need to be actuated during the test. These loads include rider weight, chain tension, and quick release clamping force. These previously-made machines provided a starting point from which the team could generate possible soultions for the design and ranged in complexity from autmoted pneumatic systems to simply hanging weights on the frame.

Bearing Research

AMI Bearings, Inc. (n.d.). *Accu-Loc® Concentric Collar Locking Pillow Block Unit, UEP200 Series*. Retrieved January 16, 2013, from AMI Bearings: http://catalog.amibearings.com/viewitems/accu-loc-concentric-collar-locking/ric-collar-locking-pillow-block-unit-uep200-series

Baldor Electric Company. (2013). *Grip Tight Adapter Ball Bearing.* Retrieved January 19, 2013, from Baldor-Dodge: http://www.dodge-pt.com/products/bearing/griptight/index.html

FYH BEARING UNITS USA INC. (2009, September). *NU Concentric-LOC BALL BEARING UNITS.* Retrieved January 15, 2013, from fyhbearings.com: http://www.fyhbearings.com/catalog/NU-LOC_E_3401.pdf

New Way Air Bearings. (2006, January). *AIR BEARING APPLICATION .* Retrieved November 8, 2012, from www.newwayairbearings.com: https://dl-web.dropbox.com/get/ME%20428/Lab/Background%20Research/Air%20Bearing%20Specifics.pdf?w=078d5cef

New Way Air Bearings. (2007, December 16). *RADIAL AIR BEARING PRODUCT SPECIFICATIONS.* Retrieved November 8, 2012, from www.newwayairbearings.com: https://dl-web.dropbox.com/get/ME%20428/Lab/Background%20Research/Air%20Bearing%20Basics%20-%20New%20Way.pdf?w=ffd22b5f

The Timken Company. (2013). *Concentric Locking Collar* . Retrieved January 16, 2013, from Timken: http://www.timken.com/EN-US/products/bearings/productlist/HousedUnits/BallBearing/Pages/ConcentricLockingCollar.aspx

Xie, X. (2003). *Comparison of Bearings-- For the Bearing Choosing of High-speed Spindle Design .* Salt Lake City: Dept. of Mechanical Engineering, University of Utah .

Zinn, L. (2012). *Bearing It All: Ceramic Bearings*. Retrieved November 17, 2012, from Active: http://www.active.com/cycling/Articles/Bearing_It_All__Ceramic_Bearings

The above sources gave concise information analyzing the performance characteristics of different bearing types as well as how these characteristics rank relatively between types of bearings. This relative comparison was done both quantitatively and qualitatively, giving the team multiple different

perspectives of determining which bearings would/could be feasible in incorporating into any proposed conceptual design.

Control and Data Acquisition Systems

National Instruments Corporation. (2012). *LabVIEW for Students*. Retrieved January 17, 2013, from National Instruments: http://www.ni.com/academic/students/

National Instruments Corporation. (2012). *NI USB-6341 X Series Data Acquisition*. Retrieved January 16, 2013, from National Instruments: http://sine.ni.com/nips/cds/view/p/lang/en/nid/209069

National Instruments Corporation. (2012). *What is Signal Conditioning?* Retrieved January 12, 2013, from National Instruments: http://sine.ni.com/np/app/main/p/ap/daq/lang/en/pg/1/sn/n17:daq,n21:11/fmid/2998/

Omega Engineering Inc. (2013). *Introduction to Load Cells*. Retrieved January 15, 2013, from omega.com: http://www.omega.com/prodinfo/loadcells.html

Transducer Techniques, Inc. (2013). *Load Cell Systems*. Retrieved January 17, 2013, from transducertechniques.com: http://www.transducertechniques.com/load-cell.aspx

Vishay Precison Group, Inc. (2012). *Micro-Measurements Strain Gauges and Instrumentation*. Retrieved January 14, 2013, from vishaypg.com: http://www.vishaypg.com/micro-measurements/instruments/d4/

The sources above contain pertinent details for identifying all the necessary data acquisition instruments involved in determining power, namely load cells, signal conditioners, cable adapters, etc. These sources, along with their supplier's technical data sheets, were vital to selecting specific models for the final design as they contained explicit details on required parameters such as calibration range, sampling rate, number of input/output channels, etc.

Dynamometer Research

Anaheim Automation, Inc. (2011). *Servo Motor Guide*. Retrieved January 12, 2013, from Anaheim Automation Motion Control: http://www.anaheimautomation.com/manuals/forms/servo-motor-guide.php

Automationdirect.com, Inc. (2011). *750 W Low Inertia System Torque/Speed*. Retrieved January 11, 2013, from www.sureservo.com: http://www.sureservo.com/750w_low_comp_system.htm

Bilal Ali, E. N. (2011, June 10). *Performance Dynamometer with Motor Car Model*. Retrieved January 10, 2013, from NI Community: https://decibel.ni.com/content/docs/DOC-16521

Daniel Meine, G. G. (2012, December 20). Mechanical Design Engineer, Micro-computer Specialist. (R. Williams, Interviewer)

J. S. Brar, R. K. (2004). *A Text Book of Theory of Machines.* Firewall Media.

joeqsmith. (2011, March 9). *Lockridge Device*. Retrieved January 17, 2013, from energeticforum.com: http://www.energeticforum.com/renewable-energy/6792-lockridge-device-peter-lindemann-23.html

Killedar, J. S. (2012). *Dynamometer: Theory and Application to Engine Testing.* Xlibris Corporation.

Leadshine Technology Co., LTD. (n.d.). *Motor Torque Calculation.* Retrieved January 18, 2013, from leadshine.com: http://www.leadshine.com/Pdf/Calculation.pdf

These sources were critical for defining the instrumentation and method required for precisely determining power lost within the hub bearings. With the information derived, a speed-controlled servo motor system using an attached torque arm was selected as the best method for acquiring this measurement. These sources also defined the method for how this driven dynamometric system would allow support for the motor while not skewing the torque magnitudes being driven through the torque arm to the load cell.

Coupling Considerations

Helical Products Company, Inc. (n.d.). *Standard Coupling Guide*. Retrieved January 18, 2013, from heli-cal.com: http://heli-cal.com/cm/Products/Flexible-Couplings/Home.html

R+W Coupling Technology. (n.d.). *Product Finder for Couplings and Line Shafts*. Retrieved January 14, 2013, from R+W Coupling Technology: http://www.couplings-selection.com/

The sources above were extremely useful in determining the most accurate coupling method for transferring motor speed and torque from the motor shaft to the driven axle. With the descriptions given on each respective coupling's speed, size, and torque capabilities, the proper model and size coupler could be found.

Load-Actuating Systems

Generic Slides . Manual Positioning Slides . n.d. 21 January 2013 <http://www.genericslides.com/manual_positioning_slides.html>.

Joyce Dayton. Machine Screw Jacks. 2013. 22 January 2013 <http://joycedayton.com/products/machine-screw-jacks>.

The sources above were used during the detail design phase to aid in properly selecting the componentry needed to actuate the chain and rider loads. The information derived from these sources discusses critical parameters such as mechanism travel, material, and load capacity.

Appendix B: Management Plan

Taking on a project with as large of magnitude as this requires a clearly defined plan of attack. Without having defined individual and group assignments as well as judicious time management, the quality of the final design would be compromised. Because of this, it was prudent to dictate team roles so that the most efficient working environment can be created and the best possible design be produced. Each team member's roles were defined by his academic/engineering strengths, applicable work experience, and personal interests and are described below.

Team Members

Dylan Harper

Due to Dylan's ability to effectively transfer abstract concepts to a distinct, plausible design, he was placed in charge of Conceptual Fundamentals and their application to the final design. This role requires Dylan to develop clear, working models of the proposed and final solutions. While the entire group will contribute in conceptualizing solutions, Dylan is recognized as this area's lead and holds the responsibility of putting group ideas to paper. Dylan has also had extensive exposure to Microsoft Excel and will be in charge of developing and maintaining System Trades Analysis done via computer. This analysis includes the parametric modeling of all system variables and allows the team to see interdependencies and influences within proposed designs.

Kevin Hom

Kevin is an avid mountain biker whom has been competitively racing for the past four years. Kevin's experiences have exposed him to the inner dynamics of the cycling industry and have given him a detailed knowledge of how a bicycle's components interact during operation. The fact that Kevin can provide design input from both the rider and engineer's perspective makes his involvement a crucial determinant of the project's success. Kevin also has extensive experience in the rapid prototyping industry including all aspects of the design to fabrication process. Because of these qualities he has been designated as the group's lead in bicycle reference, fabrication, and manufacturing.

Ross (Alex) Williams

Alex's strengths as a student and team member stem from his ability to manage time. Doing so allows him to complete multiple assignments in parallel without the concern of

missing a deadline. Because of this, Alex's role is to maintain maximum group productivity and to ensure that team resources are being used as efficiently as possible. Alex will also maintain professional communication with the project's sponsor (Specialized) and their corresponding contact (Sam Pickman). This administrative role is critical in preserving group synergy and will ensure the timely completion of both short and long-term tasks. Alex also has engineering experience with bearing lubrication optimization and its specific application to bicycles. Because of this, Alex will act as the team reference for the analysis and testing of bearing lubrication.

Collective Assignments

In addition to team member individual roles and in order to maintain an industry level of professionalism, there will be several tasks and expectations delegated throughout all team members. This includes thorough documentation of all research, concept designs, meeting minutes, and any other information pertinent to the project. Also, group members are required to maintain a strict level of punctuality and must give notice well in advance of team meetings in the event of an absence. Lastly and perhaps the most important group responsibility is to adhere to all relevant standards and codes specified by professional organizations such as ASME, NSPE, ASTM, etc. Being diligent in the following of these rules ensures the project will run at optimum efficiency and represents engineering best practices.

Project Phases and Milestones

Table 4. Dates of significant project deliverables and events

Deliverable	Date
Initial Meeting with Sponsor	10-5-12
Project Proposal	10-19-12
Conceptual Model	11-8-12
Conceptual Design Report	12-3-12
Conceptual Design Review with Sponsor	12-4-12
Detail Design Report	2-5-13
Manufacturing and Test Review	3-7-12
Project Update Memo to Sponsor	4-8-12
Project Hardware/Assembly Demo	5-1-2
Design Expo	5-30-12
Final Report	6-11-12

The above table summarizes key deadlines and project milestones taking place throughout the academic year. As shown, the project goes through many detailed phases starting with team introductions in September then transitioning through

conceptual and detail design before culminating with the Design Expo in June. To ensure all assignments are completed in a timely and efficient manner corresponding with these dates, a Gantt chart was developed showing the order and dependencies of all necessary tasks leading to project completion. This chart details the progression of these tasks and can be found in Appendix I.

Teaming

After being paired as a group, it became instantly necessary for the three team members to become as comfortable and open with each other as possible. This phase, seemingly trivial, ensures the group works at maximum efficiency and allows each team member to work in a role that improves the quality of the final product while advancing his engineering ability. An additional benefit of taking the time to initially "gel" as a team is that it allows each team member to contribute in areas both in and not relating to his designated group role.

Background Research

The problem solving approach began with background research into any various topics and/or technologies thought to be relevant to the project. A detailed overview of this initial research can be found in the previous background section. As understanding of the project has grown, research has become more refined and will continue to do so for the remainder of the project as needed. From this launching point, and with detailed knowledge of all engineering requirements, the team can develop multiple conceptual designs fulfilling the needs of sponsor.

Requirement definition and Quality Functional Deployment

Clearly defining all engineering specifications and targets is perhaps the most important step of the project's introductory phase. A lack of knowledge or an undetailed analysis of the machine's function and necessary capabilities could lead the team to produce a design inconsistent with sponsor demands. Fortunately for the team, these specifications were clearly given in the project's introductory presentation. These requirements as well as others later defined by the group can be found in the Objectives section as well as Appendix C which document how each successive requirement was relatively compared to find its overall importance to the final design.

Conceptual Design Phase

As stated above, performing preliminary research combined with having each engineering requirement's importance relatively defined allows the team to begin the conceptual design phase. During this time, the team tried to develop and define any possible method of testing that could satisfy these requirements. These designs ranged from tests operating in single and multiple different fixtures to schematics using different wheel spinning and force-actuating mechanisms. After some preliminary analysis defining which concepts or aspects of a specific concept could be feasibly constructed, three top concepts were selected and presented separately to the sponsor and advisor. Receiving feedback from these two parties enabled the team to perform more detailed analyses on each concept which could then yield a defined top concept the team could defend in a formal presentation.

Detail Design Phase

Following the selection of a clear top concept allows the detail design phase to begin. During this phase, all necessary components and costs involved in constructing the machine will be specified. From this, a dimensioned solid model with a corresponding bill of materials can be formed giving a defined engineering layout to follow in building the machine. This will make machine fabrication a much more efficient process as the method of building or purchasing each specific component will be known.

Machine Fabrication and Detail Design Iteration

Upon sponsor approval of the detail design at the Critical Design Review, the construction process mentioned in the above paragraph can begin. Completing this phase successfully requires the team to take full advantage of all resources and funds available to the group. This will most likely result in many hours spent in Cal Poly machine shops testing critical components of the machine as well as sending out detail drawings of parts to be machined by Specialized. Due to the complex nature of any concept selected for the detail phase, it is anticipated machine fabrication will involve many iterations and amendments to the detail design. These changes could involve re-specifying a specific sensor or redesigning a structurally weak part. As such, the team will make sure an emergency set of funds are available to account for the costs involved with these iterations.

Appendix C

QFD House of Quality

Customer Requirements		Weighting (Total 100)	Power Lost (W)	Vertical Load(N)	Chain Tension (N)	Wheel Speed (km/hr)	Can fit both F/R hubs (Y/N)	Clamping Force (N)	Can turn drive load off/on (Y/N)	Accounts for ranging stiffnesses (N/m)	Can turn different loads off/on (Y/N)	Effective Cost ($)	% of Shop Employees that can use it without help	Volume (m^3)	Maintainence Time/mo (hrs)	Error %	Benchmarks: Bearing Tester	Bike Dynomometer	Power Hubs
Engineering Requirements																			
Customer Requirements	Measures hub bearing friction	14	9	3	3	3		3				1				3	5	3	3
	Simulate static vertical load from rider	6	3	9						1	3	1				3	3	2	1
	simulate static drive load from chain	10	3		9				9	3	3	1				3	3	5	1
	controls wheel speed	9	9			9						1			1	3	5	5	1
	front/rear wheel applicable	11					9					1	1	1	1		5	5	5
	simulates QR clamping force	4	3					9		1	3	1				3	3	2	1
	simulates coasting	7	9		9	9			9		3	1					2	5	1
	accounts for variable dropout stiffness	8	3	3	3			1		9		1				3	1	4	1
	loads able to be run simultaneously or separately	12	3	9	9			9	9		9	1					5	2	1
	cost less than or equal to $10,000	13										9			1	3	3	3	5
	able to be used by employees-intuitive operation	1											9		3		4	4	5
	doesn't take up too much shop space	0												9			5	4	5
	minimal maintenance	2											3		9	3	3	3	5
	maintains accuracy over time	3										3			3	9	4	4	5
	Units		W	N	N	km/hr	Y/N	N	Y/N	N/m	Y/N	$	%	m^3	hrs	%			
	Targets		±1	±2	±5	±2 mm/hr	Y	±2 N	Y	TBD	Y	<=10000	85	105	<=5	1			
	Benchmark #1																		
	Benchmark #2																		

9	Srong Correlation
3	Medium Correlation
1	Small Correlation
Blank	No Correlation

Engineering Requirement Pair wise Comparison

	Measures hub friction	Simulate static vertical load from rider	simulate static drive load from chain	controls wheel speed	front/rear wheel applicable	simulates QR clamping force	simulates coasting (drive load able to be turned off/on)	accounts for variable dropout stiffness	loads able to be run simultaneously or separately	cost less than or equal to $10,000	able to be used by employees-intuitive operation	doesn't take up too much shop space	minimal maintenance	maintains accuracy over time
Measures hub friction														
Simulate static vertical load from rider	3													
simulate static drive load from chain	3													
controls wheel speed	9		1											
front/rear wheel applicable		3		9										
simulates QR clamping force	3				3									
simulates coasting (drive load able to be turned off/on)	1		9	1	1									
accounts for variable dropout stiffness	3	3	3		9	1								
loads able to be run simultaneously or separately	3	3	3			3	3	1						
cost less than or equal to $10,000	1	1	1	1	1	1	3	1	3					
able to be used by employees-intuitive operation		1	1	1	3	1	1	1	3	3				
doesn't take up too much shop space		1	1	1	3	1	1	1	3	1				
minimal maintenance		1	1	1	3	1	1	1	3	3	1			
maintains accuracy over time	1	1	1	3	1	1	1	1	3	9			3	

Appendix D: Conceptual Design Schematics

Preliminary Concept # 2: Regression Method

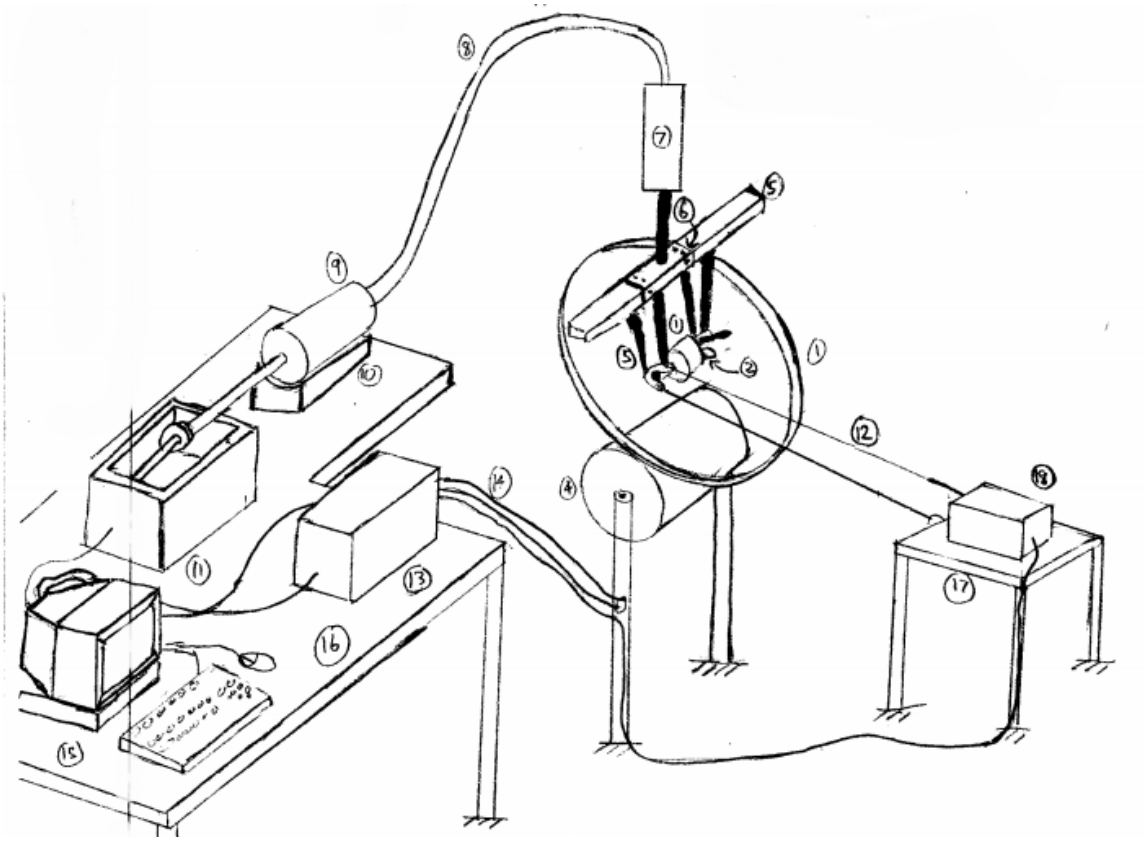

Figure 25. Initial Design Concept #2

Regression Test w/ Hydraulic Load Application

- Description - a single test spinning the wheel in a mechanical test stand with all loads present
  - losses due to aero, rolling resistance, loads, etc. would be subtracted out from power vs. time data with the mass of the wheel known
    - : aero losses - occur when power vs time becomes non-linear (2^{nd} order)
      - : research suggests this occurs at ~20 K-/L
      - $F_D = \frac{C_D \rho A V^2}{2}$ $V = V_{air/wheel}$
      - $P = F_D V_{wheel}$
    - : Rolling Resistance - proportional to the normal force and coefficient of rolling friction C_r
      - $F_R = N C_r$
      - $P = F_R V_{wheel}$
      - should be a linear relationship
  - Once aero and rolling losses are accounted for, Bearing losses should be all that is left at a given rpm and set of loading conditions
  - Data for power derived from coast-down test where wheel is allowed to spin freely to rest from top speed
    - : Velocity vs. time measured
    - : Energy vs. time calculated from velocity data
    - : power vs. time/velocity derived from energy vs. time data

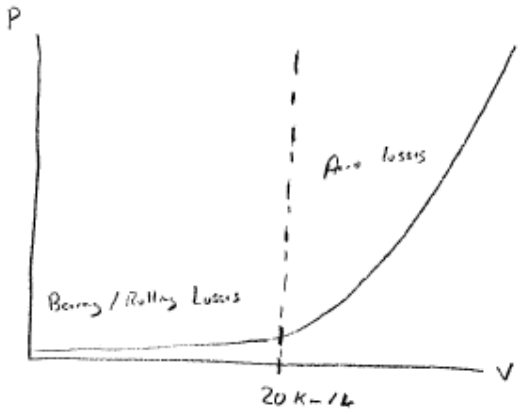

(cont. on next pg.)

Figure 26. Concept # 2 test method

Preliminary Concept # 3: Two-Test Method with One Fixture

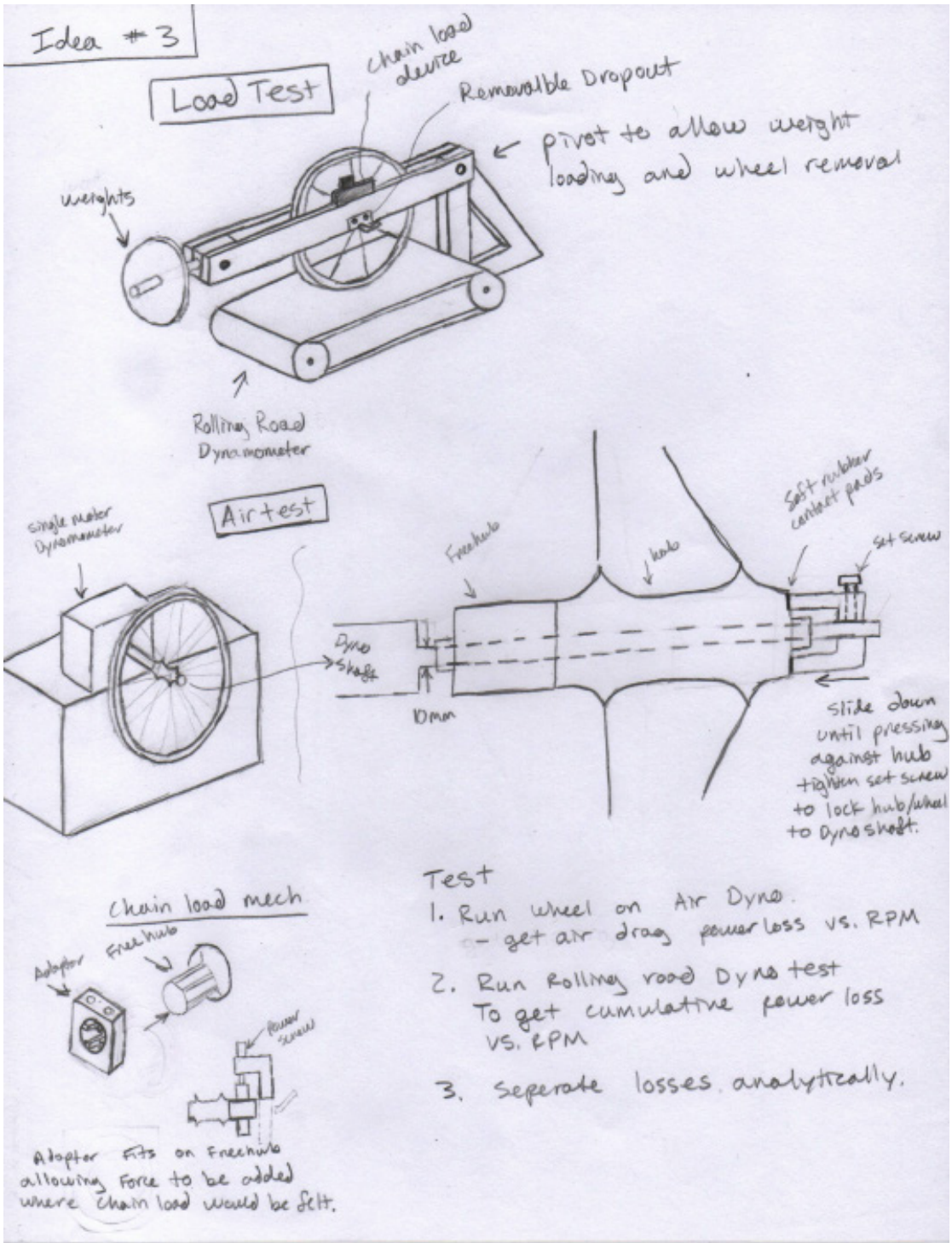

Figure 27. Initial Design Concept #3

Appendix E: Detail Design Drawing Packet

Table of Contents

System Layout **1**
Table Assembly..... ...2
Table-Top.....3
Bottom Plate.....4
2K Screw Jack Table Mount.....5
2K Jack Mount Upright.....6
2K Jack Mount Triangle.....7
2K Jack Mount Base.....8
Slider Mounting Plate.....9
Motor Mounting Block.....10
Pillow Block Mounting Block.....11
Torque Arm Load Cell Block.....12
Leg Isolator Plate.....13
Motor Assembly.....14
Torque Arm Weldment.....15
Motor Plate.....16
Arm Adapter.....17
Motor Back Plate.....18
Rider Load Assembly.....19
250 Jack Spacing Plate.....20
250 Jack Mounting Plate.....21
250 Wheel Plate.....22
Rider Load Slide Plate.....23
Flange Assembly.....24
Flange Adapter.....25
Flanged Skewer Nut.....26
Drive Side Dropout.....27
Aluminum DO Light.....28
Drive Side Dropout_Light_20mm.....29
Dropout_Medium.....30

Dropout_Stiff……31
Machined Pillow Blocks……32
Chain Load Device Assembly……33
Chain Load Roller……34
2K Jack Adapter Plate……35
Pulley Mount Assembly……36
Pulley Mount Base……37
Pulley Mount Tower……38
Pulley Mount Triangle……39
Top Level Wiring Diagram……40
Diagram 1: Fused Disconnect……41
Diagram 2: Compact Disconnect……42
Diagram 3: Load Cell Power Supply (PSM-F10) ……43
Diagram 4: NI SB-6341 DAQ……44
Diagram 5: ZipLINK ZLRTB50……45
Diagram 6:Servo Drive……46
Diagram 7: Receptacle……47

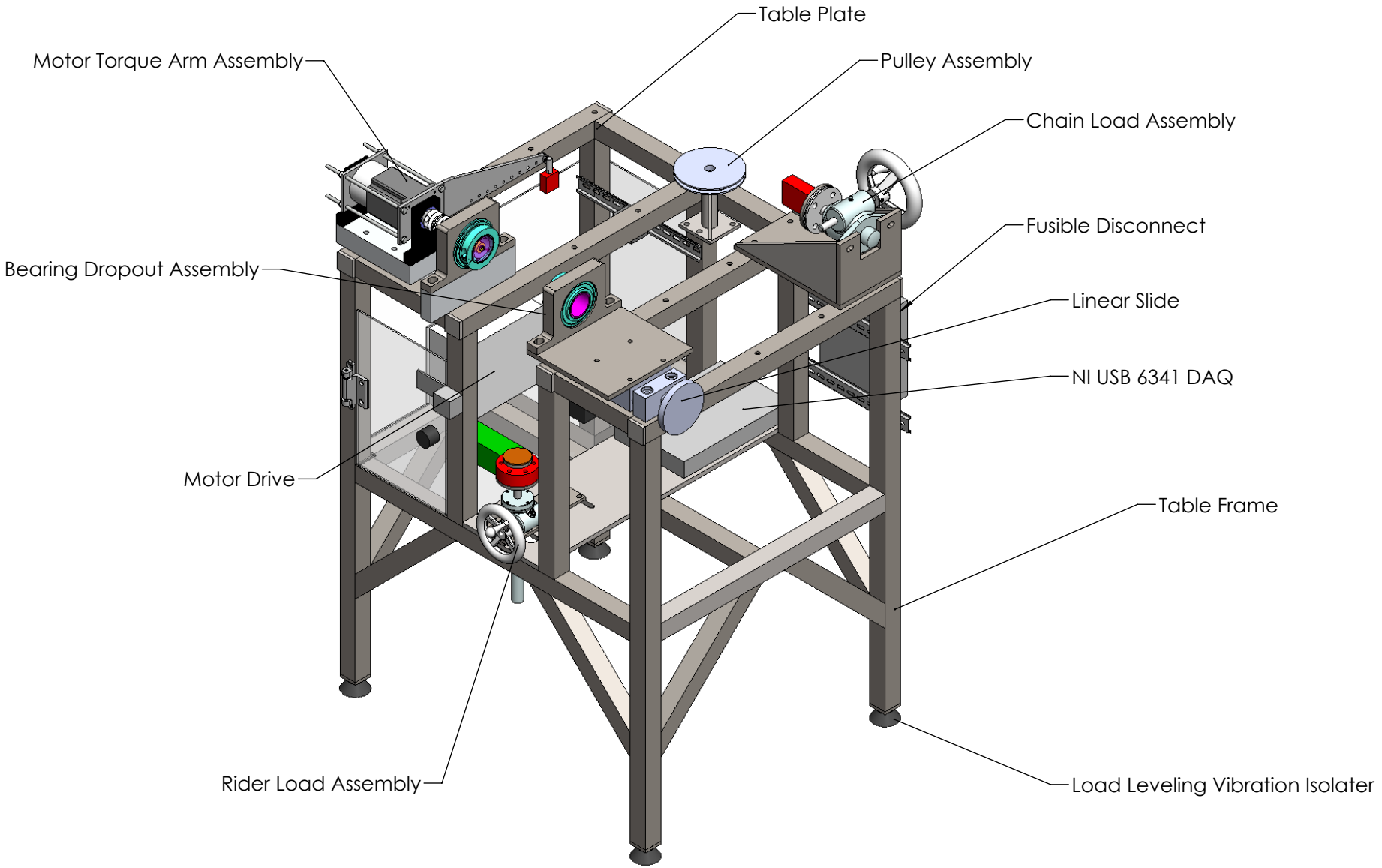

ME429 Winter 2013

Mechanical Engineering CAL POLY

SCALE: 1:10	PART: Table Assembly
UNITS:	MATERIAL:
TOLERANCE:	DATE: 6/8/2013
DWG #:	

5 4 3 2 1

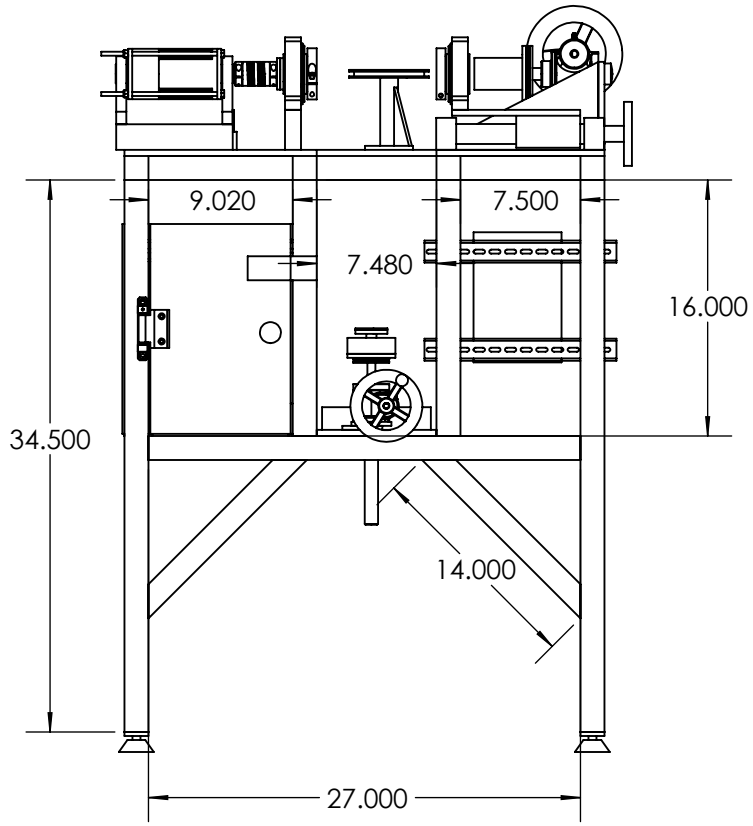

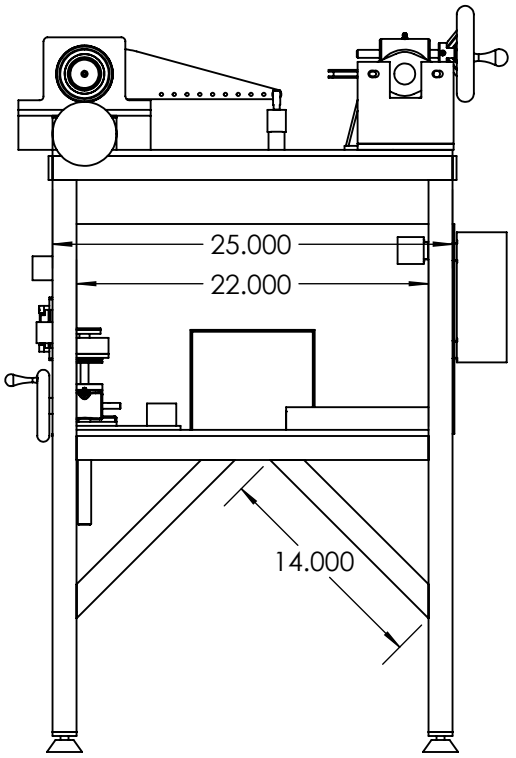

ME429 Winter 2013

Mechanical Engineering CAL POLY

SCALE: 1:12	PART: Table Frame
UNITS: Inches	MATERIAL: ASTM A36 Steel
TOLERANCE: +/- .01	DATE: 3/16/2013
DWG #:	

5 4 3 2 1

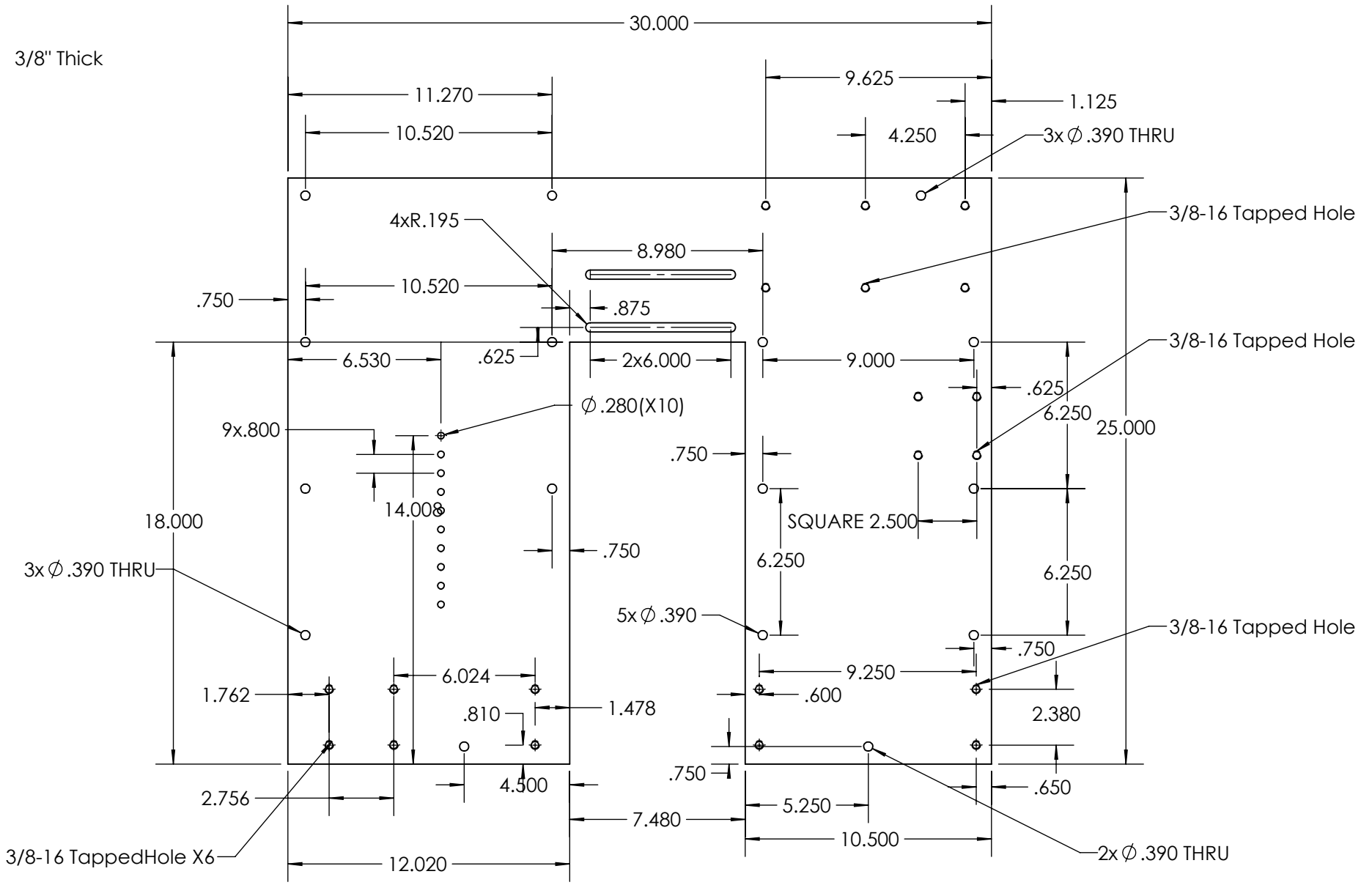

ME429 Winter 2013

Mechanical Engineering CAL POLY

SCALE: 1:8	PART: Test Tabletop
UNITS: Inches	MATERIAL: ASTM A-36 Steel
TOLERANCE: +/- .01	DATE: 4/17/2013
DWG #:	

5 4 3 2 1

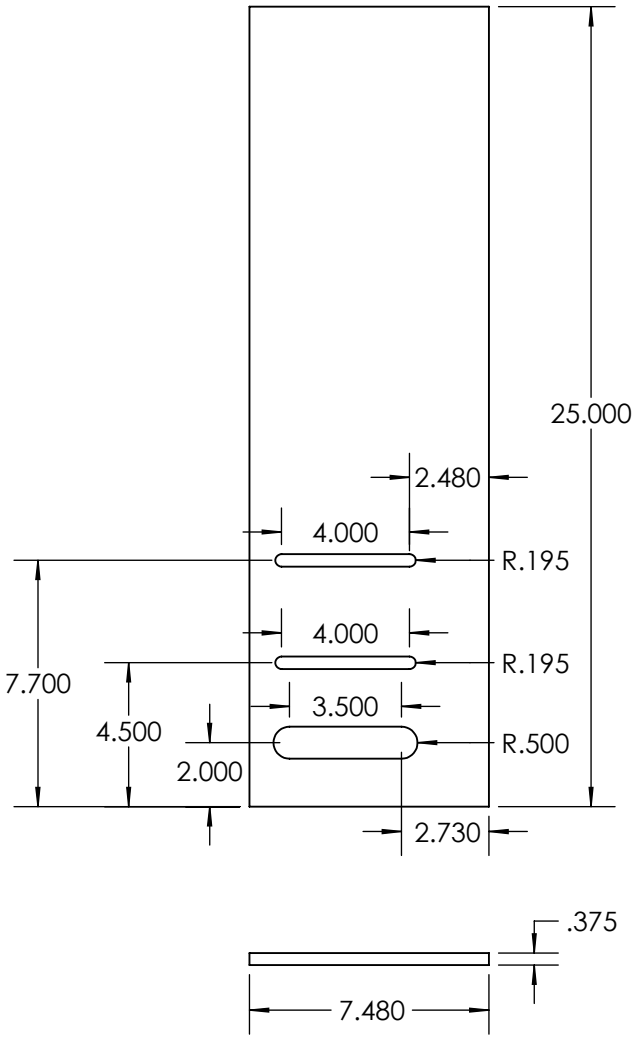

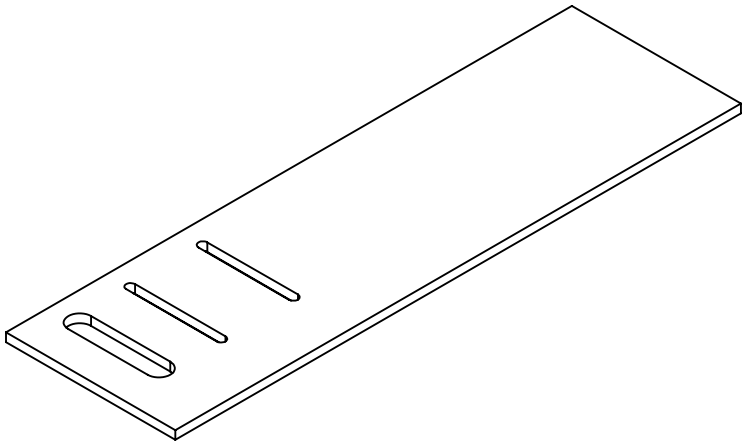

ME429 Winter 2013	SCALE: 1:6	PART: Bottom Plate
Mechanical Engineering CAL POLY	UNITS: Inches	MATERIAL: ASTM A36 Steel
	TOLERANCE: +/- .01	DATE: 3/16/2013
	DWG #:	

5 4 3 2 1

1/4" Fillet/Square welds

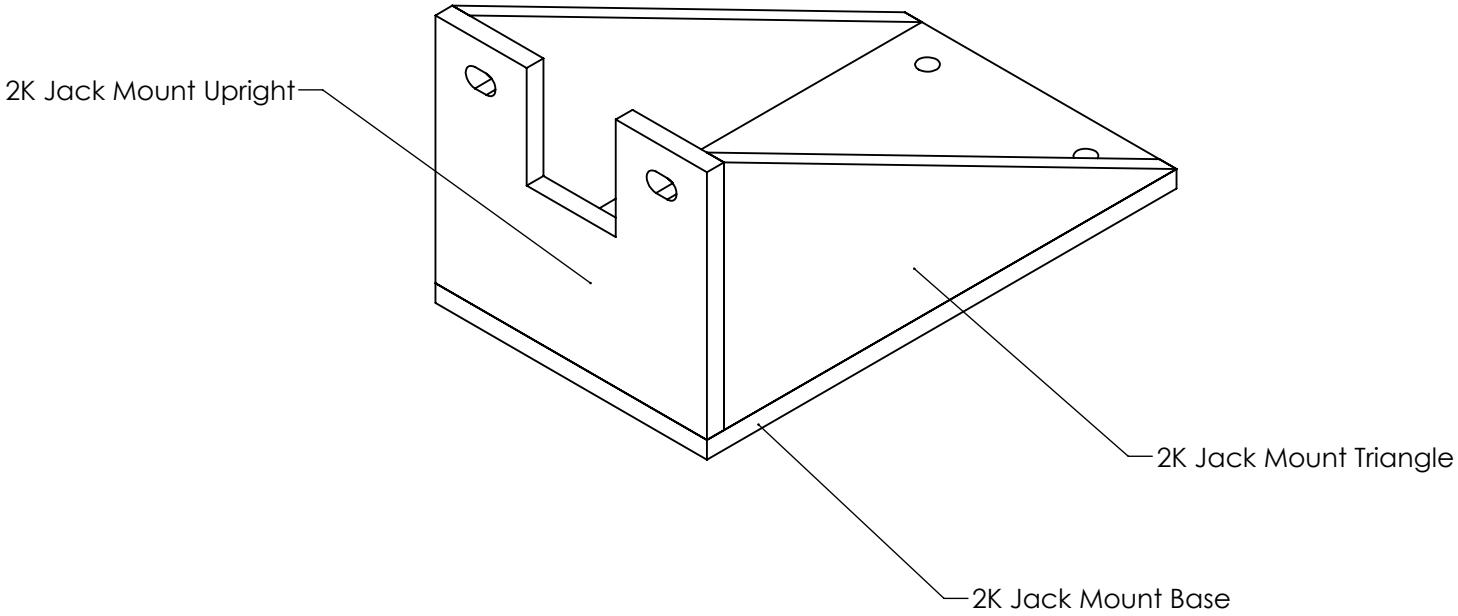

ME429 Winter 2013 Mechanical Engineering CAL POLY	SCALE: 1:2	PART: 2K ScrewJack Table Mount
	UNITS: Inches	MATERIAL: ASTM A-36 Steel
	TOLERANCE: +/- .01	DATE: 2/15/2013
	DWG #:	

5 4 3 2 1

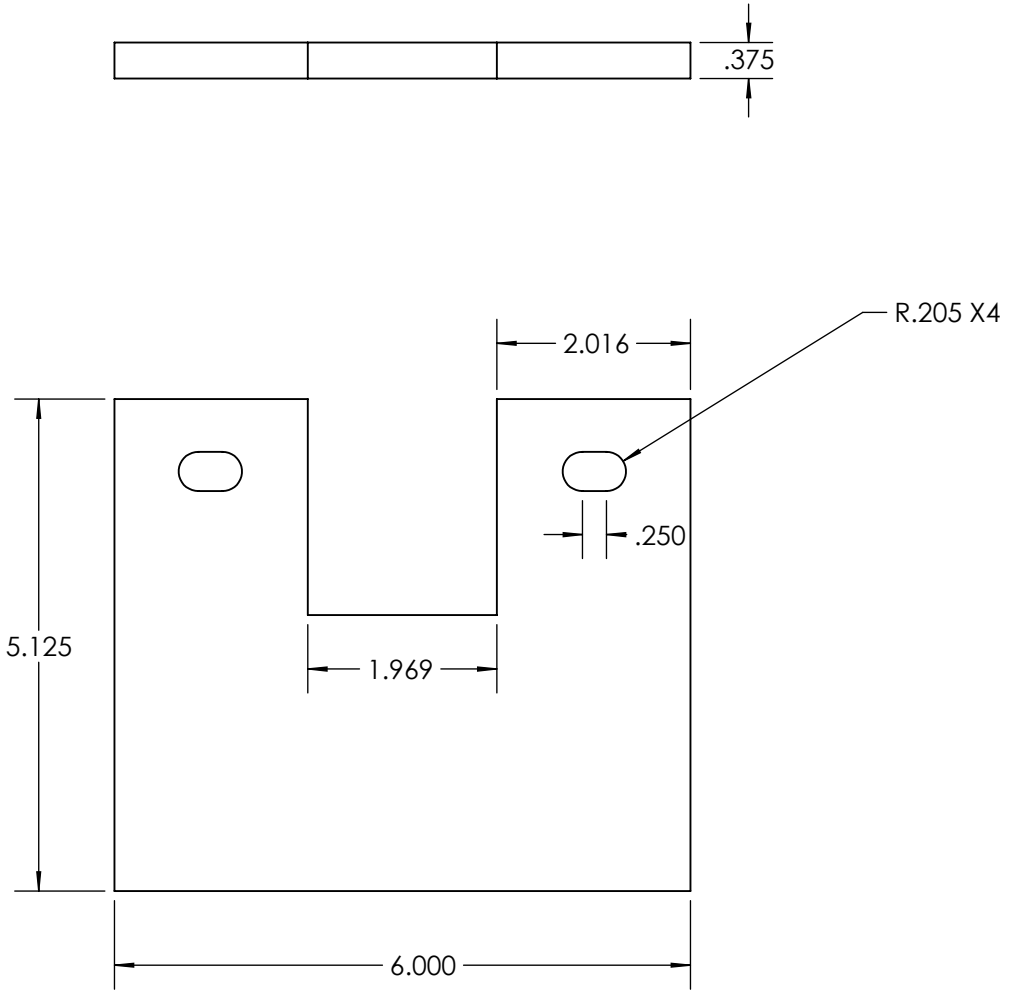

ME429 Winter 2013 Mechanical Engineering CAL POLY	SCALE: 1:1	PART: 2K Jack Mount Upright
	UNITS: Inches	MATERIAL: ASTM A36 Steel
	TOLERANCE: +/- .005	DATE: 3/16/2013
	DWG #:	

5 4 3 2 1

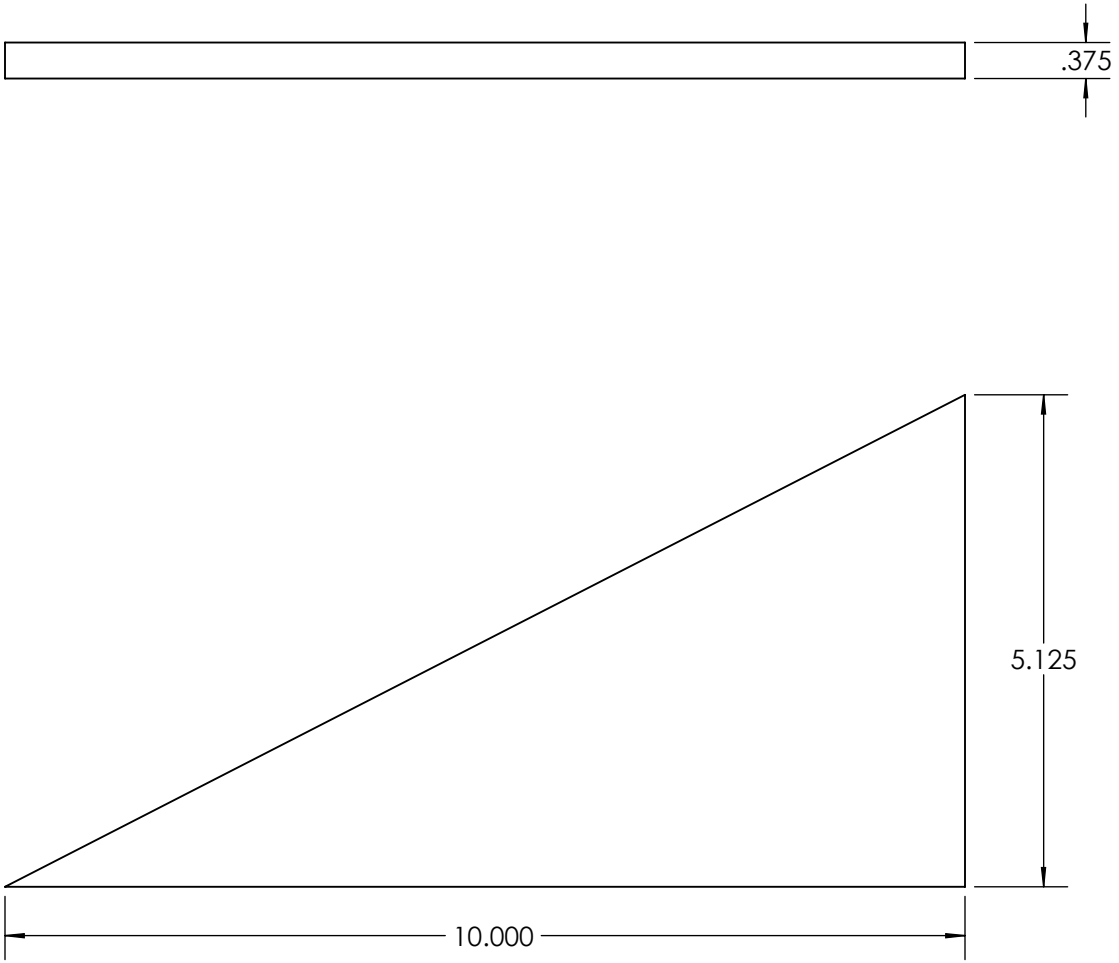

ME429 Winter 2013

Mechanical Engineering CAL POLY

SCALE: 1:1	PART: 2K Jack Mount Triangle
UNITS: Inches	MATERIAL: ASTM A36 Steel
TOLERANCE: +/- .01	DATE: 3/16/2013
DWG #:	

5 4 3 2 1

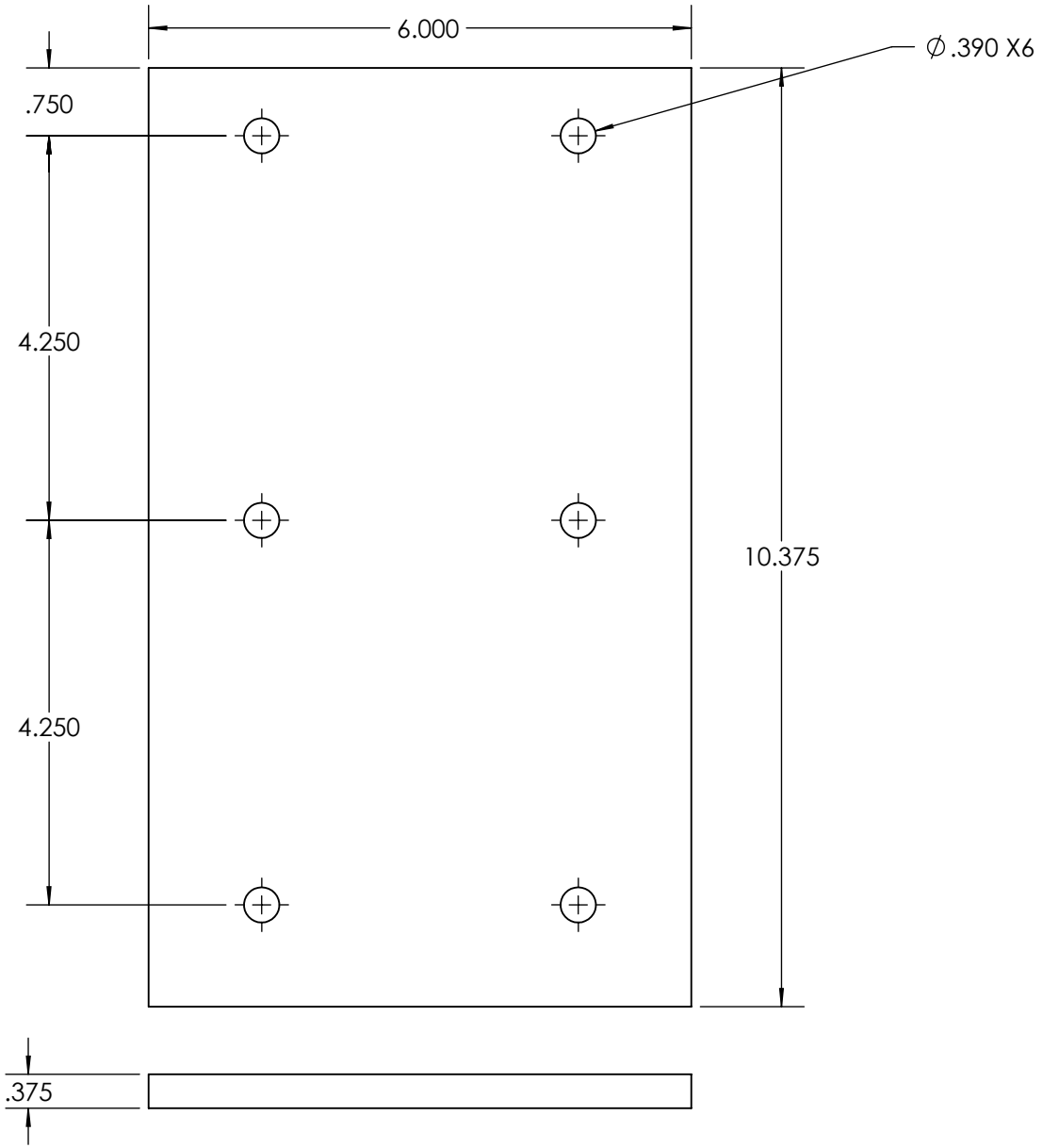

ME429 Winter 2013

Mechanical Engineering CAL POLY

SCALE: 1:1	PART: 2K Jack Mount Base
UNITS: Inches	MATERIAL: ASTM A36 Steel
TOLERANCE: +/- .005	DATE: 3/16/2013
DWG #:	

5 4 3 2 1

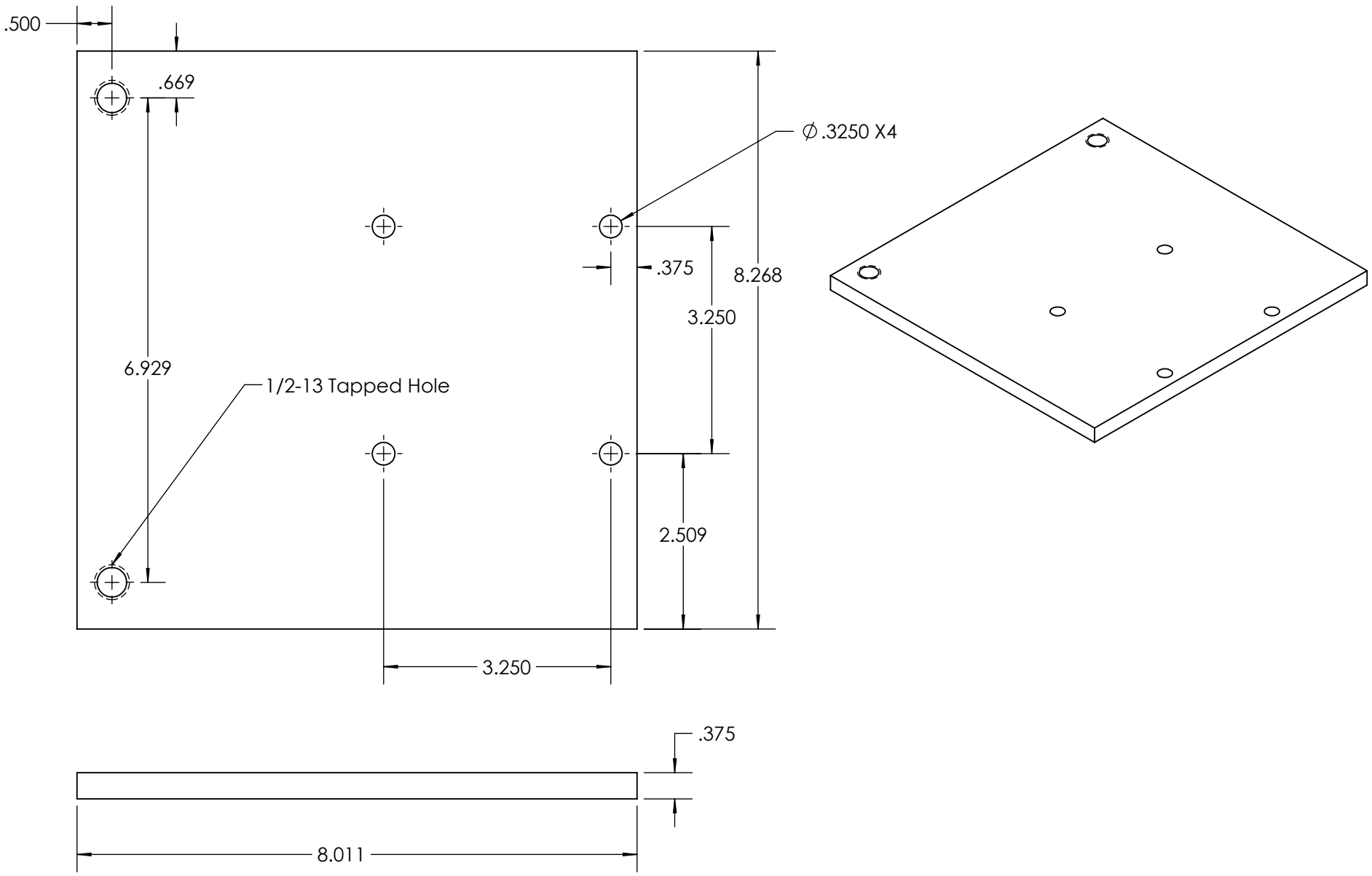

ME429 Winter 2013	SCALE: 1:2	PART: Slider Mounting Plate
Mechanical Engineering CAL POLY	UNITS: Inches	MATERIAL: ASTM A-36 Steel
	TOLERANCE: +/- .05	DATE: 2/2/2013
	DWG #:	

5 4 3 2 1

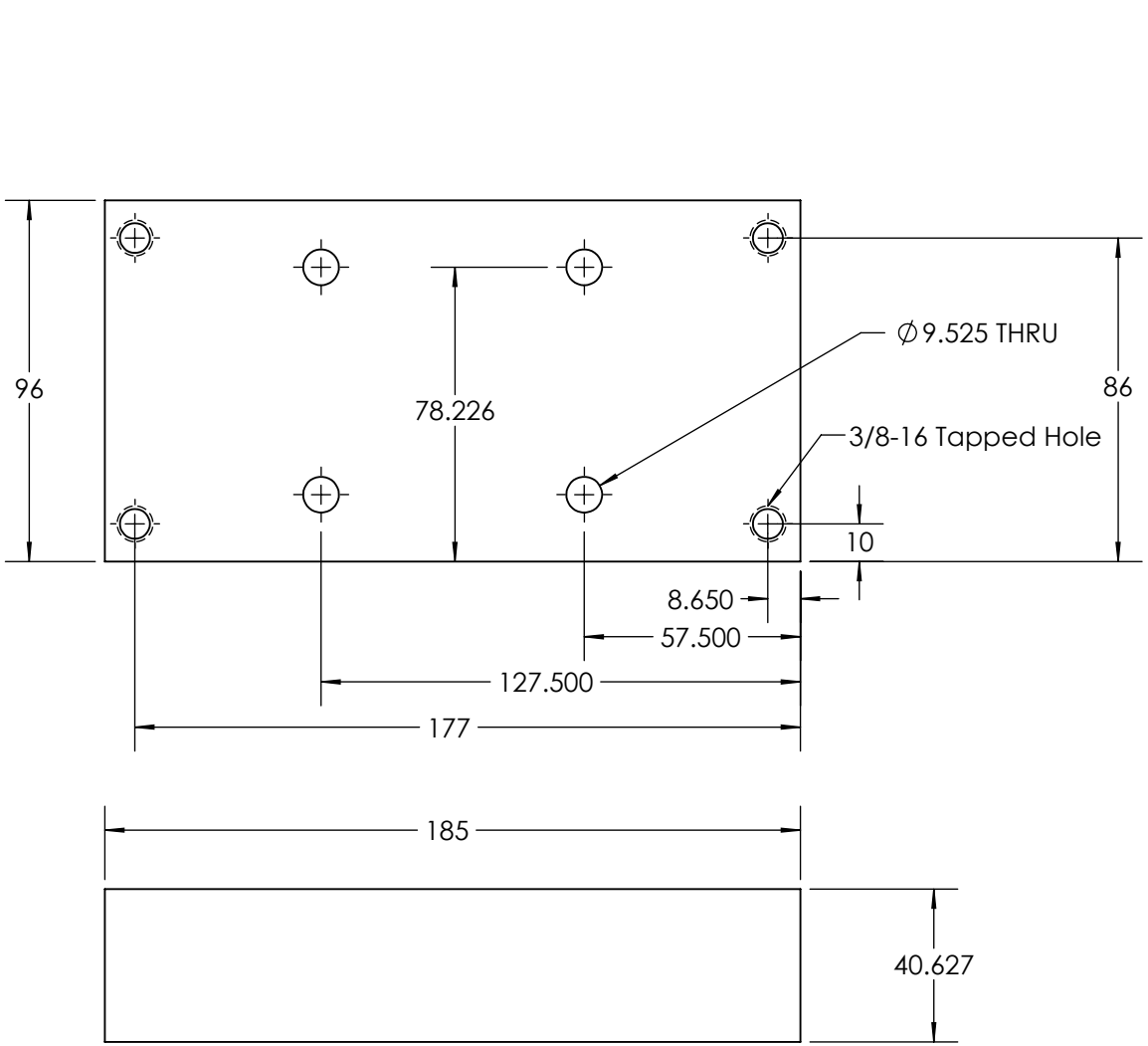

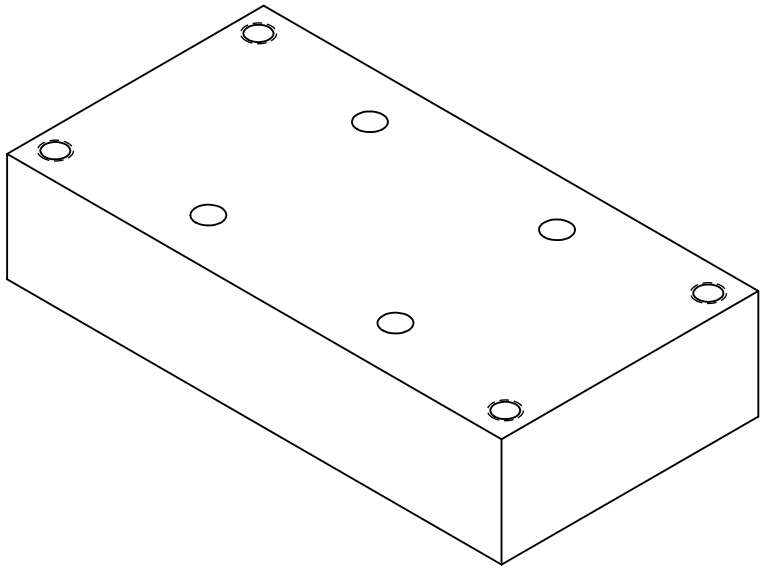

ME429 Winter 2013 Mechanical Engineering CAL POLY	SCALE: 1:2	PART: Motor Mounting Block
	UNITS: Millimeters	MATERIAL: 6061 Aluminum
	TOLERANCE: +/- .127	DATE: 2/2/2013
	DWG #:	

5 4 3 2 1

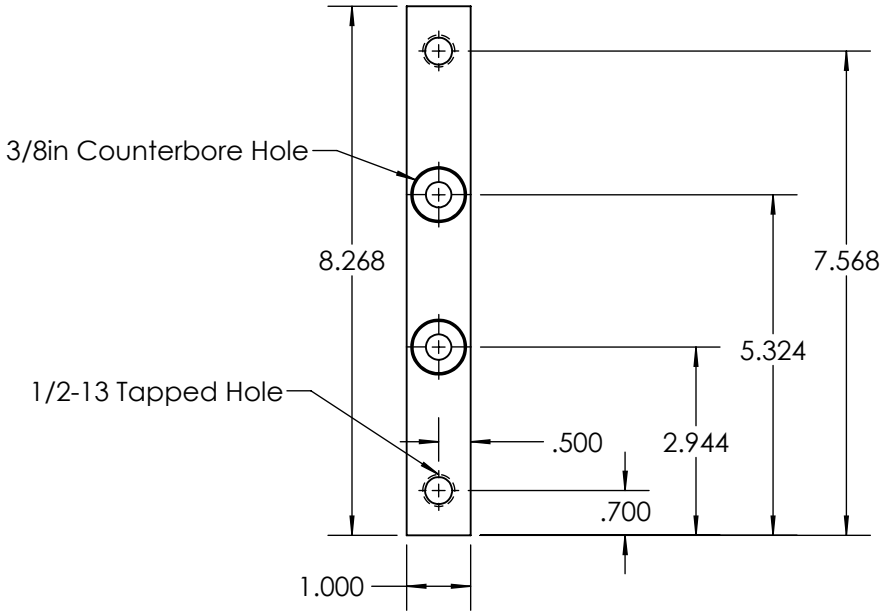

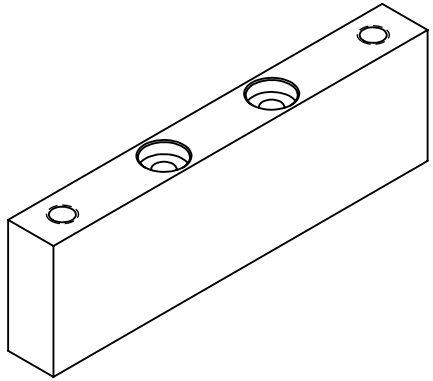

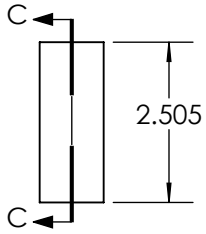

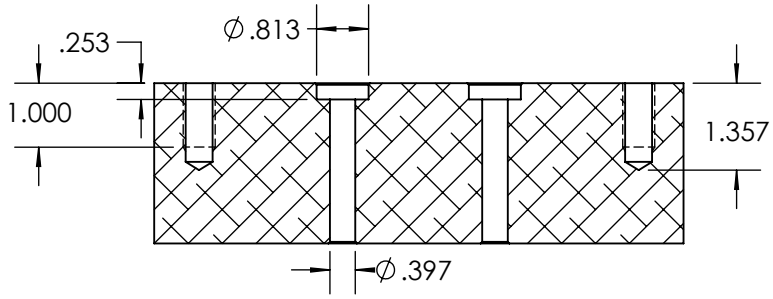

SECTION C-C
SCALE 1 : 3

ME429 Winter 2013 Mechanical Engineering CAL POLY	SCALE: 1:3	PART: Pillow Block Mounting Block
	UNITS: Inches	MATERIAL: 6061 Aluminum
	TOLERANCE: +/- .005	DATE: 2/2/2013
	DWG #:	

5 4 3 2 1

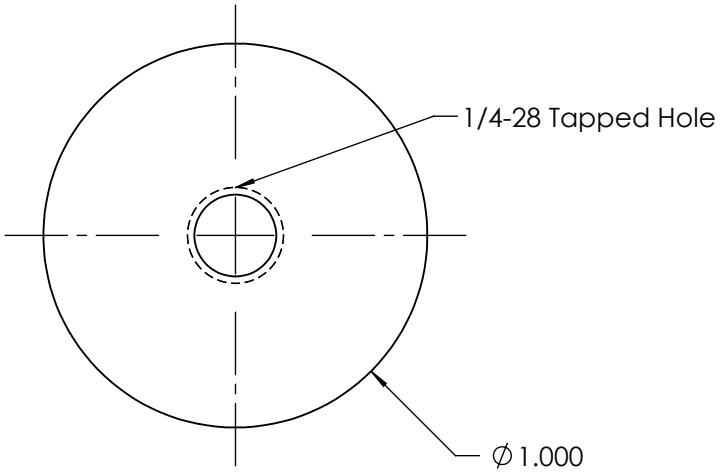

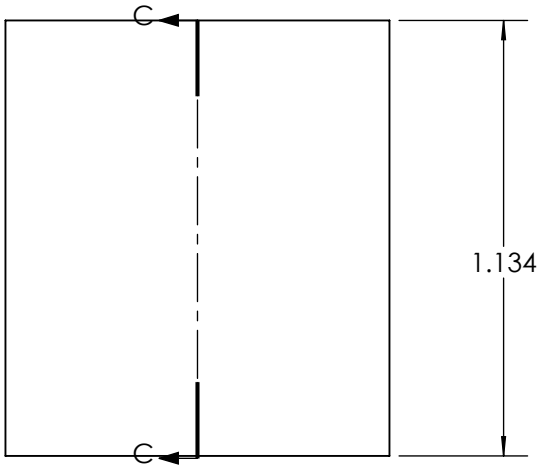

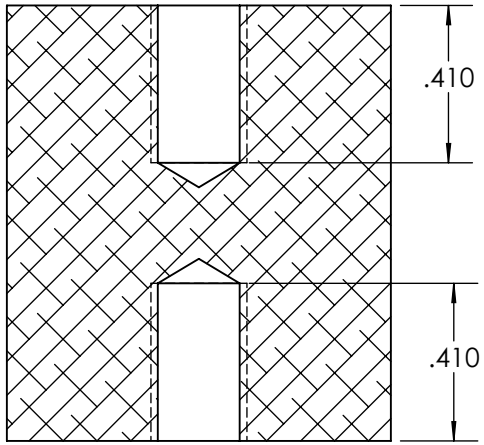

SECTION C-C

SCALE 2 : 1

ME429 Winter 2013 Mechanical Engineering CAL POLY	SCALE: 2:1	PART: Torque Arm Load Cell Block
	UNITS: Inches	MATERIAL: ASTM A 36 Steel
	TOLERANCE: +/- .05	DATE: 5/3/2013
	DWG #:	

5 4 3 2 1

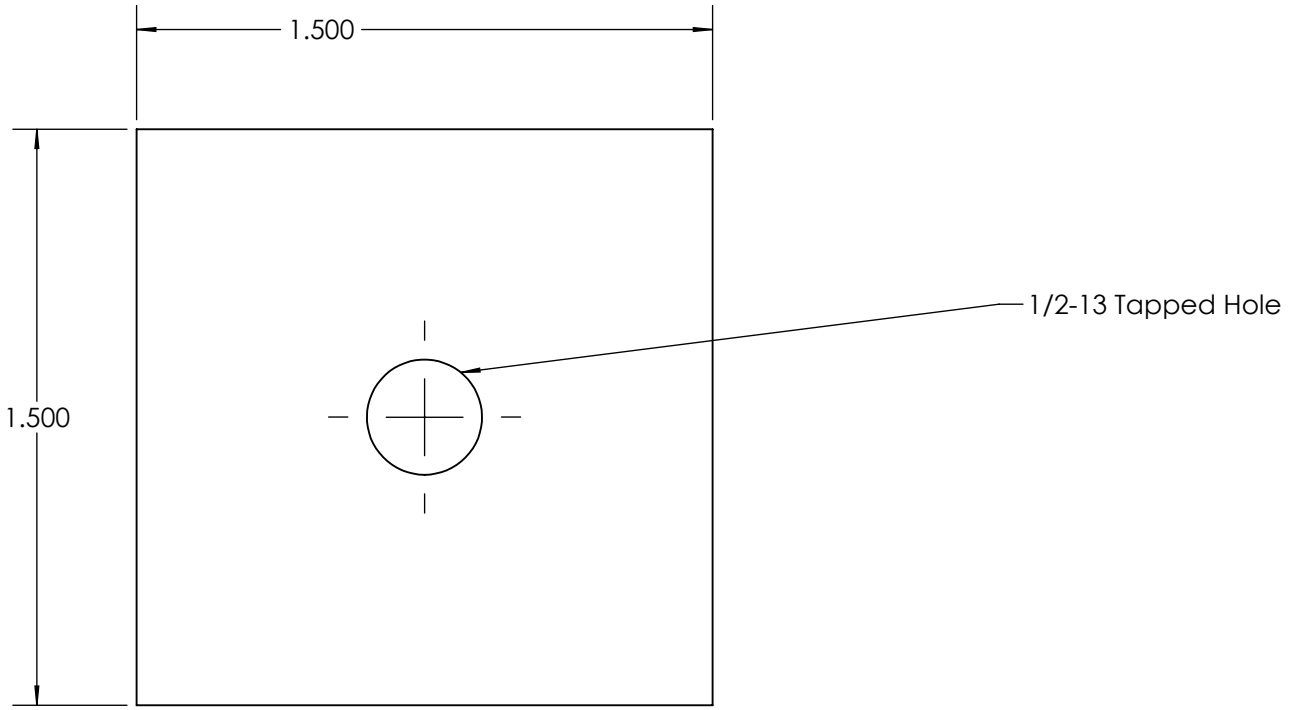

ME429 Winter 2013 Mechanical Engineering CAL POLY	SCALE: 1:1	PART: Leg Isolator Plate
	UNITS: Inches	MATERIAL: ASTM A36 Steel
	TOLERANCE: +/- .005	DATE: 4/18/2013
	DWG #:	

5 4 3 2 1

ITEM NO.	PART NUMBER	QTY.
1	Motor_SV207	1
2	Motor_Pillow Block	2
3	Motor_Back Plate	1
4	BIG BOLT CORP Hex Head Bolt_1_4_20_7_1_2	4
5	97135A210	4
6	Torque Arm Assembly_Weldment	1
7	Phillips pan head_Stainless steel 18_8__10_32 x 1_2	2

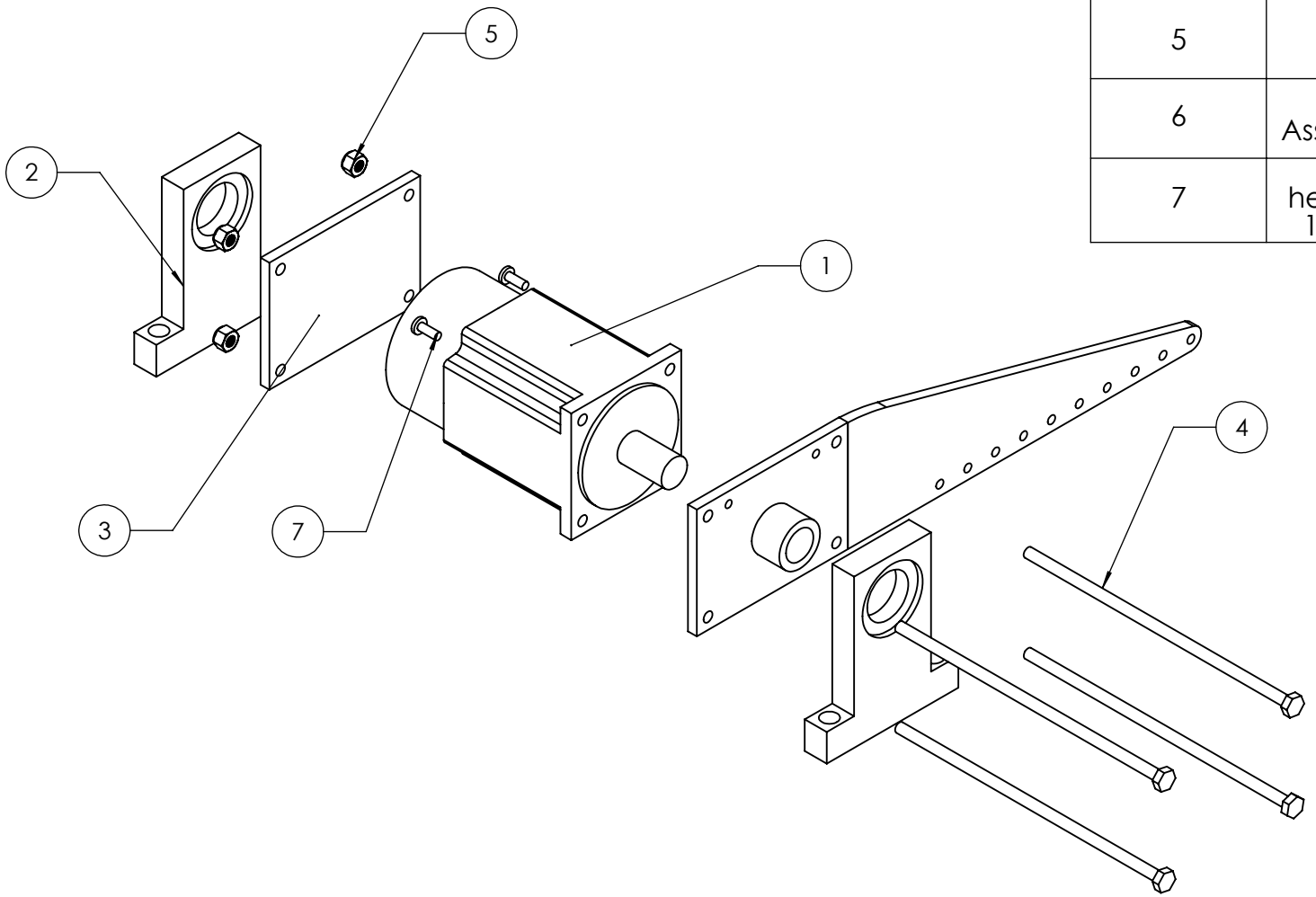

ME 429 Winter 2013

Mechanical Engineering CAL POLY

SCALE: 1:3.5	PART: Motor Torque Arm Pillow Block
UNITS:	MATERIAL:
TOLERANCE:	DATE: 2/2/2013
DWG #:	

5 4 3 2 1

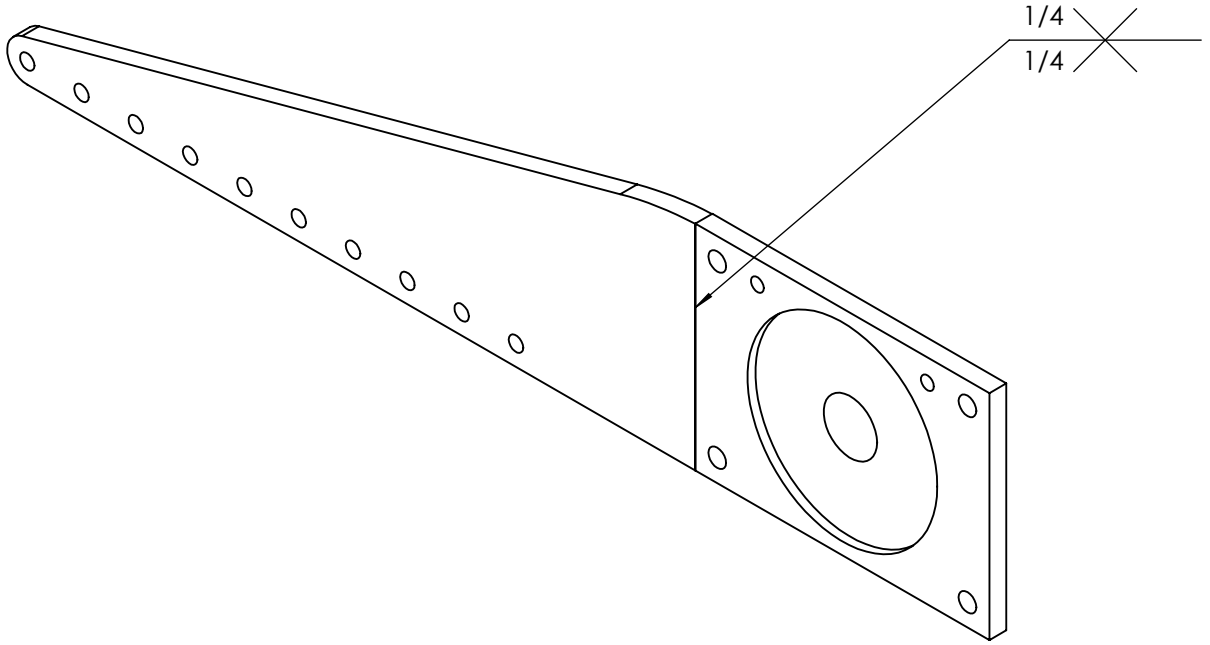

ME429 Winter 2013

Mechanical Engineering CAL POLY

SCALE: 1:2	PART: Torque Arm Assembly
UNITS:	MATERIAL: ASTM A36 Steel
TOLERANCE:	DATE: 6/6/2013
DWG #:	

5 4 3 2 1

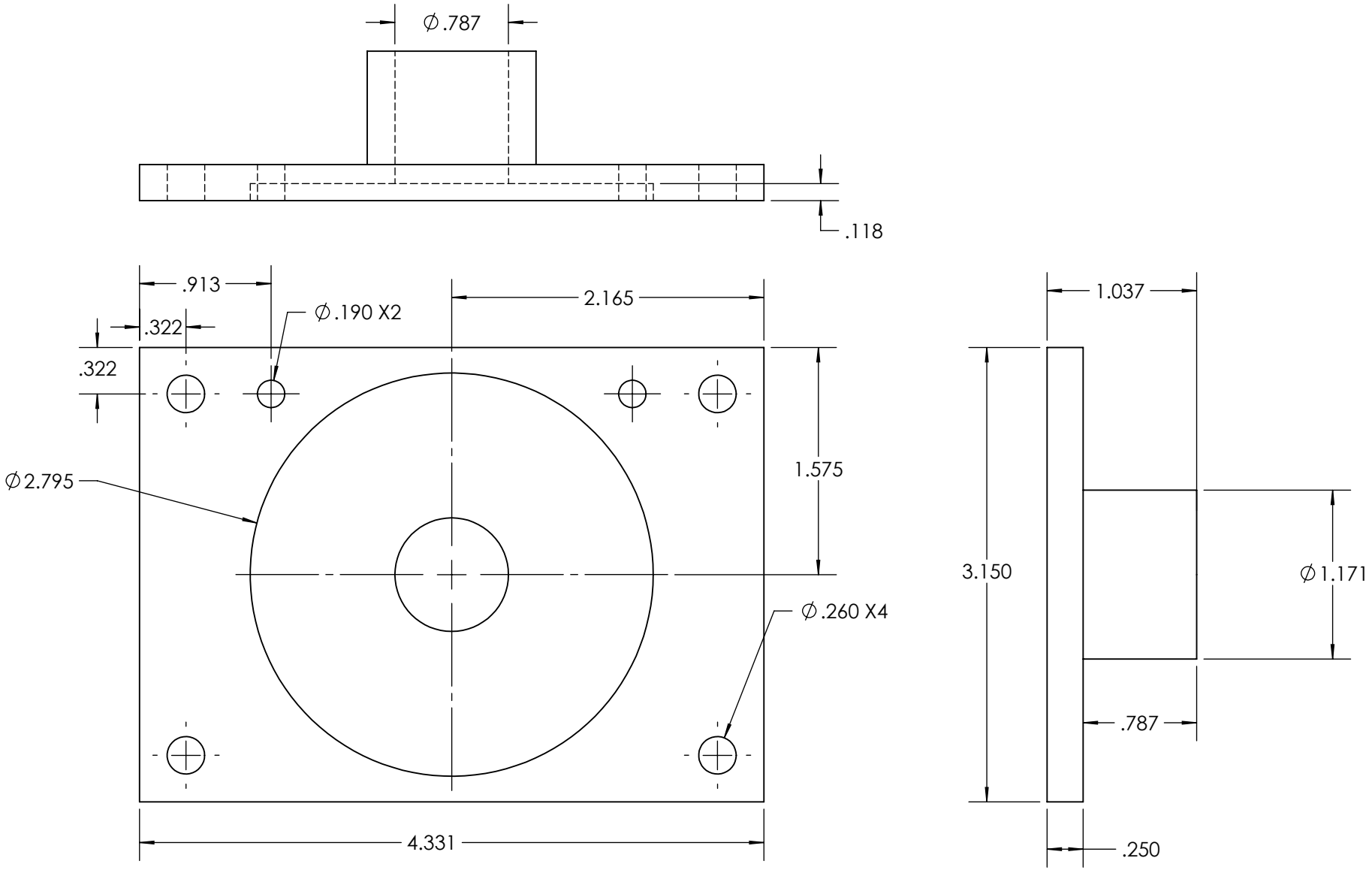

ME429 Winter 2013	SCALE: 1:1	PART: Torque Arm Adaptor_Motor Plate
Mechanical Engineering CAL POLY	UNITS: Inches	MATERIAL: ASTM A36 Steel
	TOLERANCE: +/- .005	DATE: 3/14/2013
	DWG #:	

5 4 3 2 1

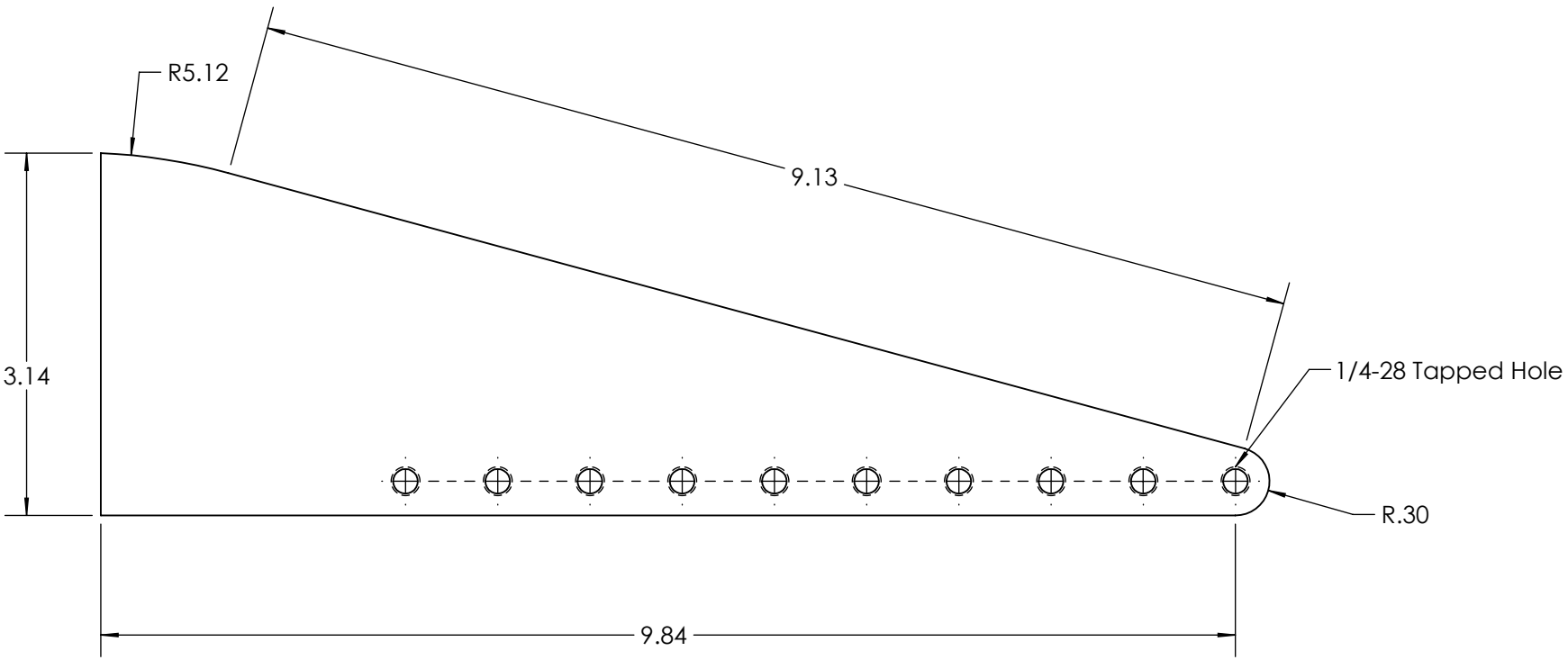

ME429 Winter 2013 Mechanical Engineering CAL POLY	SCALE: 2:3	PART: Torque Arm Adaptor
	UNITS: Inches	MATERIAL: ASTM A36 Steel
	TOLERANCE: +/- .5	DATE: 2/13/2013
	DWG #:	

5 4 3 2 1

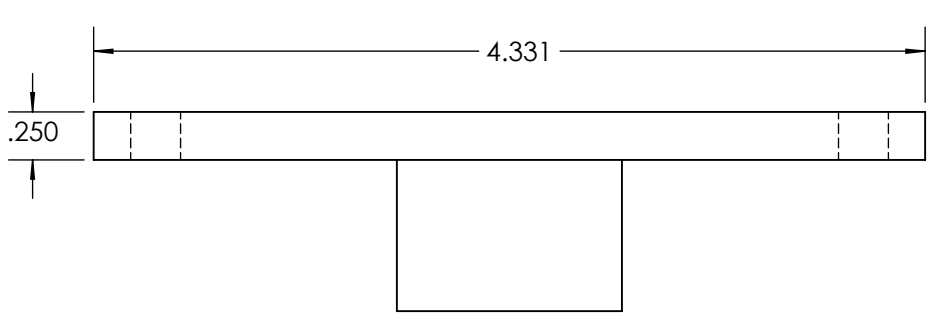

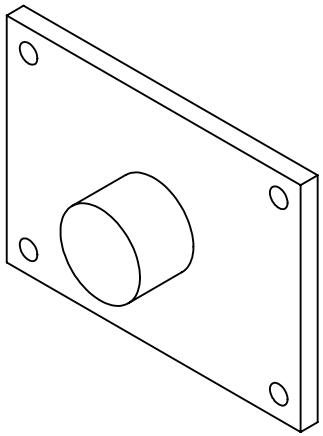

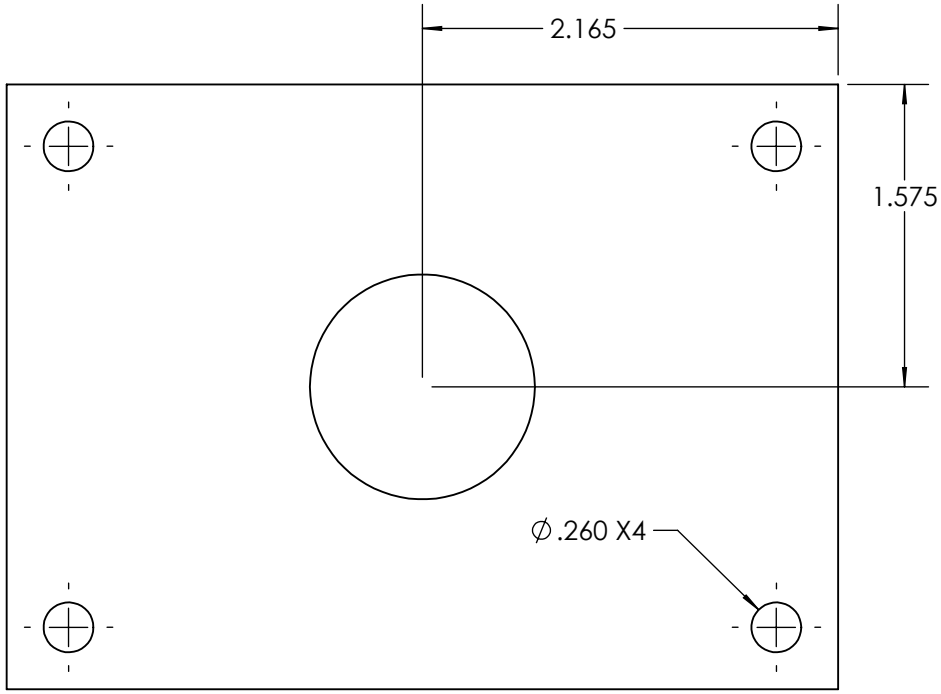

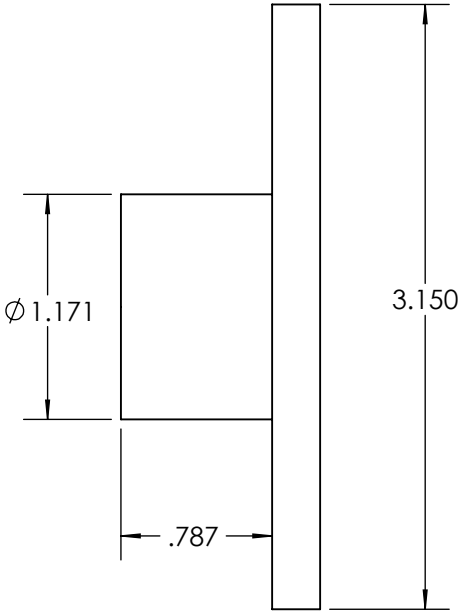

ME429 Winter 2013

Mechanical Engineering CAL POLY

SCALE: 1:1	PART: Motor Back Plate
UNITS: Inches	MATERIAL: ASTM A36 Steel
TOLERANCE: +/- .005 unless stated otherwise	DATE: 3/14/2013
DWG #:	

5 4 3 2 1

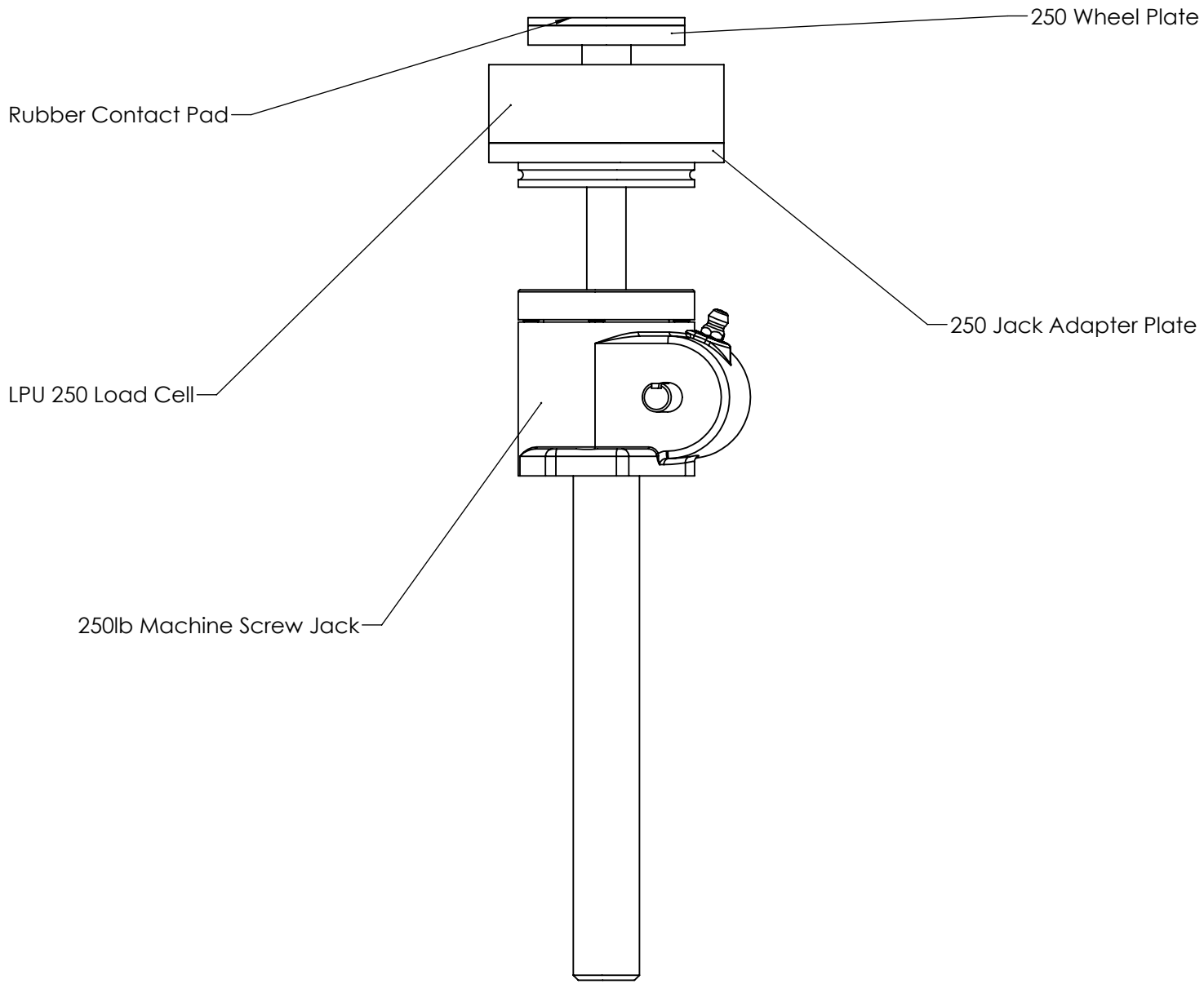

ME429 Winter 2013

Mechanical Engineering CAL POLY

SCALE: 1:4	PART: Rider Load Screw Jack Assembly
UNITS:	MATERIAL:
TOLERANCE:	DATE: 2/13/2013
DWG #:	

5 4 3 2 1

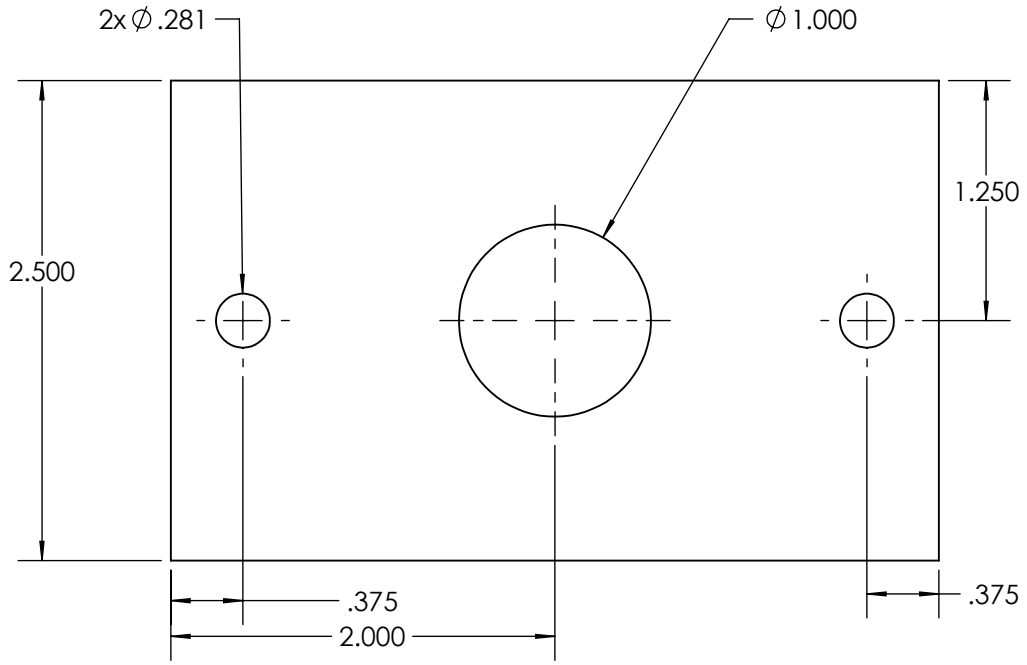

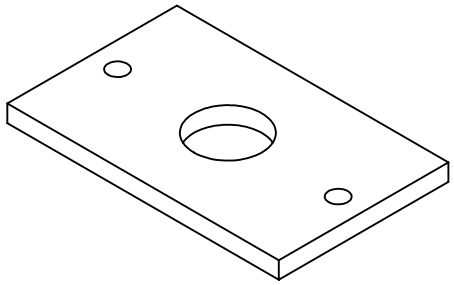

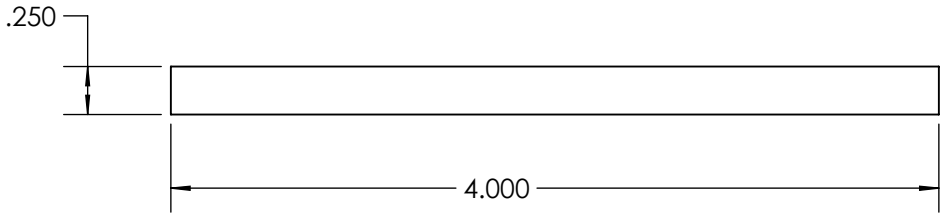

ME429 Winter 2013 Mechanical Engineering CAL POLY	SCALE: 1:8	PART: 250 Jack Spacing Plate
	UNITS: Inches	MATERIAL: ASTM A-36 Steel
	TOLERANCE: +/- .01	DATE: 2/15/2013
	DWG #:	

5 4 3 2 1

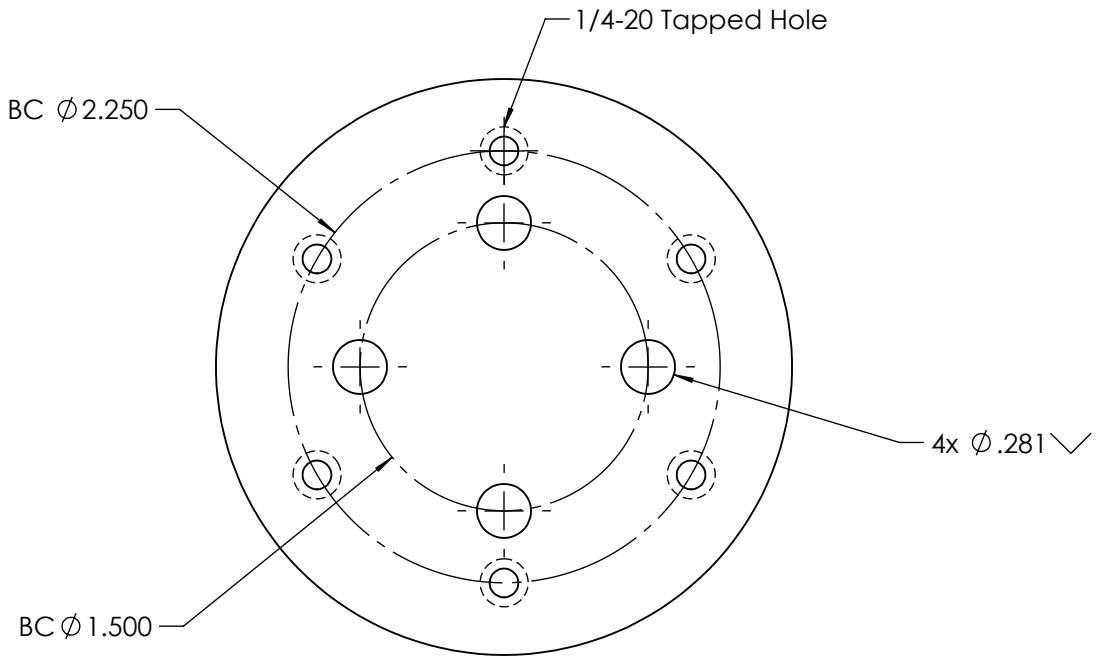

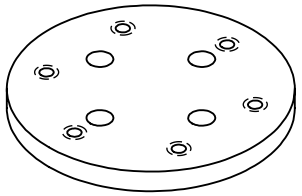

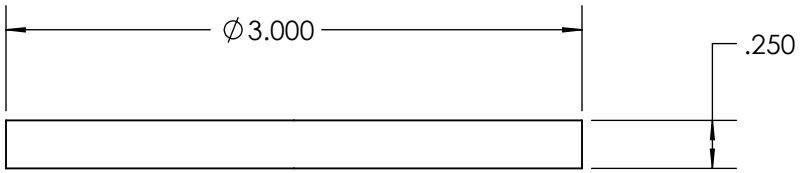

ME429 Winter 2013

Mechanical Engineering CAL POLY

SCALE: 1:2	PART: 250 Jack Mounting Plate
UNITS: Inches	MATERIAL: ASTM A36 Steel
TOLERANCE: +/-.01	DATE: 2/2/2013
DWG #:	

5 4 3 2 1

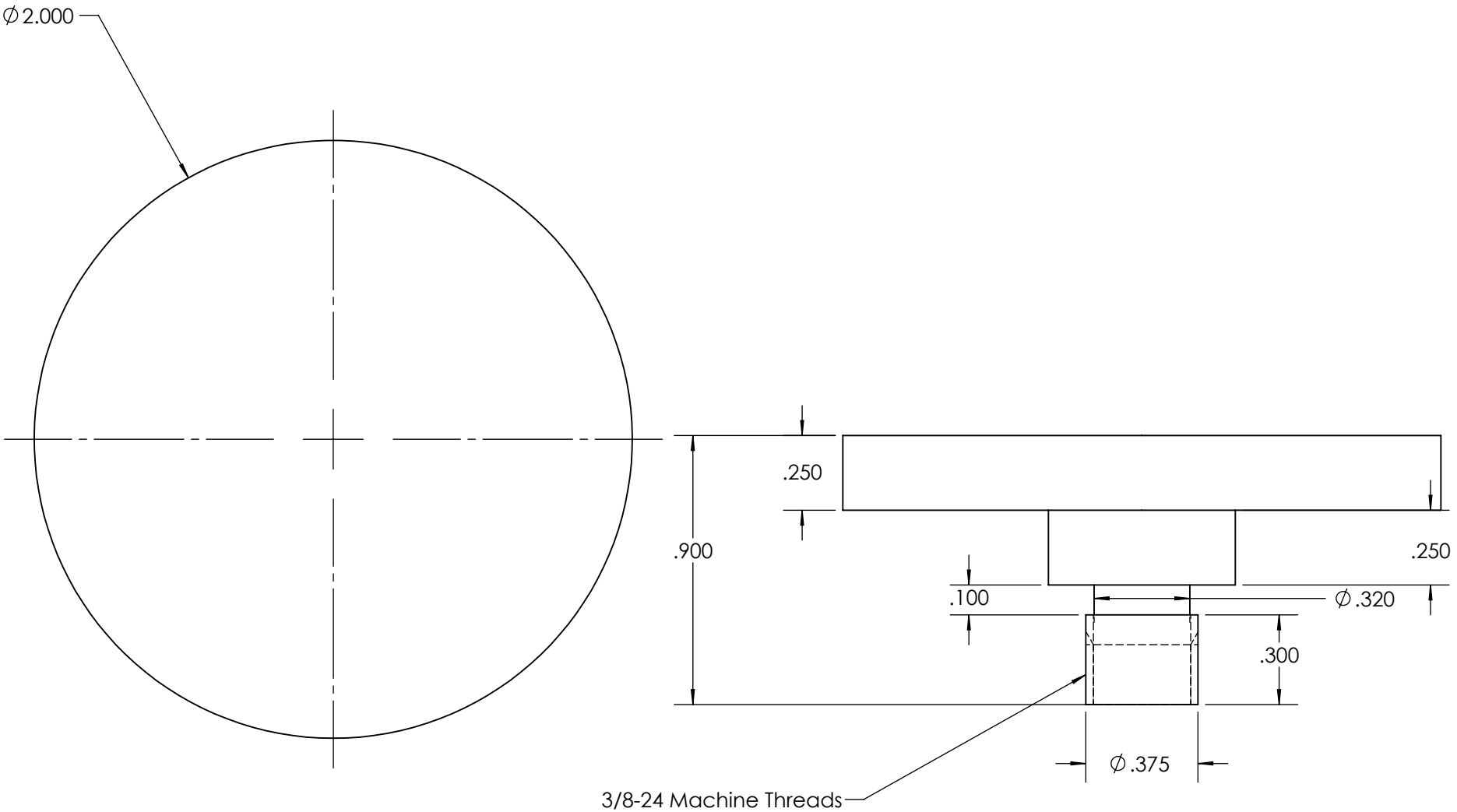

ME429 Winter 2013

Mechanical Engineering CAL POLY

SCALE: 2:1	PART: 250 Wheel Plate
UNITS: Inches	MATERIAL: Aluminum
TOLERANCE: +/- .005	DATE: 5/3/2013
DWG #:	

5 4 3 2 1

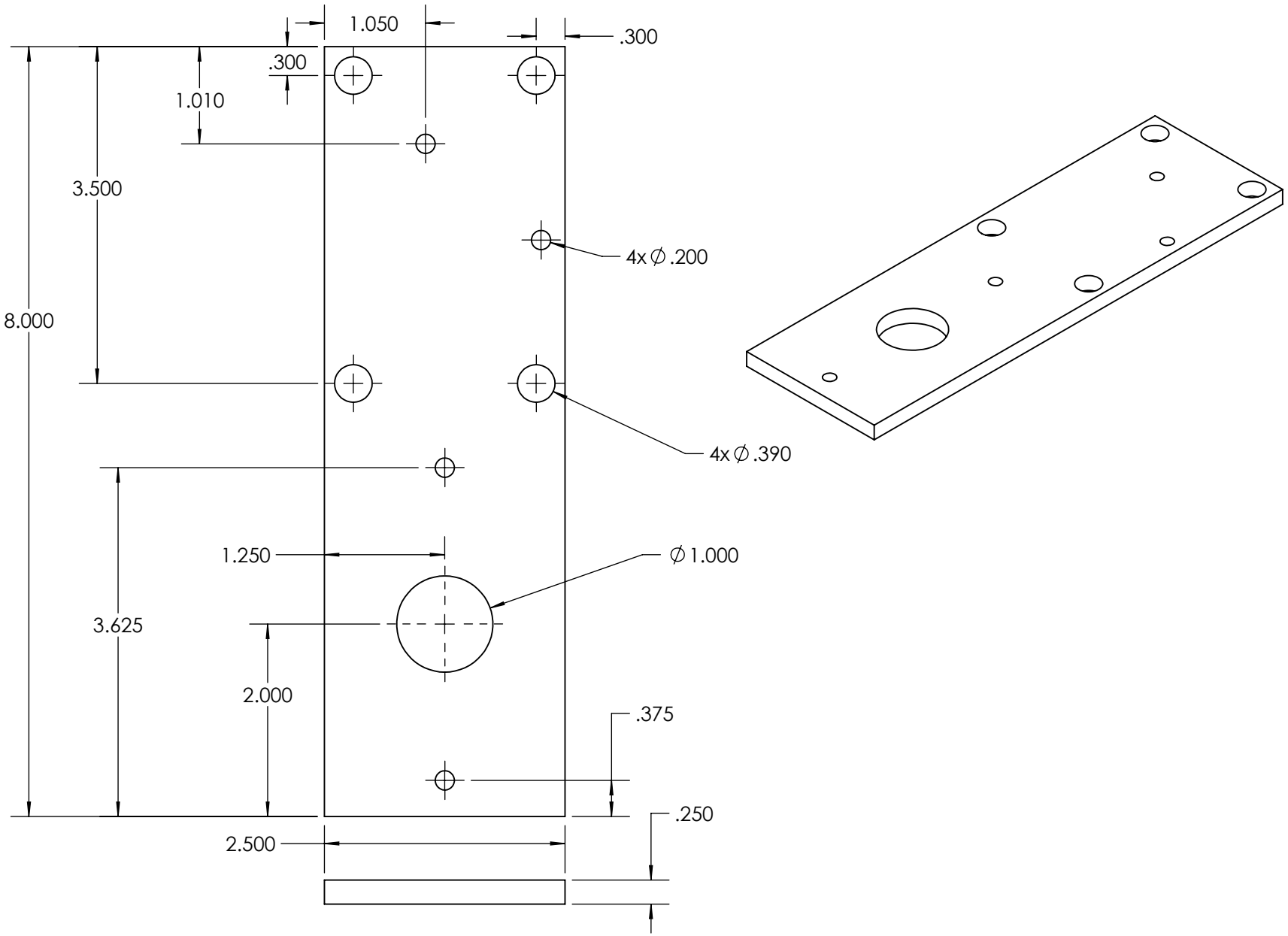

ME429 Winter 2013

Mechanical Engineering CAL POLY

SCALE: 1:1	PART: Rider Load Slide Plate
UNITS: Inches	MATERIAL: ASTM A36 Steel
TOLERANCE: +/-.05	DATE: 2/2/2013
DWG #:	

5 4 3 2 1

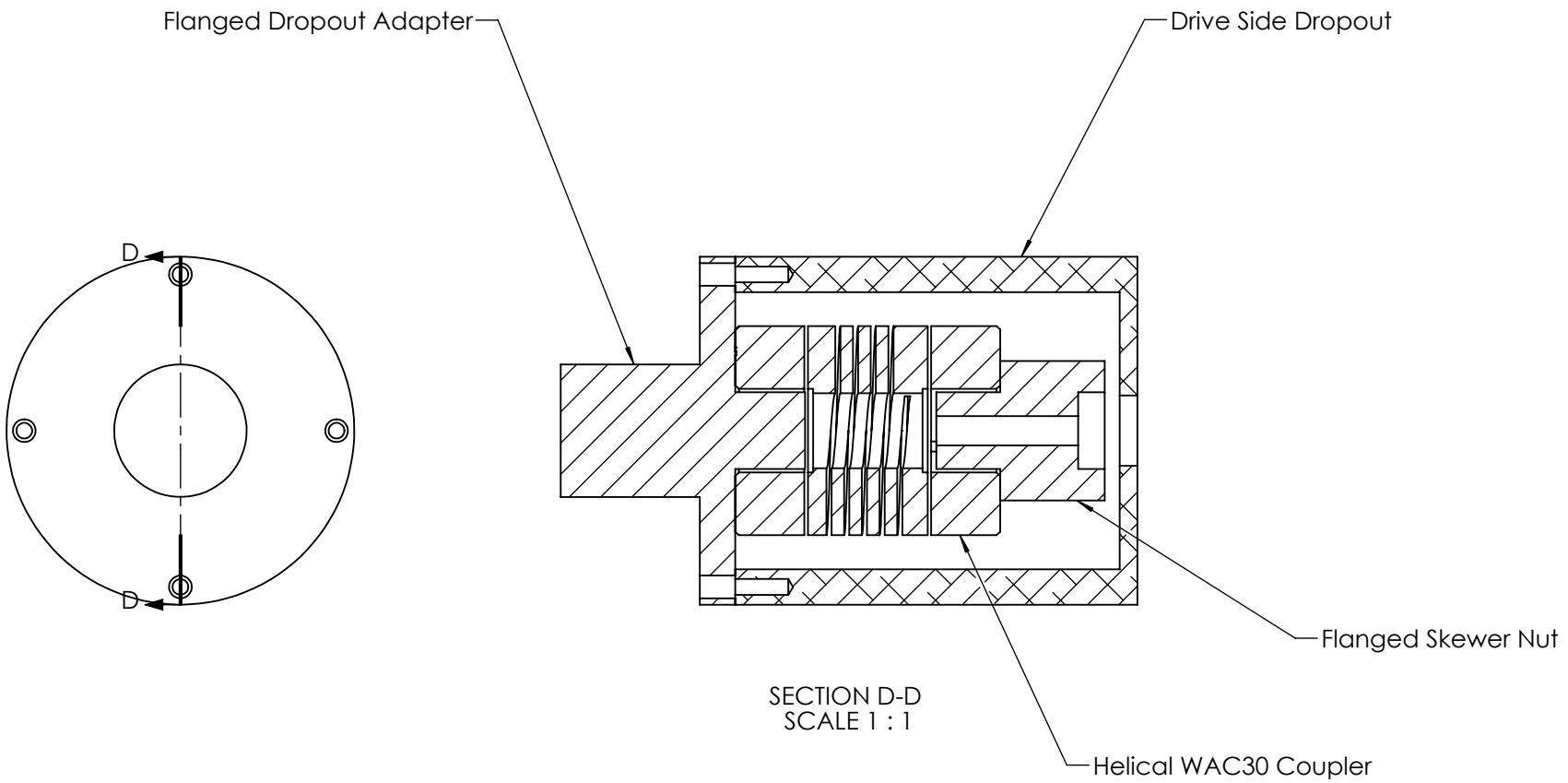

ME429 Winter 2013 Mechanical Engineering CAL POLY	SCALE: 1:1	PART: Flange Assembly
	UNITS:	MATERIAL:
	TOLERANCE:	DATE: 2/2/2013
	DWG #:	

5 4 3 2 1

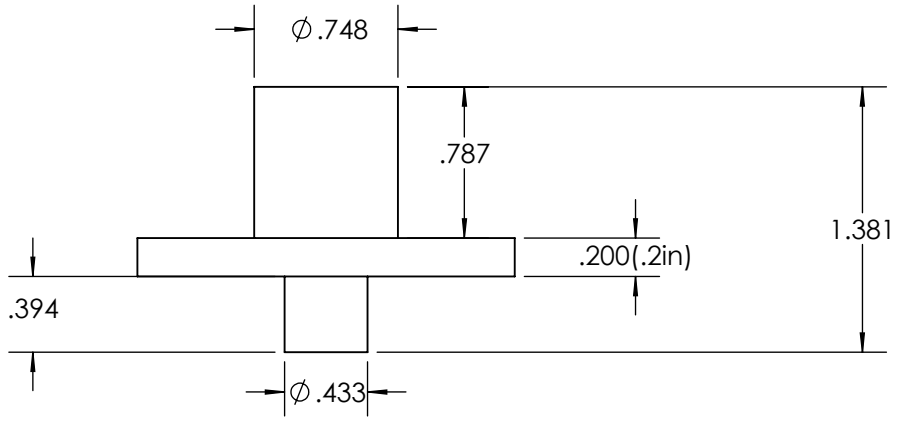

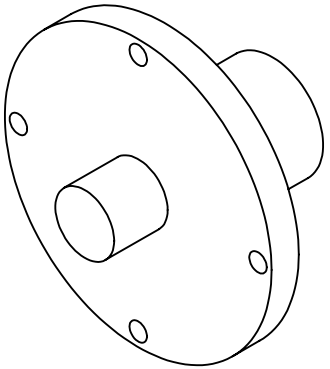

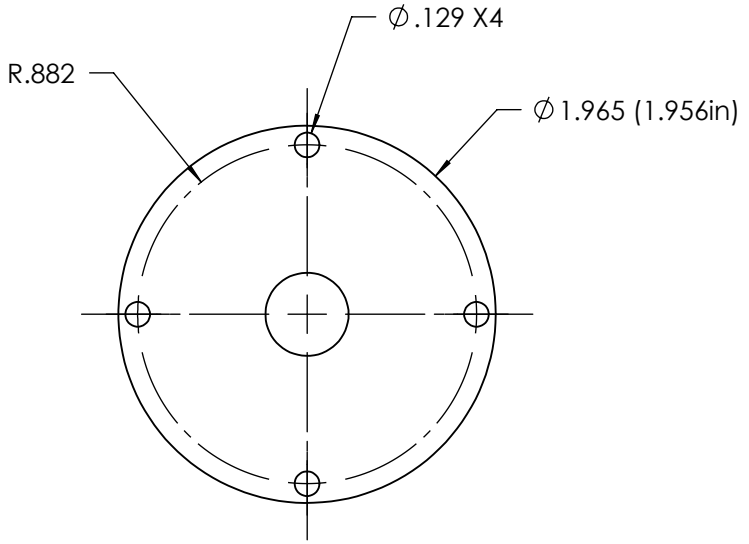

ME429 Winter 2013 Mechanical Engineering CAL POLY	SCALE: 1:1	PART: Flanged Adaptor
	UNITS: Inches	MATERIAL: 6061 Aluminum
	TOLERANCE: +/- .5	DATE: 2/2/2013
	DWG #:	

5 4 3 2 1

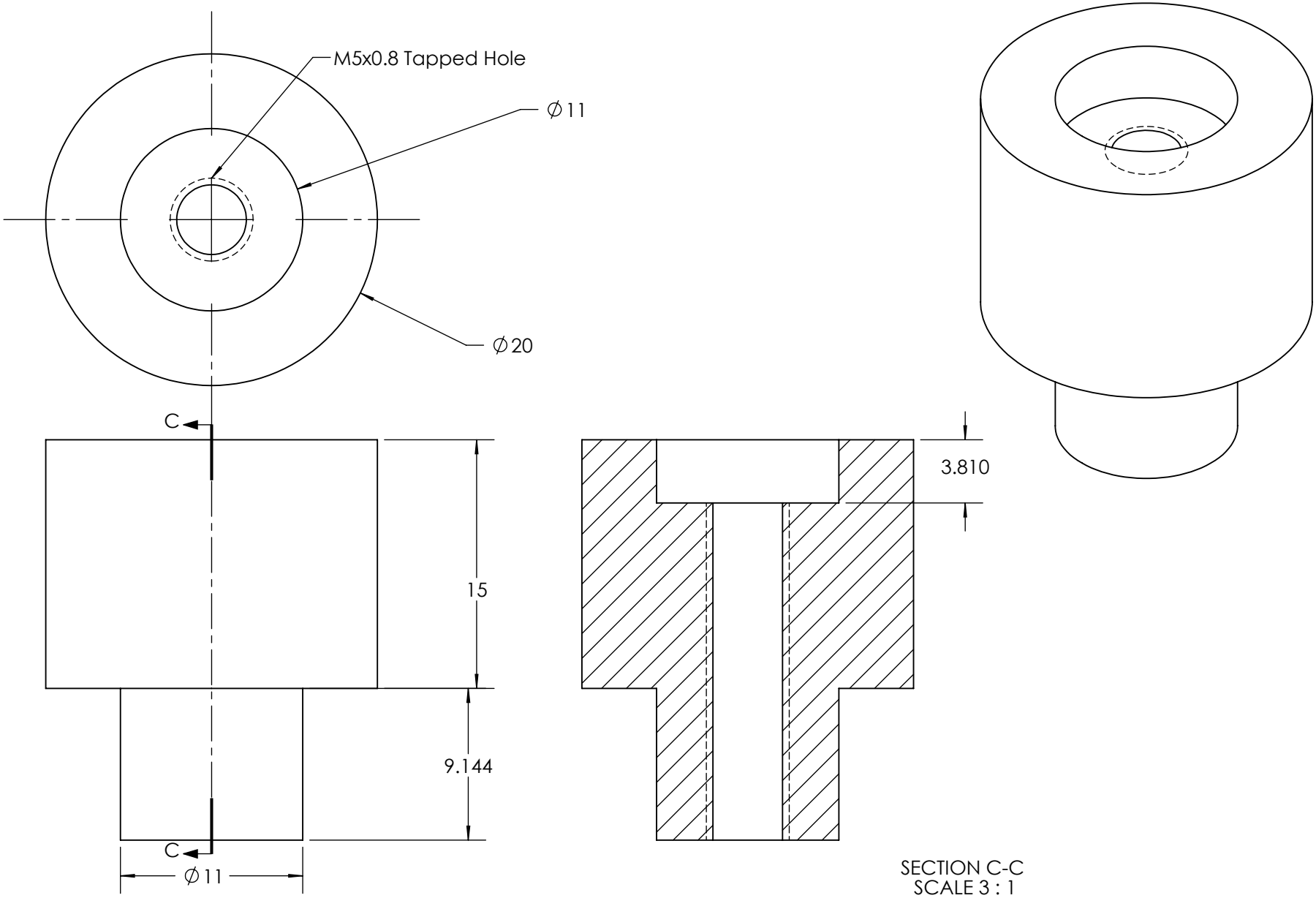

SECTION C-C
SCALE 3 : 1

ME429 Winter 2013

Mechanical Engineering CAL POLY

SCALE: 3:1	PART: Flanged Skewer Nut
UNITS: Millimeters	MATERIAL: 6061 Aluminum
TOLERANCE: +/- .5	DATE: 2/2/2013
DWG #:	

5 4 3 2 1

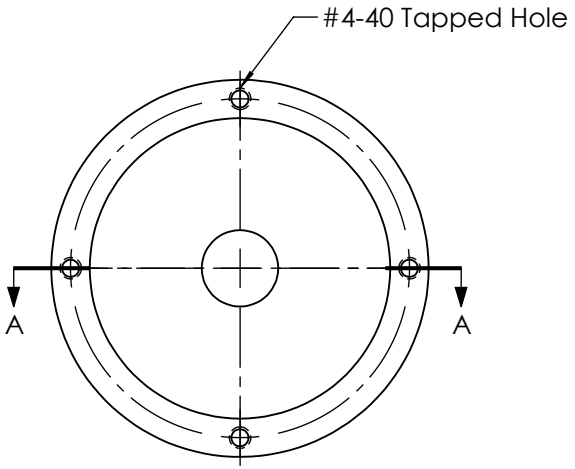

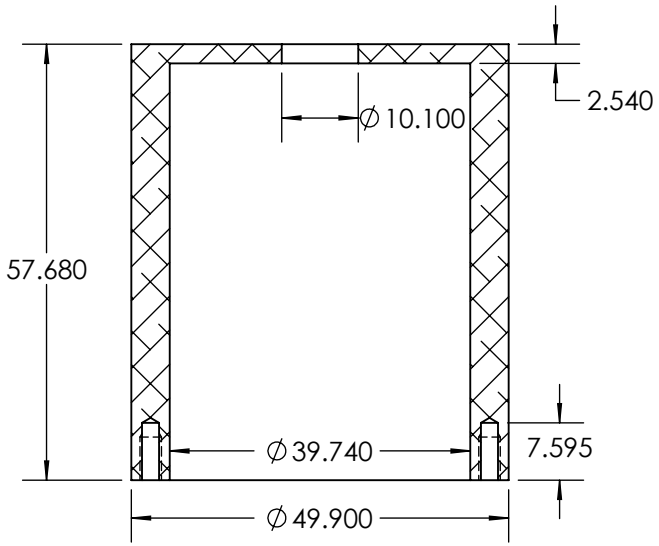

SECTION A-A
SCALE 1 : 1

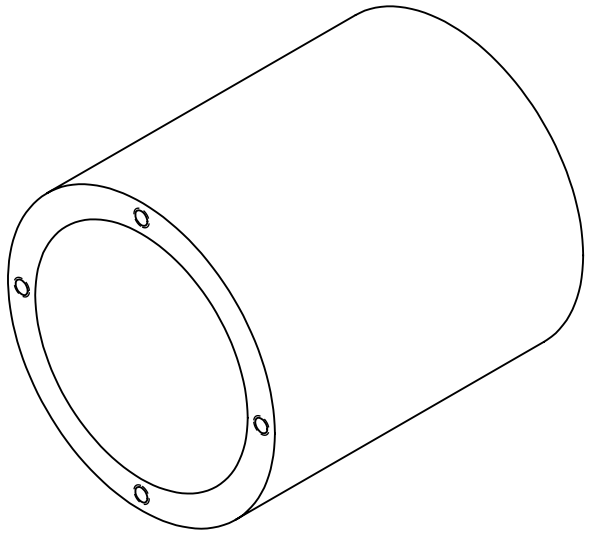

ME429 Winter 2013

Mechanical Engineering CAL POLY

SCALE: 1:1	PART: Drive Side Dropout
UNITS: Inches	MATERIAL: 6061 Aluminum
TOLERANCE: +/- .01	DATE: 3/16/2013
DWG #:	

5 4 3 2 1

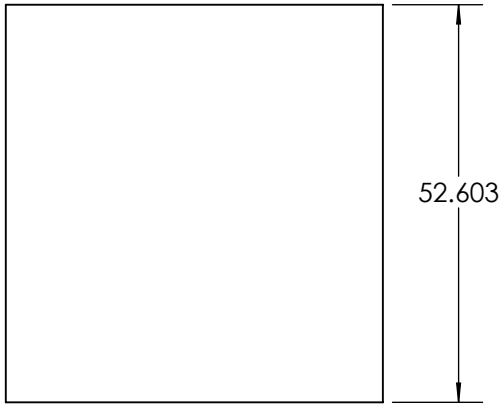

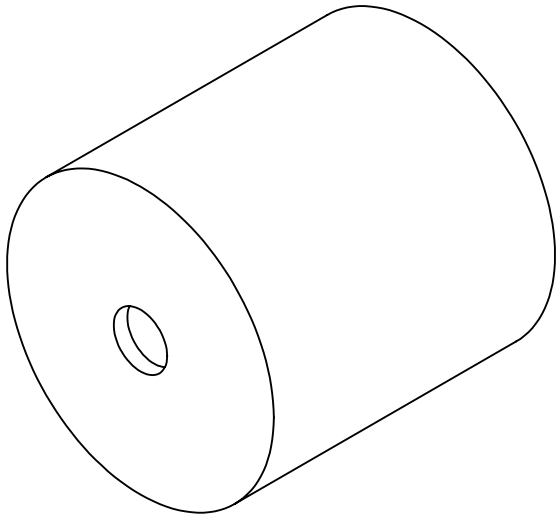

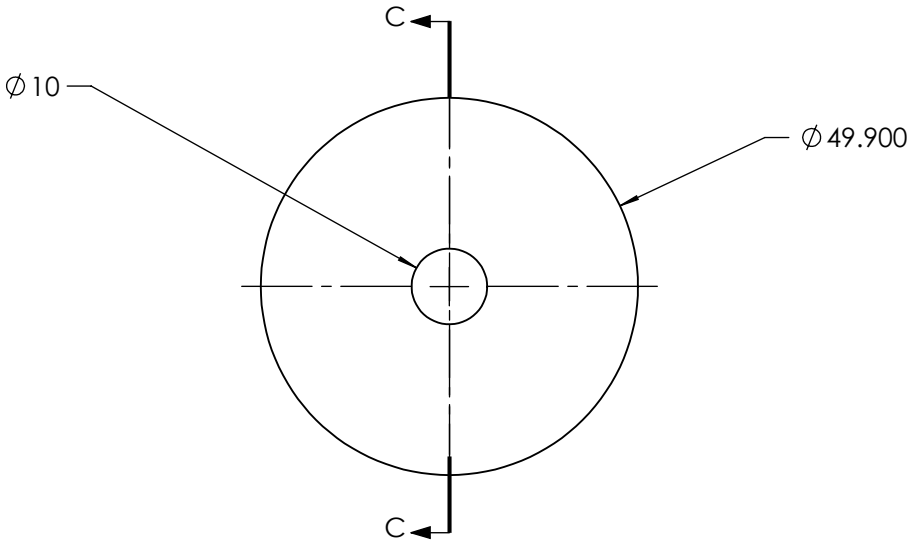

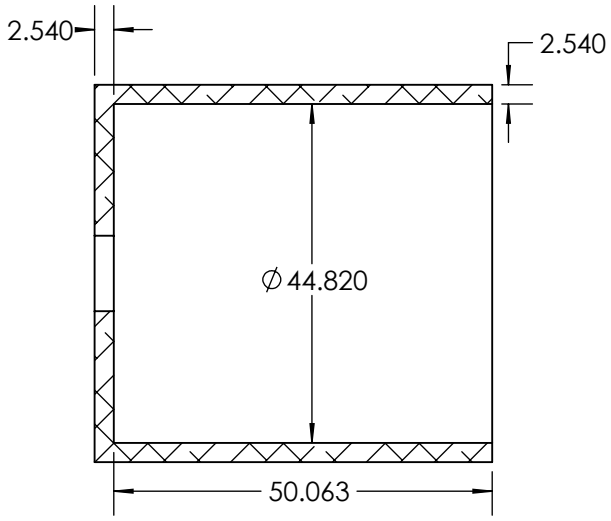

SECTION C-C
SCALE 1 : 1

ME429 Winter 2013

Mechanical Engineering CAL POLY

SCALE: 1:1	PART: Aluminum DO light
UNITS: Inches	MATERIAL: 6061 Aluminum
TOLERANCE: +/- .002	DATE: 2/2/2013
DWG #:	

5 4 3 2 1

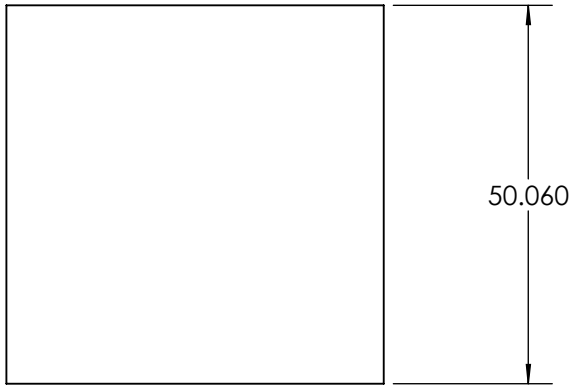

20mm hole can be tapped to accept whatever axle is selected

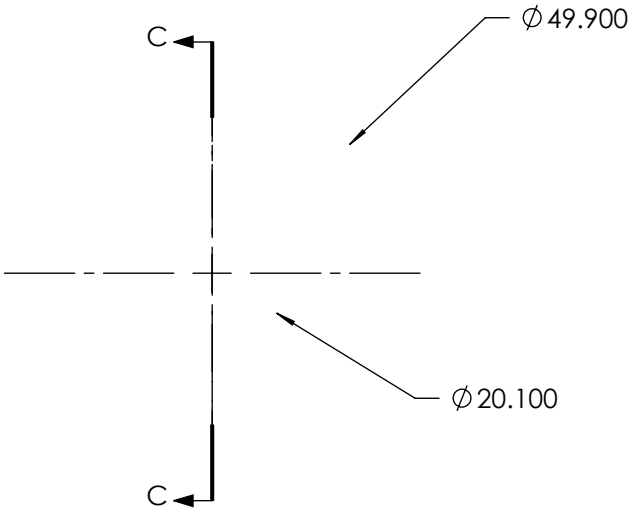

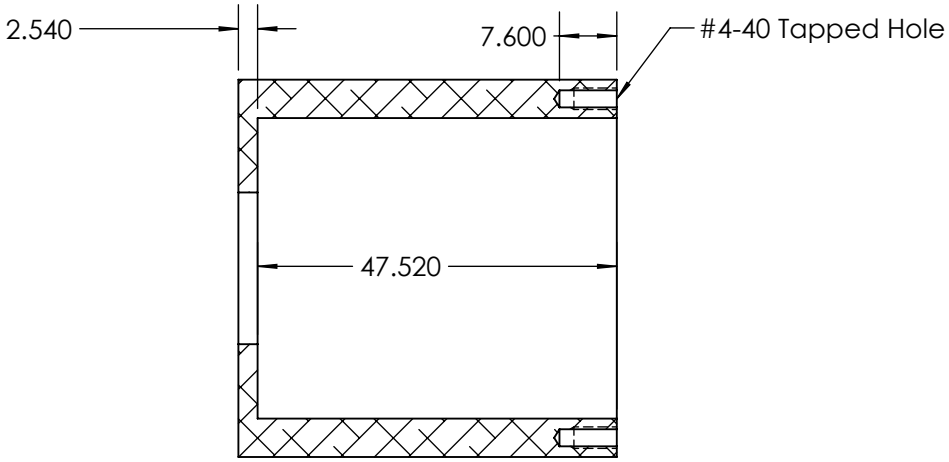

SECTION C-C

ME429 Winter 2013 Mechanical Engineering CAL POLY	SCALE: 1:1	PART: Drive Side Dropout_Light_20mm
	UNITS: Millimeters	MATERIAL: 6061 Aluminum
	TOLERANCE: +/- 0.1	DATE: 6/10/2013
	DWG #:	

5 4 3 2 1

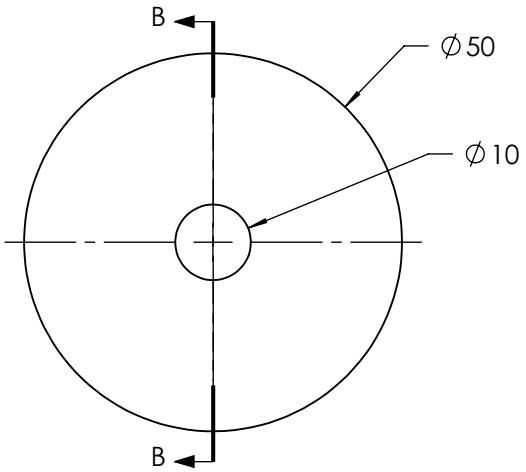

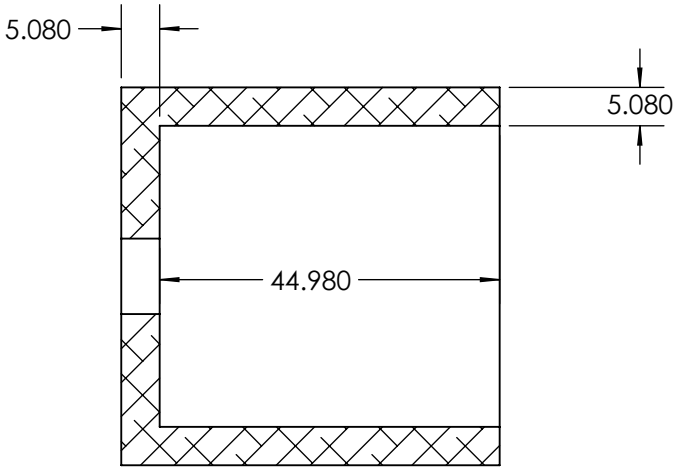

SECTION B-B

ME429 Winter 2013 Mechanical Engineering CAL POLY	SCALE: 1:1	PART: Dropout_Medium
	UNITS: Millimeters	MATERIAL: 6061 Aluminum
	TOLERANCE: +/- 0.1	DATE: 6/10/2013
	DWG #:	

5 4 3 2 1

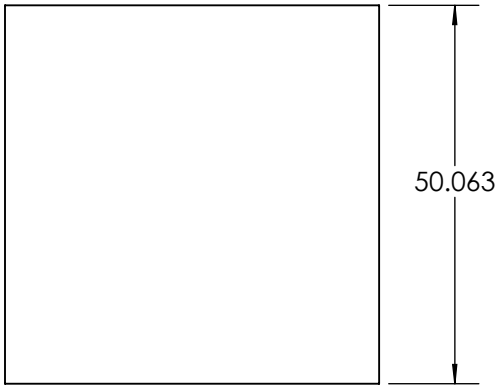

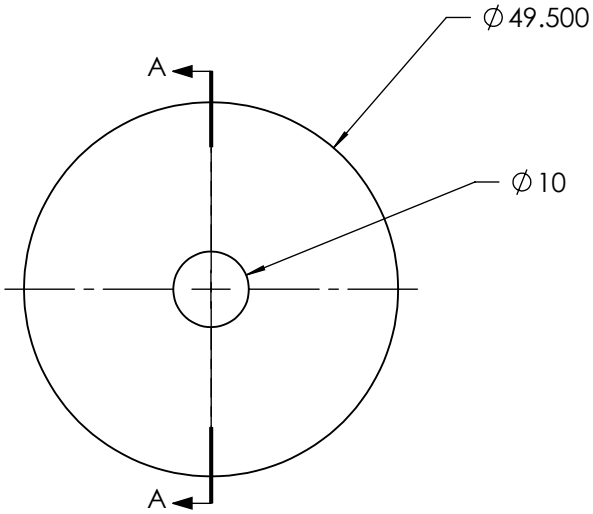

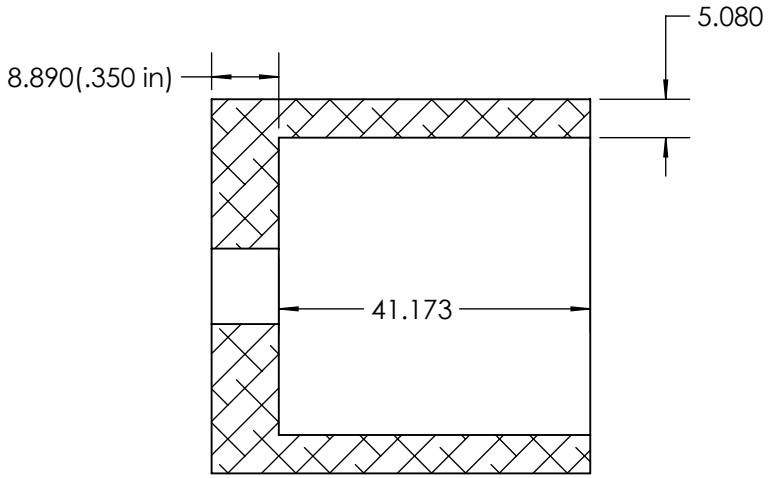

SECTION A-A

ME429 Winter 2013 Mechanical Engineering CAL POLY	SCALE: 1:1	PART: Dropout_Stiff
	UNITS: Millimeters	MATERIAL: 6061 Aluminum
	TOLERANCE: +/- 0.1	DATE: 6/10/2013
	DWG #:	

5 4 3 2 1

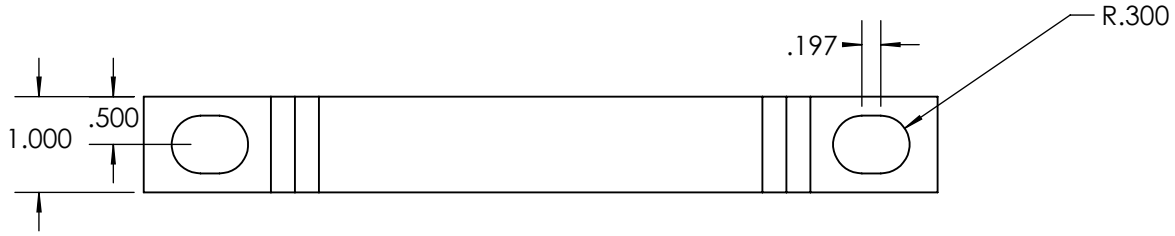

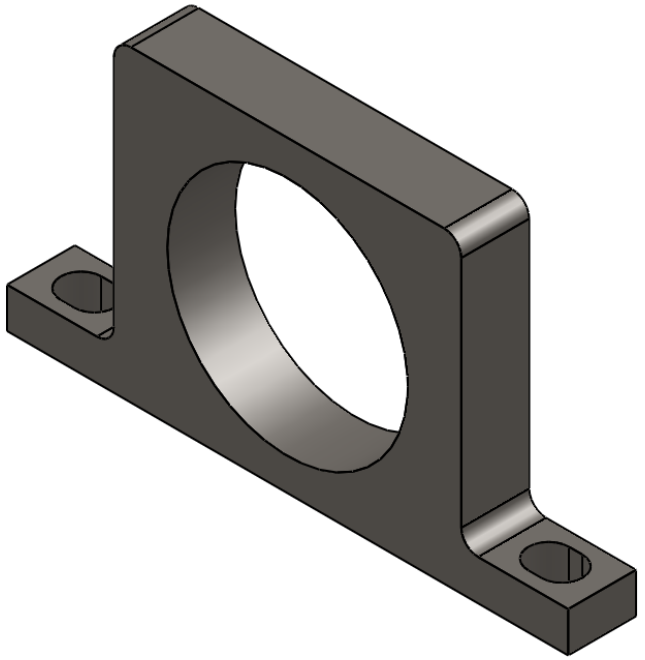

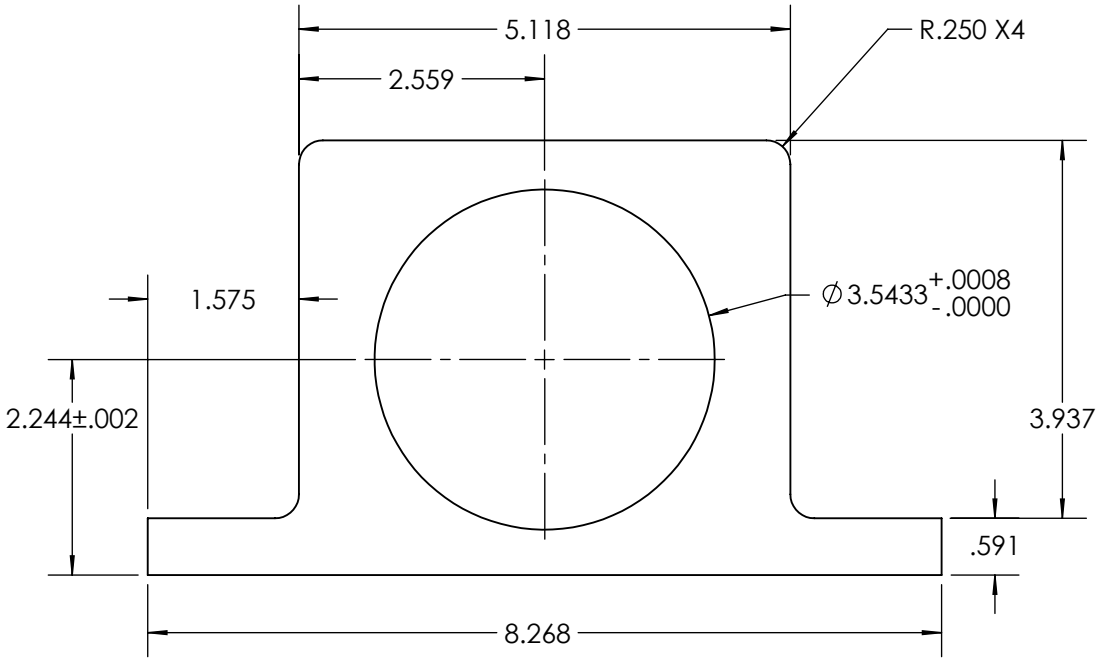

ME429 Winter 2013	SCALE: 1:2	PART: Machined Pillow Blocks
Mechanical Engineering CAL POLY	UNITS: Inches	MATERIAL: ASTM A36 Steel
	TOLERANCE: +/- .005 unless stated otherwise	DATE: 4/8/2013
	DWG #:	

5 4 3 2 1

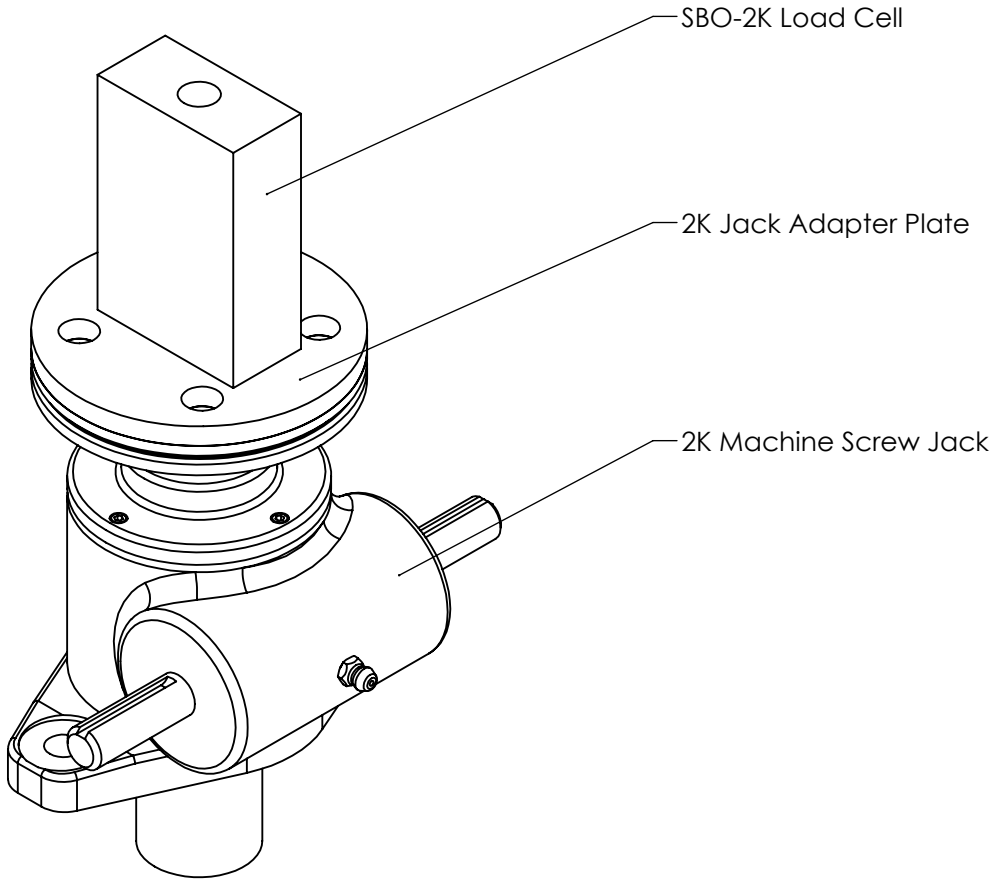

ME429 Winter 2013

Mechanical Engineering CAL POLY

SCALE: 1:2	PART: Chain Load Device Sub Asm
UNITS:	MATERIAL:
TOLERANCE:	DATE: 2/2/2013
DWG #:	

5 4 3 2 1

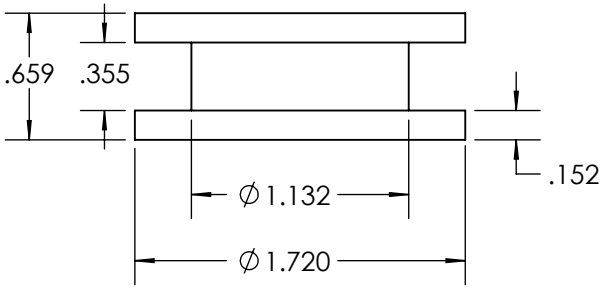

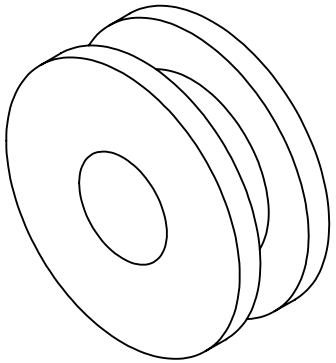

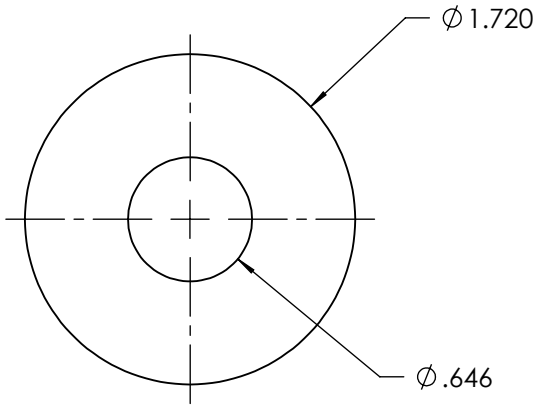

ME429 Winter 2013

Mechanical Engineering CAL POLY

SCALE: 1:1	PART: Chain Load Roller
UNITS: Inches	MATERIAL:Delrin
TOLERANCE: +/- .01	DATE: 2/2/2013
DWG #:	

5 4 3 2 1

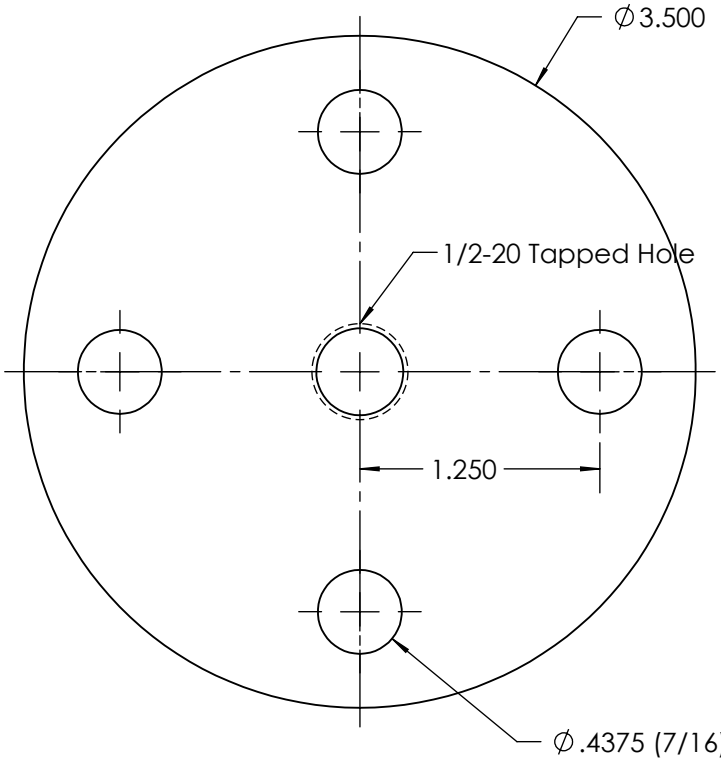

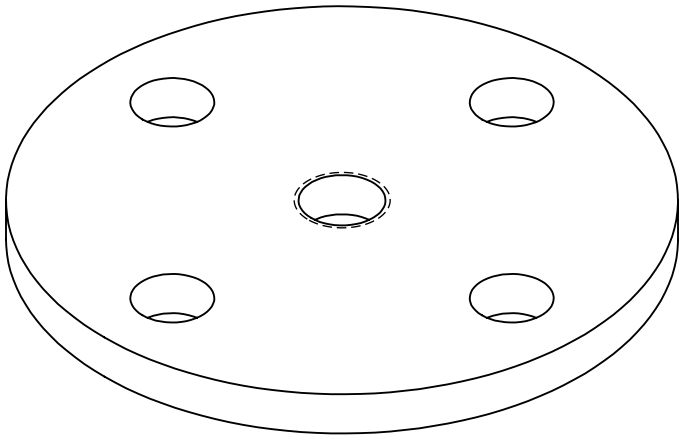

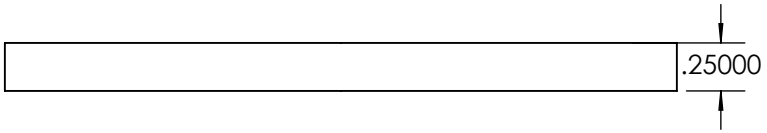

ME429 Winter 2013

Mechanical Engineering CAL POLY

SCALE: 1:1	PART: 2K Jack Adaptor Plate
UNITS: Inches	MATERIAL: ASTM A36 Steel
TOLERANCE:	DATE: 2/2/2013
DWG #:	

5 4 3 2 1

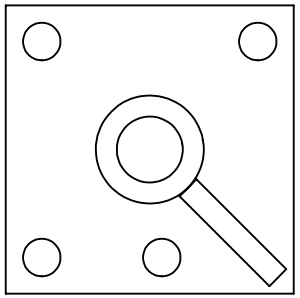

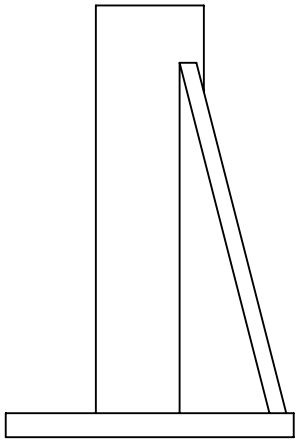

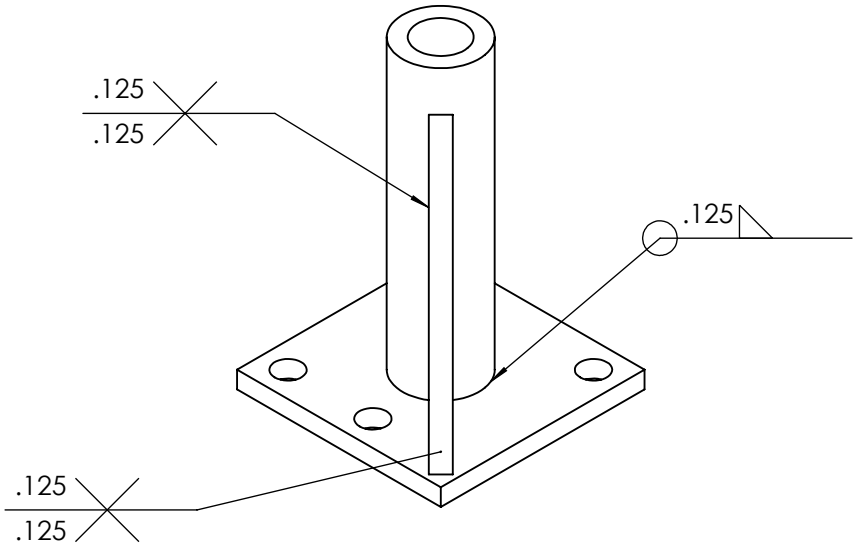

ME429 Winter 2013	SCALE: 1:1	PART: Pulley Mount Assembly
Mechanical Engineering CAL POLY	UNITS: Inches	MATERIAL: ASTM A36 Steel
	TOLERANCE: +/- .005	DATE: 3/16/2013
	DWG #:	

5 4 3 2 1

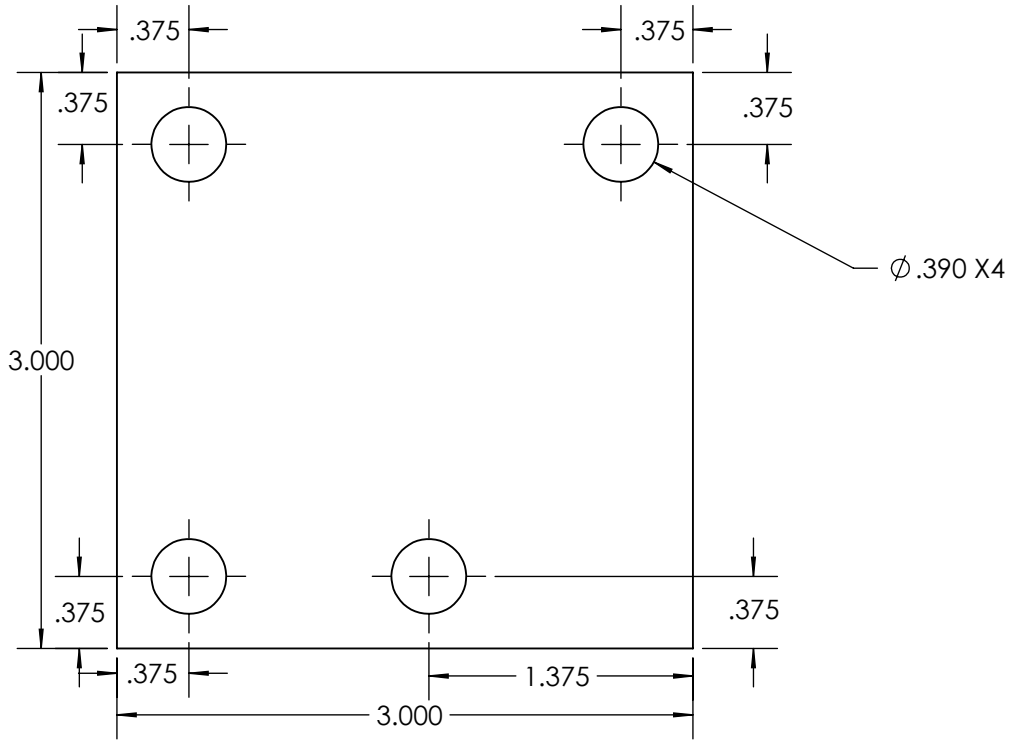

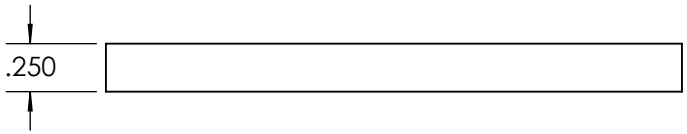

ME429 Winter 2013 Mechanical Engineering CAL POLY	SCALE: 1:1	PART: Pulley Mount Base
	UNITS: Inches	MATERIAL: ASTM A36 Steel
	TOLERANCE: +/- .005	DATE: 3/16/2013
	DWG #:	

5 4 3 2 1

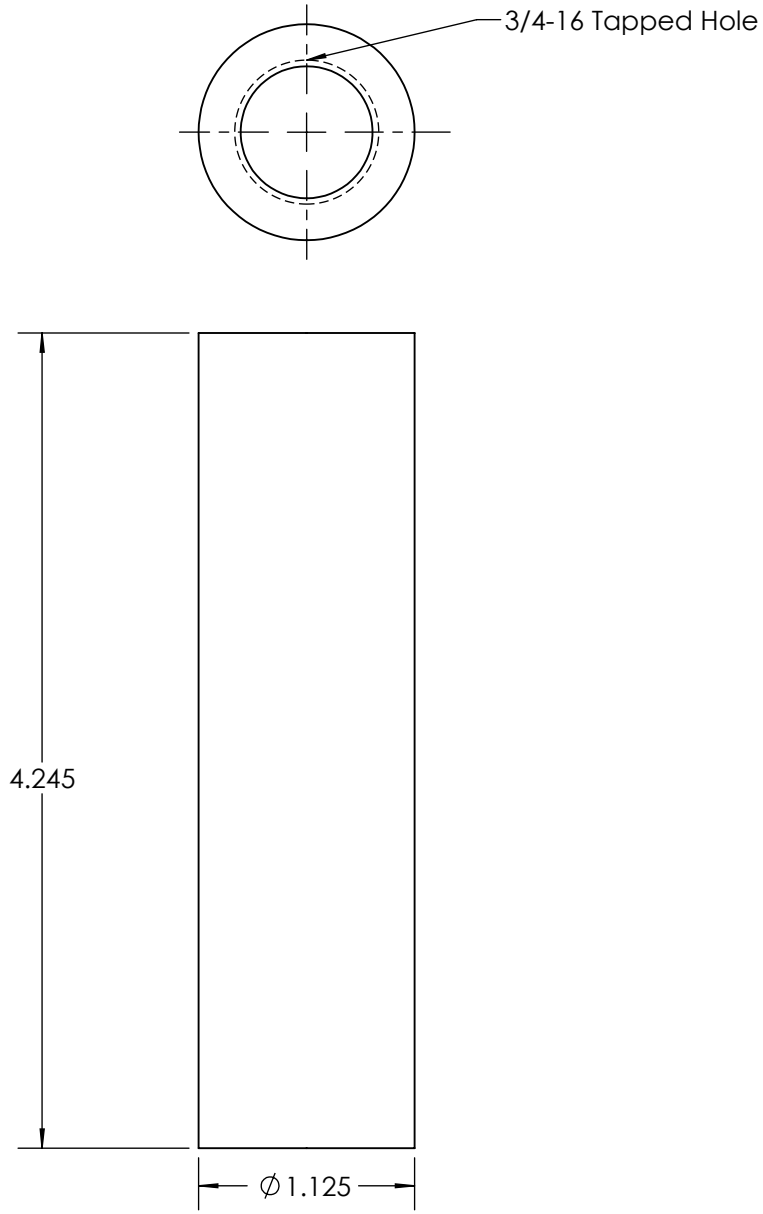

ME429 Winter 2013

Mechanical Engineering CAL POLY

SCALE: 1:1	PART: Pulley Mount Tower
UNITS: Inches	MATERIAL: ASTM A36 Steel
TOLERANCE: +/- .005	DATE: 3/16/2013
DWG #:	

5 4 3 2 1

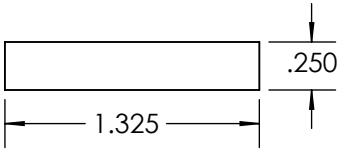

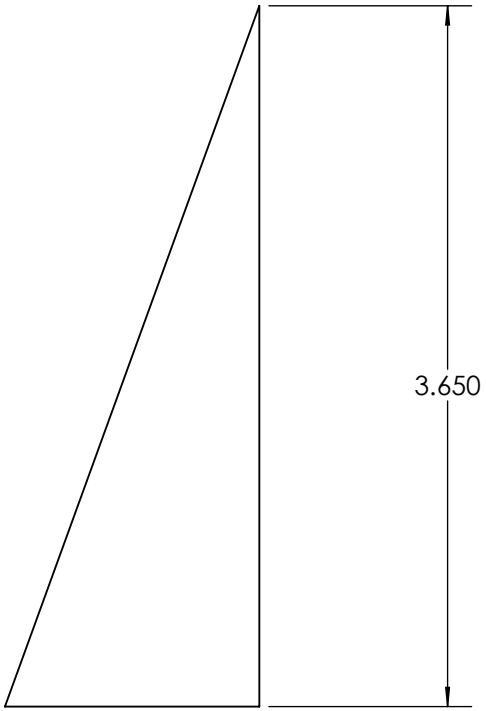

ME429 Winter 2013

Mechanical Engineering CAL POLY

SCALE: 1:1	PART: Pulley Mount Triangle
UNITS: Inches	MATERIAL: ASTM A36 Steel
TOLERANCE: +/- .005	DATE: 3/16/2013
DWG #:	

5 4 3 2 1

A. LINE COLOR DENOTES WIRE COLOR ON MACHINE

B. LINE REPRESENTS 3 SETS OF WIRES GOING INTO PSM-F10

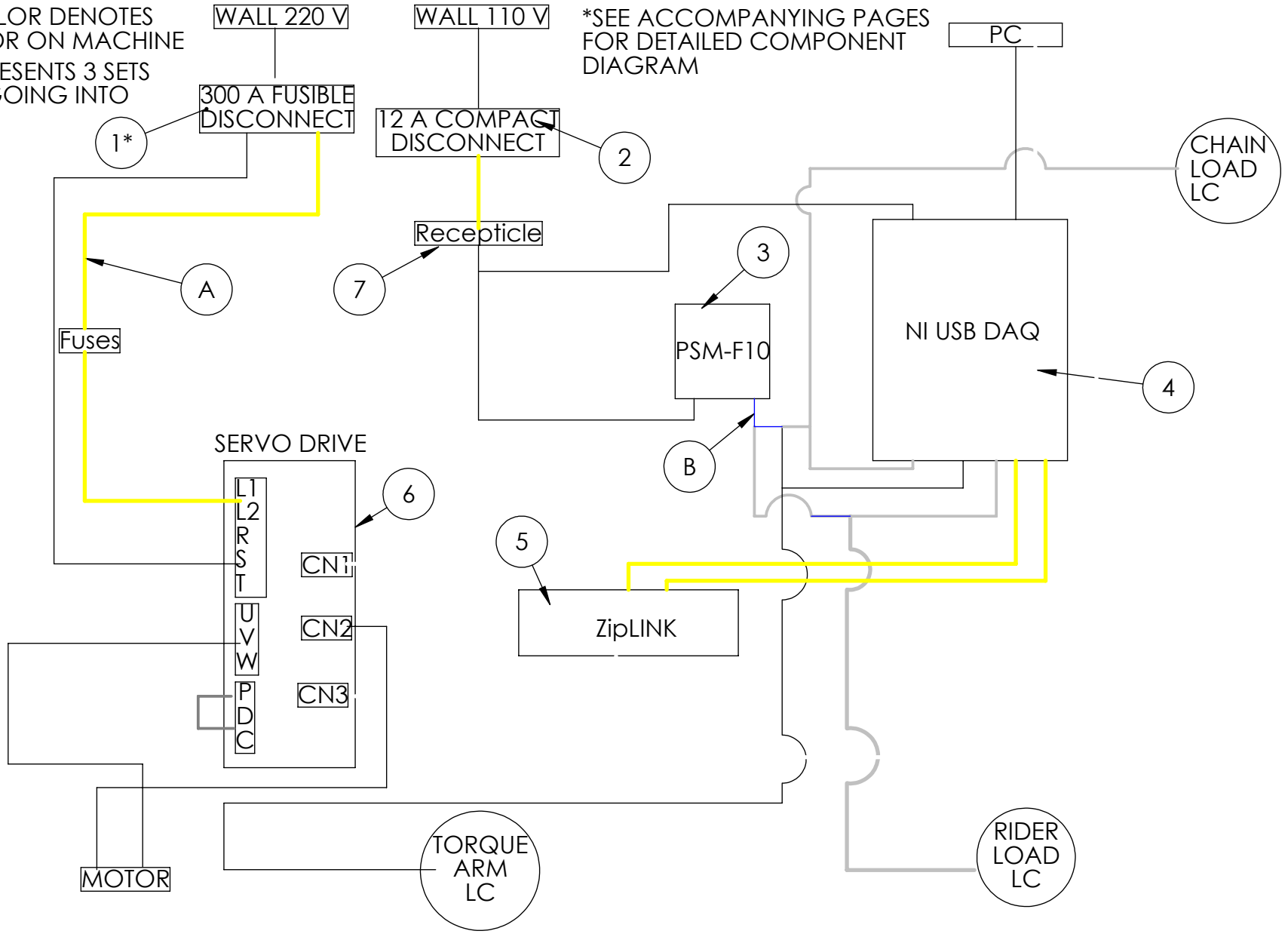

ME430 SPRING 2013

Mechanical Engineering CAL POLY

SCALE:	PART:
UNITS:	MATERIAL:
TOLERANCE:	DATE:
DWG #:	

5 4 3 2 1

DIAGRAM 1:FUSED DISCONNECT

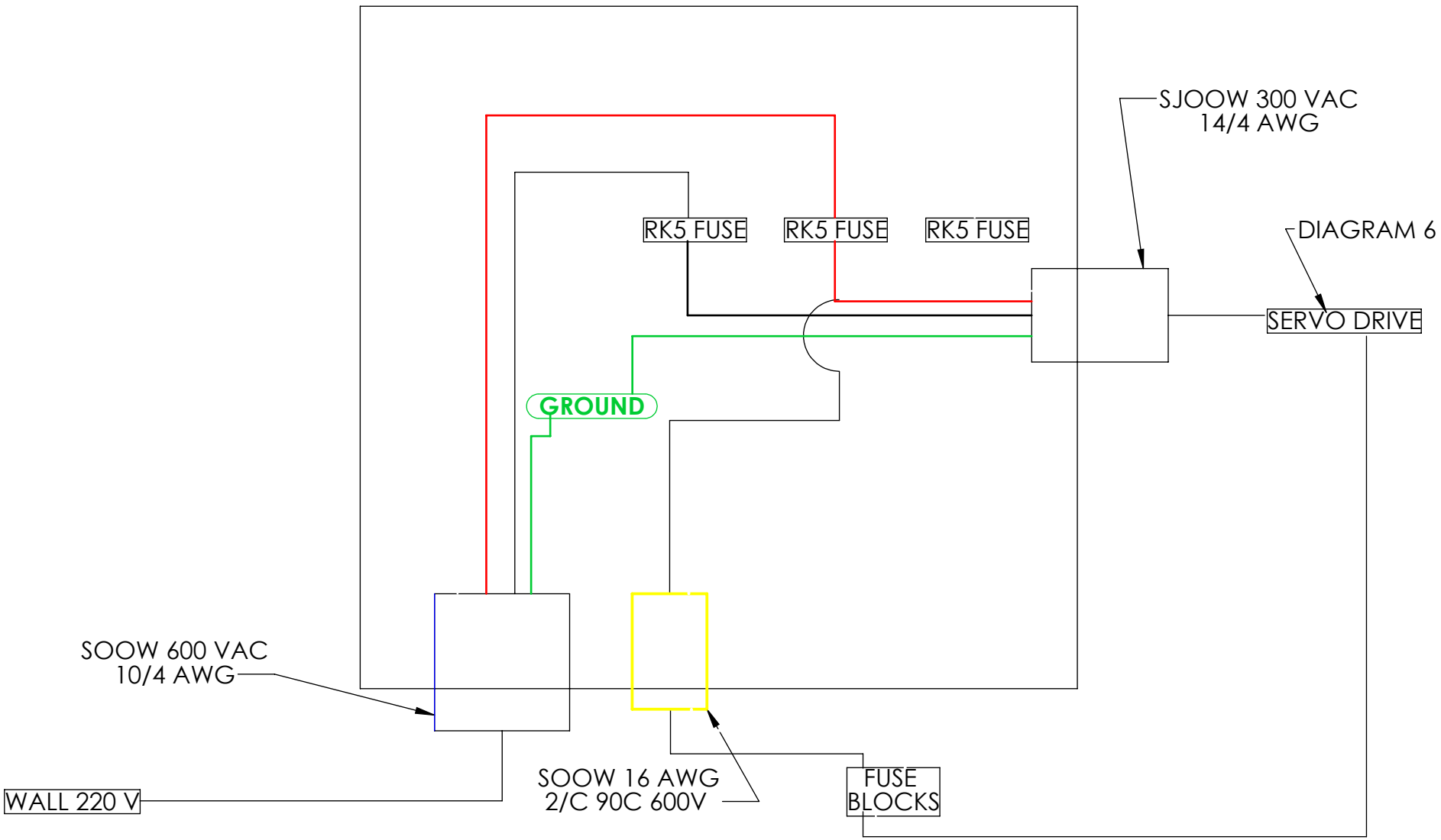

ME430 SPRING 2013

Mechanical Engineering CAL POLY

SCALE:	PART:
UNITS:	MATERIAL:
TOLERANCE:	DATE:
DWG #:	

5 4 3 2 1

DIAGRAM 2: COMPACT DISCONNECT

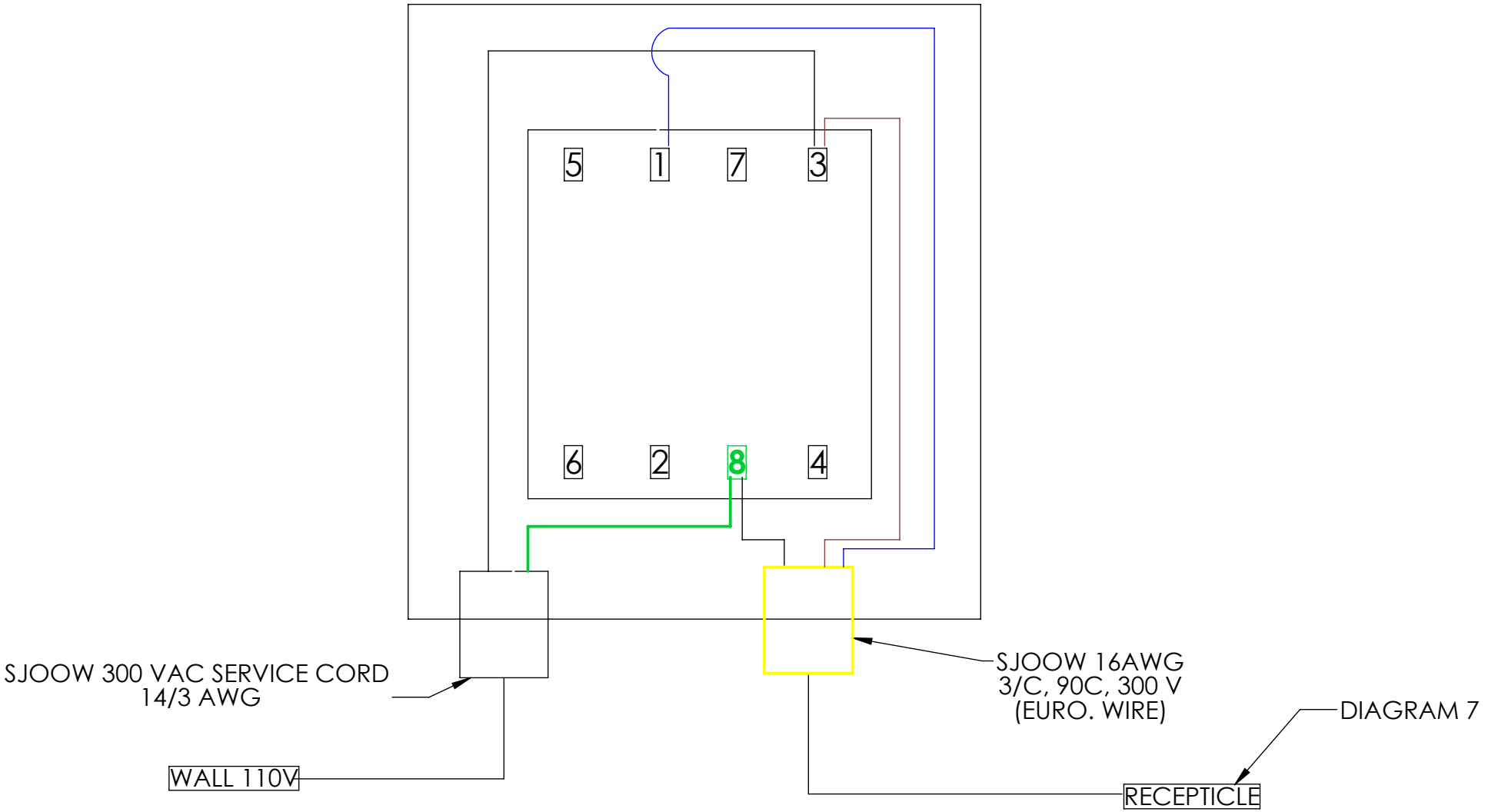

ME430 SPRING 2013 Mechanical Engineering CAL POLY	SCALE:	PART:
	UNITS:	MATERIAL:
	TOLERANCE:	DATE:
	DWG #:	

5 4 3 2 1

DIAGRAM 3: LOAD CELL POWER SUPPLY
(PSM-F10)

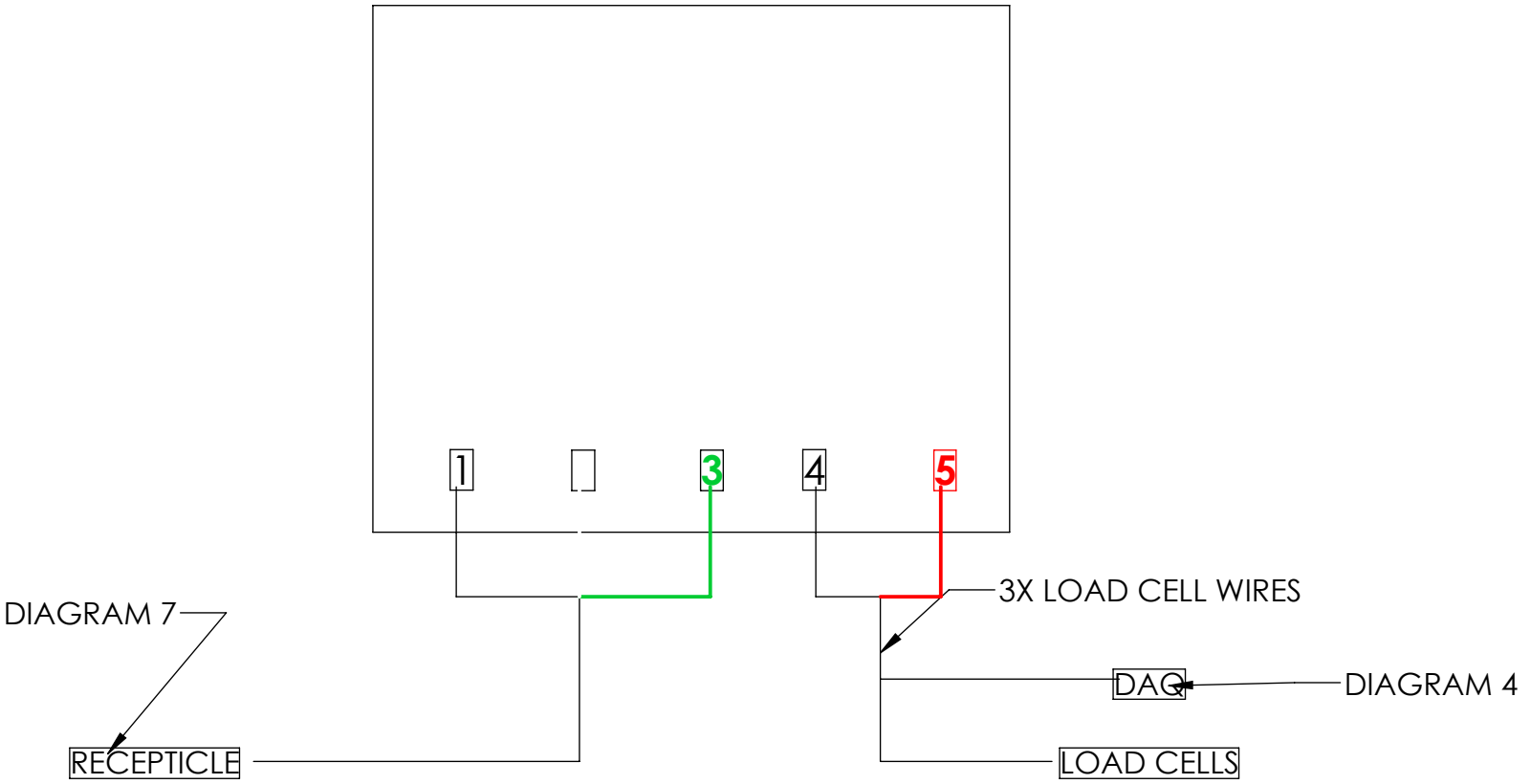

ME430 SPRING 2013 Mechanical Engineering CAL POLY	SCALE:	PART:
	UNITS:	MATERIAL:
	TOLERANCE:	DATE:
	DWG #:	

5 4 3 2 1

DIAGRAM 4: NI USB-6341 DAQ

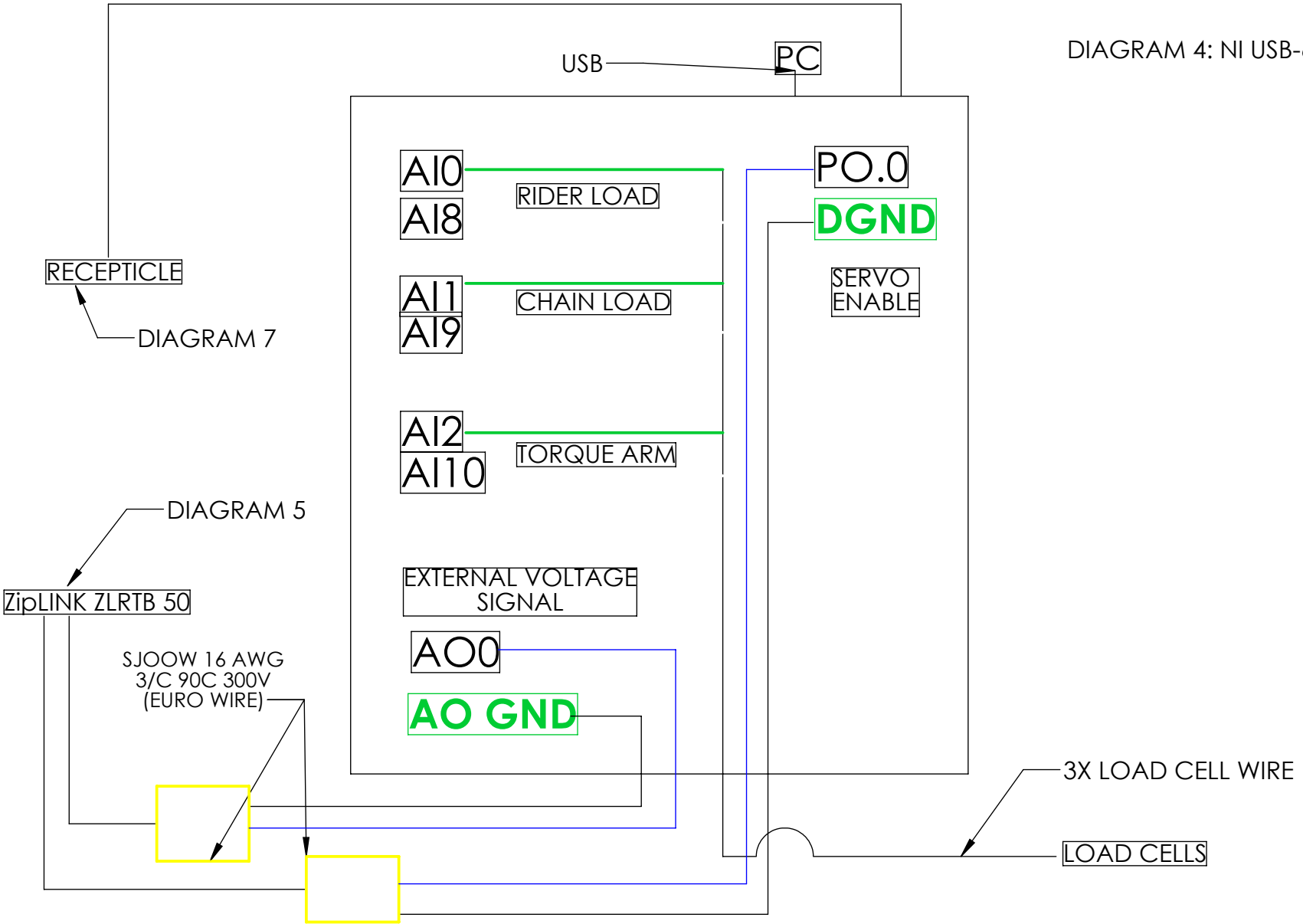

ME430 SPRING 2013	
Mechanical Engineering CAL POLY	
SCALE:	PART:
UNITS:	MATERIAL:
TOLERANCE:	DATE:
DWG #:	

5 4 3 2 1

DIAGRAM 5: ZipLINK ZLRTB50

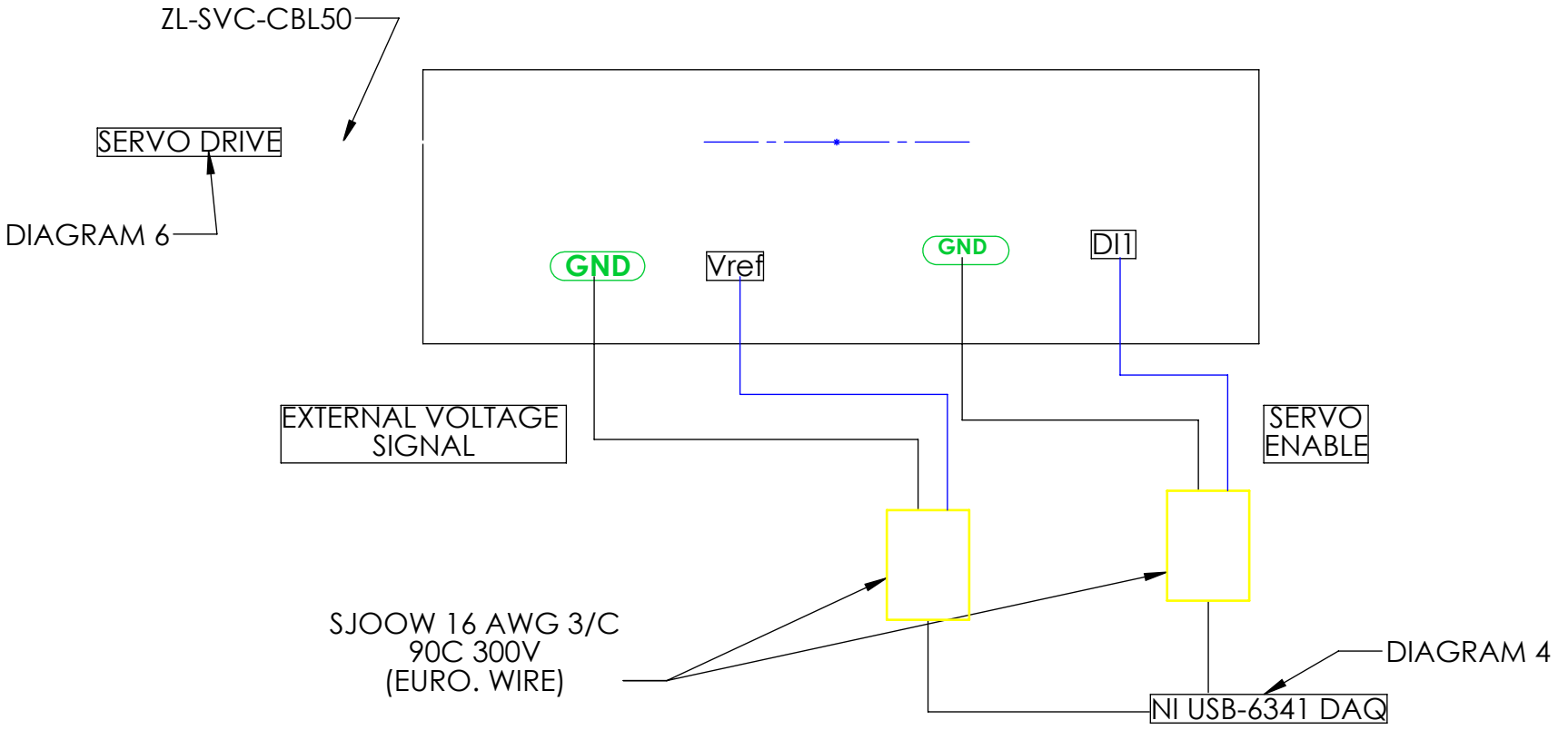

ME430 SPRING 2013 Mechanical Engineering CAL POLY	SCALE:	PART:
	UNITS:	MATERIAL:
	TOLERANCE:	DATE:
	DWG #:	

5 4 3 2 1

DIAGRAM 6: SERVO DRIVE

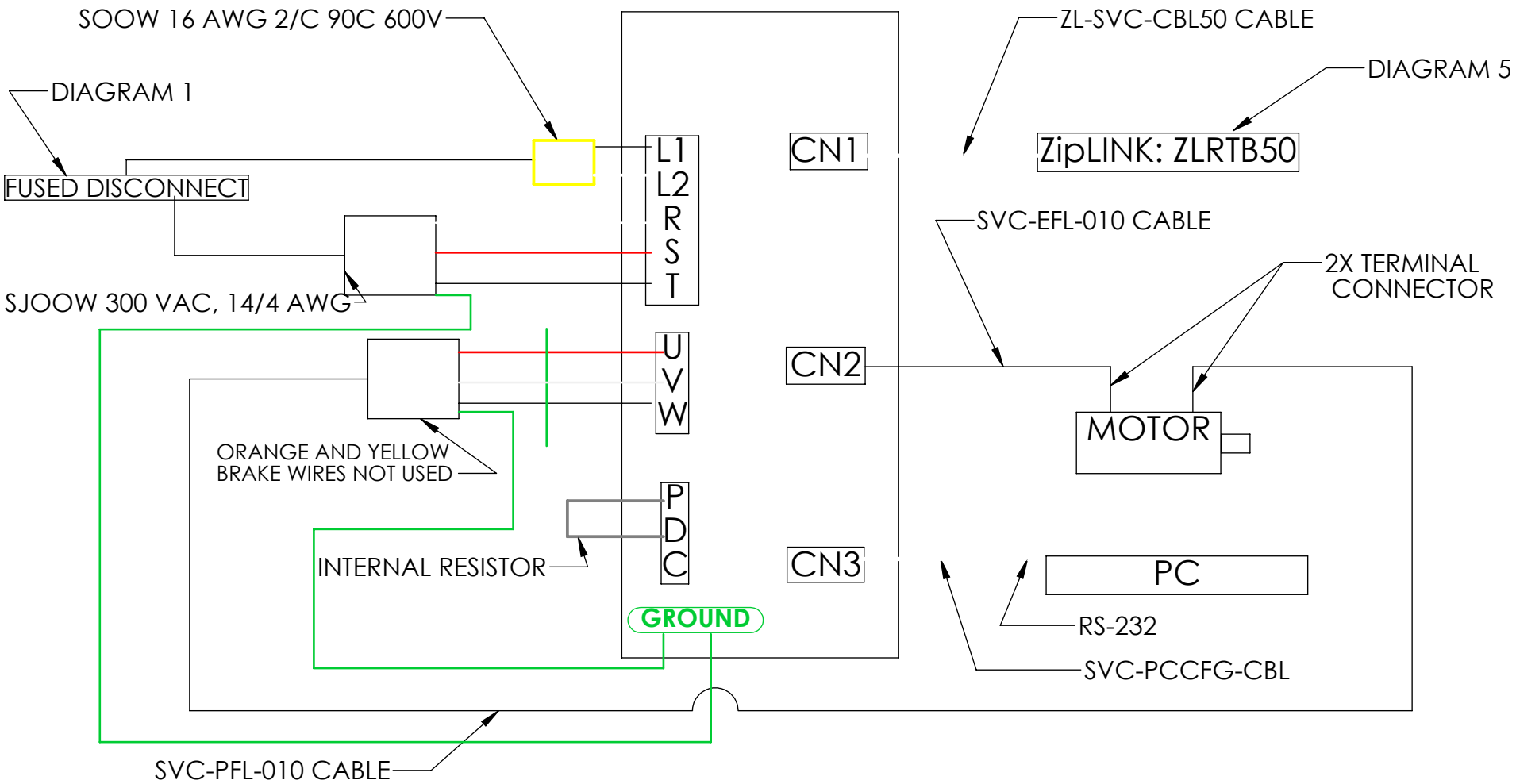

ME430 SPRING 2013 Mechanical Engineering CAL POLY	SCALE:	PART:
	UNITS:	MATERIAL:
	TOLERANCE:	DATE:
	DWG #:	

5 4 3 2 1

DIAGRAM 7: RECEPTICLE

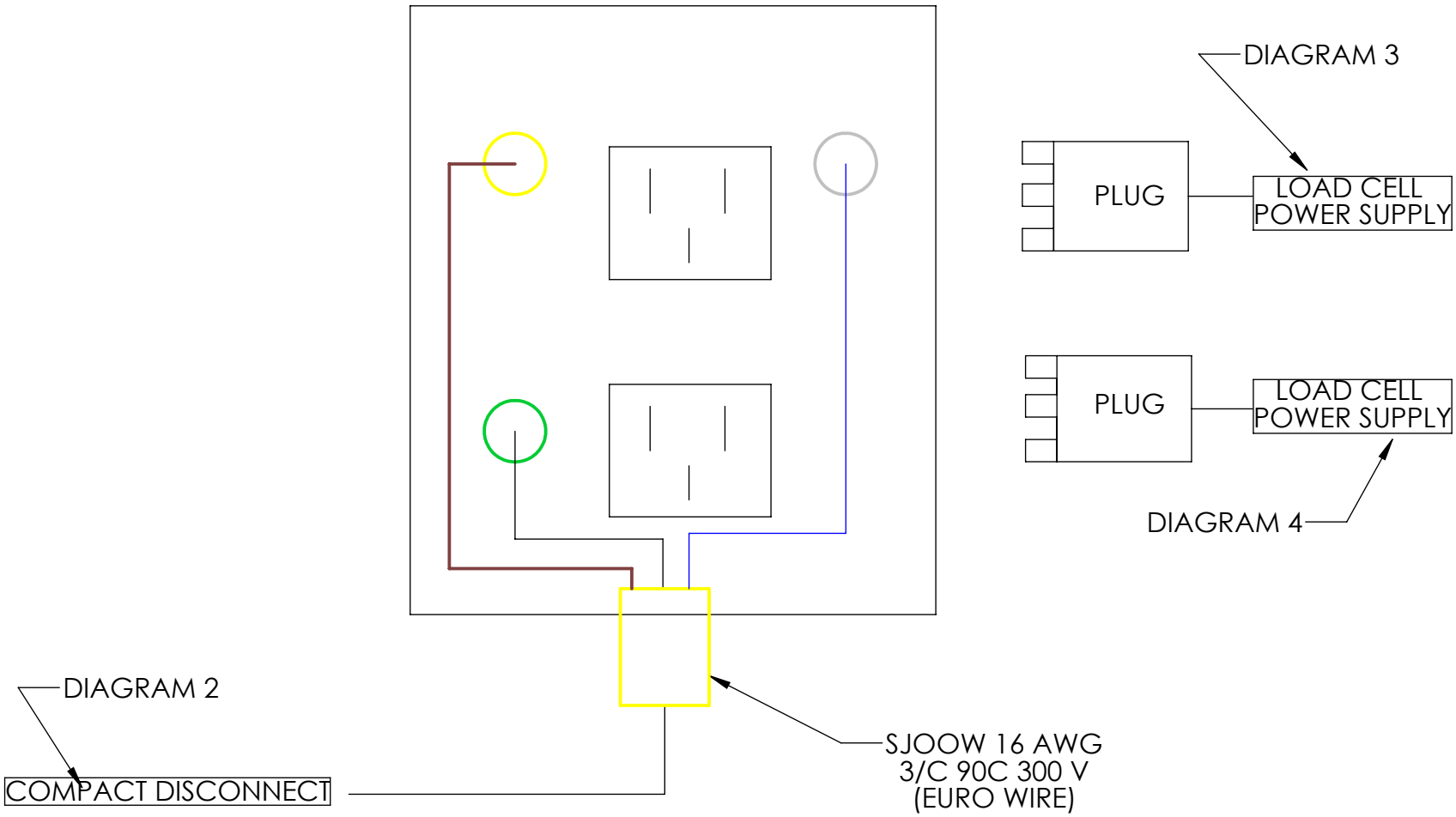

ME430 SPRING 2013	
Mechanical Engineering CAL POLY	
SCALE:	PART:
UNITS:	MATERIAL:
TOLERANCE:	DATE:
DWG #:	

5 4 3 2 1

Appendix F: Contact Information

Specialized Correspondent

Sam Pickman
408-779-6229
sam.pickman@specialized.com

Team Advisor

Joseph D. Mello
805-756-1356
jdmello@calpoly.edu

Vendors and Suppliers

AMI Bearings, Inc.
570 North Wheeling Road
Mount Prospect, IL 60056
Phone: 800.882.8642

Automationdirect.com
3505 Hutchinson Road
Cumming, GA 30040

Daniel Meine, Keiser Corporation
Mechanical Design Enginer
danielm@keiser.com

GENERIC SLIDES
1049 William Flynn Highway Suite 300
Glenshaw, PA 15116
Phone: 412/ 492-7272
Fax: 412/ 492-7271
Email: sales@genericslides.com

Helical Products Company, Inc.
901 West McCoy Lane
Santa Maria, California 93455

Joyce/Dayton Corporation
3300 S Dixie Dr.
Kettering, OH 45439
(937) 294-6261

MISUMI USA, INC
1717 Penny Lane, Suite 200
Schaumburg, IL 60173
Tel: 847-843-9105 or 800-681-7475
Fax: 847-843-9107 or 800-681-7402
E-mail: inquire@misumiusa.com

National Instruments Corporation
11500 N Mopac Expwy
Austin, TX 78759-3504

Transducer Techniques, Inc.
42480 Rio Nedo
Temecula, CA 92590
800-344-3965
tti@ttloadcells.com

Appendix G: Vendor Technical Data Sheets

Table of Contents

Rotating Dropout Assembly.....**1-3**

AMI Bearings: SUE210

Generic Slide: MS400

Load Cells.....4-7

Transducer Techniques: SBO

Transducer Techniques: MDB

Transducer Techniques: LPU

Coupler.....8-11

Helical: WAC30-12-12

Helical: WAC50-19-19

Load Actuators.....12-14

Joyce & Dayton WJ201

Joyce & Dayton WJ250

Motor Control System Assembly.....**15-37**

SureServo™ AC Servo SystemsUser Manual

National Instruments X Series Multifunction Data Acquisition

MiSUMI Bearings with Housings-T-Shaped, Base Mount, Retained

Appendix H: Supporting Analysis

Table of Contents

Pillow Block Bearing Assembly……1-3

Hydrodynamic Bearing Analysis

Load Shaft Size Determination

Motor Control System Assembly……4-7

Motor Selection Process2

Dynamometer Power Method

Dynamometer Power Uncertainty Determination

Appendix I: Team Gantt Chart

*See Separated Attachment